Sepsis Proteome Analysis by the Combination of Immunodepletion, Two-dimensional HPLC and nanoLC-MS/MS

Dissertation

zur
Erlangung des Doktorgrades
der Naturwissenschaften
(Dr. rer. nat.)

dem Fachbereich Chemie
der Philipps-Universität Marburg
vorgelegt von

Wei Zhang

Geb. am 11. Juli 1980 in Wuhan

Marburg/ Lahn 2011

Die Untersuchungen zur vorliegenden Arbeit wurden vom Juni 2006 bis Juni 2010 am Fachbereich Medizin der Philipps-Universität Marburg unter der Betreuung von PD Dr. Dr. H.-G. Wahl durchgeführt.

Vom Fachbereich Chemie der Philipps-Universität Marburg als Dissertation am 07. Feb. 2011 angenommen.

Erstgutachter: Prof. Dr. M. A. Marahiel
Zweitgutachter: PD Dr. Dr. H. G. Wahl

Tag der mündlichen Prüfung: den 17. Feb. 2011

für meine Eltern...

Die Wissenschaft unter der Optik des Künstlers zu sehen,

die Kunst aber unter der des Lebens.

--- Friedrich Nietzsche

Erklärung

Ich versichere, dass ich meine Dissertation mit dem Titel „Sepsis Proteome Analysis by the combination of Immunodepletion, Two-Dimensional HPLC and nano LC-MS/MS“ selbständig, ohne unerlaubte Hilfe angefertigt und michdabei keiner anderen als der von mir ausdrücklich bezeichneten Quellen und Hilfen bedient habe. Die Dissertation wurde in der jetzigen oder einer ähnlichen Form noch bei keiner anderen Hochschule eingereicht und hat noch keinen sonstigen Prüfungszwecken gedient.

Berlin, den 08. März 2011

(Ort, Datum)

Wei Zhang

Danksagung

Die vorliegende Arbeit wurde am Institut für Klinische Chemie und Molekulare Diagnostik des Universitätsklinikums Marburg durchgeführt. An dieser Stelle möchte ich mich bei all denen zu bedanken, die zum Gelingen dieser Arbeit beigetragen haben.

Mein Dank gilt daher vor allem Herrn PD Dr. Dr. H.-G. Wahl, Leiter des Medizinischen Labor Wahl, für die Vergabe dieses interessanten Themas, die hervorragende Betreuung und Unterstützung. Ihm gilt besonderer Dank für vier Jahre Zusammenarbeit, für das in mich gesetzte Vertrauen und für die konstruktive Kritik bei der Durchsicht meiner Arbeit.

Ebenfalls Dank gebührt Herrn Prof. Dr. M. A. Marahiel, Leiter des Instituts für Biochemie, dass er sich freundlicherweise bereit erklärt hat, die Betreuung zu übernehmen und das Erstgutachten zu schreiben.

Herrn Prof. Dr. A. Seubert und Herrn Prof. Dr. K.-M. Weitzel danke ich dafür, dass sie sich als weitere Mitglieder der Prüfungskommission bereitwillig zur Verfügung gestellt haben.

Herrn Prof. Dr. H. Renz, Leiter des Institus für Klinische Chemie und Molekulare Diagnostik, möchte ich für meine Anstellung als Doktorand sowie die Genehmigung zahlreicher Weiterbildungen herzlich danken.

Darüber hinaus gilt mein herzlicher Dank Herrn Dr. U. Linne für die Unterstützung bei unzähligen MS-Messungen, für die Beantwortung aller MS-bezogenen Fragen, für die stets offene Tür, verbunden mit intensiven fachlichen Diskussionen.

Des Weiteren möchte ich Herrn PD. Dr. T. Stief für die Hilfstellung bei zahlreichen theoretischen Fragen und für die Korrektur meiner Arbeit.

Herrn Dr. S. Sel und Frau Dr. I. Herzum möchte ich für ihre Hilfsbereitschaft sowie ihre fachliche Unterstützung zu Beginn meiner Arbeit danken.

Weiterhin möchte ich Frau Dr. S. Riedel, Frau Dr. H. Galambos, und Frau B. Kosche danken. Dafür, dass sie in privaten Bereichen stets großes Interesse für meine Person gezeigt hatten und so dass sie jederzeit ein offenes Ohr für meine Probleme hatten. Ebenso ist Frau R. Haupt für die nette Unterstützung bei bürokratischen Angelegenheiten dankend zu erwähnen.

Für die gute Zusanmmenarbeit sowie für die technische Unterstützung bedanke ich mich bei Dr. M. Souquet von Beckman Coulter.

Allen voran aber gilt der Dank meiner Familie und Freunden, insbesondere meinen Eltern für ihre großartige und bedingungslose Unterstützung in allen Lebenslagen. Ohne ihre Ermutigung wäre diese Arbeit nie entstanden.

Table of contents

Zusammenfassung

Sepsis ist eine infektionsinduzierte Inflammationsreaktion des Körpers, wobei die Intensität des infektiösen Triggers nicht mit der Intensität der Antwortreaktion des Wirtsorganismus kongruent sein muss. Während eine kontrollierte lokal beschränkte inflammatorische Reaktion der Elimination der Infektion dient, kann sie unkontrolliert systemisch zu einer Vielzahl von Ereignissen führen, die letztendlich im Multiorganversagen enden kann. Pathogenetisch bedeutsam ist hierbei die aus der Dysfunktion des unspezifischen Immunsystems resultierende Gerinnungsaktivierung und endotheliale Dysfunktion. Die frühe Erkennung der Sepsis und die Vorhersage der Mortalität sind zwingend notwendig für eine weitere Senkung der immer noch hohen Sepsissterblichkeit weltweit. Die bisherigen Sepsismarker sind für diese Aufgabe nur unzureichend geeignet.

In der vorliegenden Arbeit sollte mit Hilfe eines neuen Flüssigkeitschromatografie-basierten Verfahrens zur differenziellen Proteomanalyse versucht werden, Biomarkerkandidaten aus Plasmaproben von Sepsispatienten zu identifizieren. Dabei wurde das Proteinreinigungssystem ProteomeLab^{TM} IgY-12 zur Abtrennung der 12 High-Abundance-Plasmaproteine eingesetzt. Anschließend erfolgte mit dem Proteinseparationssystem Proteome Lab^{TM} PF2D eine zweidimensionale Auftrennung der Proteine nach isoelektrischem Punkt und Hydrophobizität. Die integrierte DeltaVue^{TM} Software zeigt die Unterschiede zwischen normalen und septischen Proteomen an. Die differenziell dargestellten Peaks wurden, fraktioniert gesammelt, zur weiteren Identifizierung potentieller Biomarker anhand von nano LC-MS/MS analysiert. Nach verschiedenen Optimierungsschritten zeigte sich die angewandte „IgY-PF2D-nanoLC-MS/MS“ – Strategie als effektive und effiziente Methode zur differentiellen Proteomanalyse humaner Plasmaproben.

In der vorliegenden Studie wurden Plasmaproben von gesunden Probanden und Patienten mit Sepsis untersucht. Von den 124 Patienten mit Sepsis, schwerer Sepsis und septischen Schock wurden Plasmaproben von 5 männlichen Patienten mit ähnlicher Krankengeschichte und Sepsisursache für die differenzielle Proteomanalyse verwendet. Als Referenzproteom wurden Plasmaproben von 5 gesunden männlichen Probanden (altersgematcht) herangezogen. Insgesamt wurden 1800 Fraktionen analysiert und 233 einzelne Proteine identifiziert. 17 Proteine, die nur in den Patientenproben mit Sepsis vorkamen, wurden als Biomarkerkandidaten postuliert. Neben bekannten Akute – Phase – Proteinen wurden auch einige neue Proteine wie z. B. Lumican, Urinary Protease Inhibitor und Cationic trypsinogen als putative Sepsismarker identifiziert, deren Rolle in der Sepsispathogenese noch zu klären sind. Alle 17 Biomarkerkandidaten sollten nun in weiteren gezielten Studien hinsichtlich ihres diagnostischen und prognostischen Wertes überprüft werden.

List of used abbreviations

1D	1st dimension
2D	2nd dimension
2-DE	two-dimensional gel electrophoresis
ACN	acetonitrile
ACT	alpha-1-antichymotrypsin
apoB100	apolipoprotein B-100
APPs	acute-phase proteins
CF	chromatofocusing
CID	collision-induced dissociation
CRP	C-reactive protein
CTG	cationic trypsinogen
DIC	disseminated intravascular coagulation
DTT	dithiothreitol
EDTA	ethylenediamine tetraacetic acid
ESI	electrospray ionization
FDA	food and drug administration
HAPs	high abundance proteins
HDLs	high density lipoproteins
HPLC	high performance liquid chromatography
HSA	human serum albumin
IaIp	inter-alpha inhibitor protein
ICU	intensive care unit
IgA	immunoglobulin A
IgG	immunoglobulin G
IgM	immunoglobulin M
IgY	immunoglobulin yolk
IL-6	interleukin 6
IL-8	interleukin 8
LAC	lactoferrin

LAPs	low abundance proteins
LPS	lipopolysaccharide
LRG	leucine-rich α2-glycoprotein
LUM	lumican
MODS	multiple organ dysfunction syndrome
MS	mass spectrometry
MS/MS	tandem mass spectrometry
MSDB	mass spectrometry protein sequence database
MW	molecular weight
NAPs	negative acute-phase proteins
NF-κB	nuclear factor-κB
NuMA	nuclear mitotic apparatus protein
PCT	procalcitonin
PF2D	two-dimensional protein fractionation
p*I*	isoelectric point
PLC	phosphoinositide phospholipase C
PTMs	post-translational modifications
PTP1B	Protein tyrosine phosphatase 1B
RP	reversed-phase
RT-PCR	real-time polymerase chain reaction
SAA	serum amyloid A
SIRS	systemic inflammatory response syndrome
SOP	standard operating procedure
TFA	trifluoroacetic acid
TNFα	tumor necrosis factor α
TOF	time-of-flight
Tris	tris-(hydroxymethyl)-aminomethane
UTI	urinary trypsin inhibitor
UV	ultraviolet

List of used scale units

%	percent
°C	degree celsius
AU	absorbance units
kDa	kilodalton
mg	milligram
min	minute
mL	milliliter
nm	nanometer
ppm	parts per million
sec	second
v/v	volume to volume
w/v	weight to volume
xg	relative centrifugal force
µL	microliter

1 Introduction

1.1 Definitions of sepsis

Since 1992, the currently used sepsis definition criteria of the American College of Chest Physicians (ACCP) and the Society of Critical Care Medicine (SCCM) improved the epidemiological data through the standardization of the inclusion criteria in clinical studies [Bone et al. 1992; Levy et al. 2003]. The definition includes five clinical entities: SIRS (Systemic Inflammatory Response Syndrome), sepsis, severe sepsis, septic shock and Multiple Organ Dysfunction Syndrome (MODS). They represent a continuum of clinical and pathophysiological severity (Figure 1-1). The process begins with an infection, with or without a systemic inflammatory response, and may progress to a systemic response with severe sepsis (hypotension, hypoperfusion, or organ dysfunction) or septic shock (hypotension not responsive to adequate fluid resuscitation with hypoperfusion or organ dysfunction). These are different degrees of the systemic inflammatory reaction to a certain trigger that occurs as a complication in the follow-up of different diseases. It was believed that the phases of the disease process form a continuum of severity which characterizes populations at increased risk of morbidity and mortality [Matot et al. 2001].

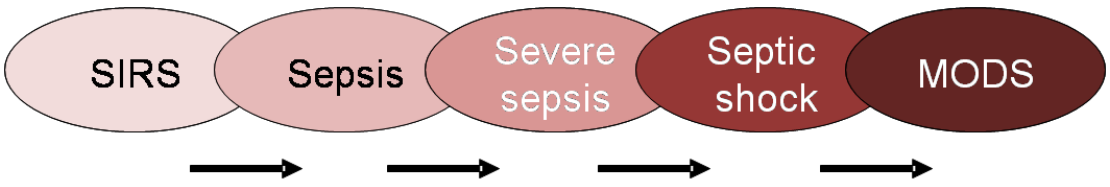

Figure 1-1: MODS represents the end of the spectrum of increasing inflammation. An overlap is usually observed during the different steps of the cascade of events leading to the manifestations of sepsis.

1.1.1 SIRS

The systemic inflammation response syndrome (SIRS) is diagnosed when patients have clinical manifestation of two or more of the following conditions reported in Table 1-1. A systemic inflammatory response may follow a variety of infectious and noninfectious insults. SIRS therefore was characterized as a clinical syndrome whose differential diagnosis includes infection as well as a number of noninfectious processes. In fact, the clinical manifestations of systemic inflammation are nonspecific. It was believed that the biochemical and/or immunologic, rather than clinical, criteria supported by further epidemiologic data may be more consistent to identify the inflammatory response.

Table 1-1: SIRS is considered to be present when patients have two or more of the following symptoms.

Clinical criteria
Body temperature > 38°C or < 36°C
Heart rate > 90/min
Respiratory rate of > 20/min or a $PaCO_2$ of < 32 mmHg
White blood cell count of > 12000 cells/μL or < 4000 cells/μL

1.1.2 Sepsis

Sepsis is defined as the clinical syndrome characterized by the presence of both infection and systemic inflammation response syndrome (SIRS) [Lever et al. 2007]. In consequence, strongly suspected infection as well as the clinical signs of SIRS (Table 1-1) is the basis diagnostic criteria for sepsis. Figure 1-2 presents the relations of infection, sepsis, and SIRS. Infection is defined as the pathological process caused by the invasion of normally sterile tissue or fluid or body cavity by pathogenic or potentially pathogenic microorganisms [Tsiotou et al. 2005]. Infections happen more often when the immune system does not function quit right. Infection may invoke a systemic host response, and sepsis refers to the clinical syndrome of systemic inflammation in response to infection.

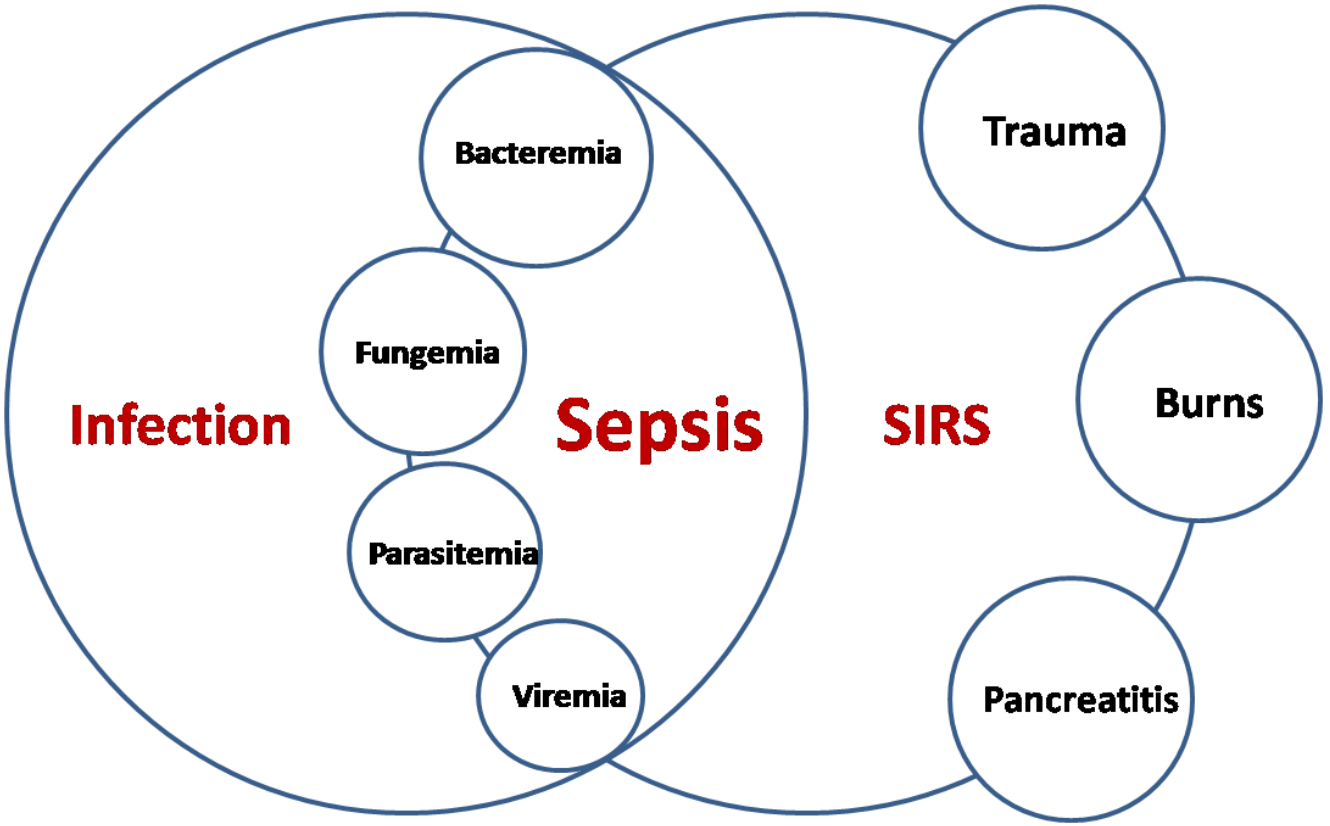

Figure 1-2: Relation between infection, sepsis, and the systemic inflammatory response syndrome (SIRS) [Bone et al. 1992]. The SIRS concept is valid to the extent that a systemic inflammatory response can be triggered by a variety of infectious and noninfectious conditions.

Furthermore, with the aid of extended epidemiologic data, a set of clinical parameter such as general, inflammatory, hemodynamic variables and organ dysfunction, tissue perfusion variables listed in Table 1-2 can be used to establish the diagnosis of sepsis.

Table 1-2: Clinical parameter as diagnostic criteria for sepsis [Levy et al. 2003]. WBC, white blood cell; SBP, systolic blood pressure; MAP, mean arterial blood pressure; SvO_2, mixed venous oxygen saturation; INR, international normalized ratio; aPTT, activated partial thromboplastin time.

Infection
documented or suspected, and some of the following:
General variables
Fever (core temperature > 38.3°C); Hypothermia (core temperature < 36°C); Heart rate > 90/min or > 2 SD above the normal value for age; Significant edema or positive fluid balance (> 20 mL/kg over 24 h); Hyperglycemia (plasma glucose > 110 mg/dL) in the absence of diabetes
Inflammatory variables
Leukocytosis (WBC count > 12,000/µL); Leukopenia (WBC count < 4000/µL); Normal WBC count with > 10% immature forms; Plasma C-reactive protein > 2 SD above the normal value; Plasma procalcitonin > 2 SD above the normal value
Haemodynamic variables
Arterial hypotension (SBP < 90 mmHg, MAP < 70 mmHg, or an SBP decrease > 40 mmHg in adults or < 2 SD below normal for age); SvO_2 > 70% (not used in newborns or children); Cardiac index > 3.5 L $min^{-1} \cdot M^{-2}$ (not used in newborns or children)
Organ dysfunction variables
Arterial hypoxemia (PaO_2/FIO_2 < 300); Acute oliguria (urine output < 0.5 mL $kg^{-1} \cdot h^{-1}$); Creatinine increase > 0.5 mg/dL; Coagulation abnormalities (INR > 1.5 or aPTT > 60 secs); Ileus (absent bowel sounds); Thrombocytopenia (platelet count < 100,000/µL); Hyperbilirubinemia (plasma total bilirubin > 4 mg/dL or 70 µmol/L)
Tissue perfusion variables
Hyperlactatemia (> 1 mmol/L); Decreased capillary refill or mottling

1.1.3 Severe sepsis

The definition of severe sepsis refers to sepsis associated with at least one organ dysfunction, hypoperfusion (low blood pressure), or hypotension (insufficient blood flow) [Matthay 2001]. Sepsis-induced hypotension and diffuse intravascular coagulation (DIC) result in organ dysfunction as consequence.

1.1.4 Septic shock

Septic shock is the syndrome characterized by a persistent arterial hypotension in patients with severe sepsis. Signs of decreased perfusion, altered alertness, or decreased urine output can round the definition of septic shock in pediatric patients [Astiz et al. 1998; Levy et al. 2003].

1.1.5 MODS

Multiple organ dysfunction syndrome (MODS) is the presence of altered organ function in an acutely ill patient such that homeostasis cannot be maintained without intervention [Bone et al. 1992]. Persons with a weakened immune system such as neonates and elderly people are most likely to develop sepsis, but the detrimental processes that may ultimately lead to the death of the patient are mostly caused by an exaggerated cell necrosis such as MODS [Van Amersfoort et al. 2003].

1.1.6 Staging system for sepsis

The staging system named PIRO (predisposition, infection, response, and organ dysfunction) is a model designed to monitor the host response to infection on the basis of factors believed to be pertinent to outcomes and has been proposed for the classification of sepsis [Angus et al. 2003; Rello et al. 2009]. This system stratifies patients on the basis of their predisposing conditions, the nature of the infection, the nature of the host response, and the degree of concomitant organ dysfunction.

1.2 Epidemiology of sepsis

It is possible to evaluate and compare epidemiological or outcome studies of sepsis since the definitions were standardized after the Consensus Conference. Increasing severity correlates with increasing mortality, which rises from 20~30% for severe sepsis up to 40~60% for septic shock. With an estimated annual mortality of between 30 and 50 deaths per 100,000 populations, this condition ranks in the top 10 causes of death and a major cause of morbidity in intensive care units. The expected number of newly diagnosed cases with severe sepsis in Germany amounts to 76~110 per 100,000 adults [Engel et al 2007]. Furthermore, epidemiology shows that sepsis was more common among men than women and among non-white persons than white persons in the United States [Martin et al. 2003]. The most cases of sepsis are due to infections in lung, abdomen, urinary tract, skin/soft tissue, and the primary bloodstream. Sepsis caused by gram-negative and gram-positive bacteria, fungi, viruses, and parasites, have become increasingly important over the past decades [Calandra et al. 1991]. The increasing sepsis rates are probably caused by the increasing use of catheters and other invasive equipment, by chemotherapy, and by immunosuppression in patients with organ transplants or inflammatory diseases [Van Amersfoort et al. 2003].

1.3 Pathophysiology of sepsis

Sepsis could be referred to as a process of malignant intravascular activation of the complex enzyme cascades of hemostasis and inflammation [Hotchkiss et al. 2003; Remick 2007]. When the inflammation occurs, toxins from infectious microorganisms activate the cellular and humoral immune defense systems in the human body such as phagocytes (neutrophils and macrophages) and natural-killer lymphocytes [Bernard et al. 2001; Buchud et al. 2003]. In the meantime, antibodies, cytokines, and inflammatory factors are present to effectively regulate these defense responses [Moshage et al. 1997]. Several signalling events are immediately evident during the initial responses to sepsis.

This is especially true for cytokines. For instance, the pro-inflammatory regulators, such as TNFα, IL-1β, IL-6, and IL-8, are frequently elevated in human sepsis; in addition, anti-inflammatory regulators, such as IL-1 receptor, IL-10, IL-11, and IL-13, are also produced in large quantities in patients with sepsis [Antonelli et al. 1999]. A complex interaction of cytokines and cytokine-neutralizing molecules probably determines the clinical presentation and course of sepsis.

1.3.1 Elements involved in sepsis

1.3.1.1 Acute-Phase Proteins

The acute-phase proteins (APPs) have been empirically defined as those whose plasma concentration increases by more than 50% following inflammatory reaction. Those proteins whose concentrations decrease by at least 50% during inflammatory response are named negative acute-phase proteins (NAPs) [Gabay et al. 1999], listed in Table 1-3.

Acute-phase proteins are synthesized almost exclusively in the liver and most are glycosylated [Baumann et al. 1994; Rivers et al. 2001]. They serve important functions in restoring homeostasis after infection or inflammation. The acute-phase response of the organism is a reaction to trauma, injury or infection aimed to repair tissue damage of the host. Monocytes and other cells of the innate immune system are the key components of the inflammatory response, as they are susceptible for microorganisms or fragments of microorganisms. Activated cells secrete inflammatory mediators like IL-1, IL-2, IL-6 and TNFα, which regulate the cascade of inflammation.

Table 1-3: Human acute-phase proteins [Gabay et al. 1999].

Acute-Phase Proteins	
Complement system	C3, C4, C9, Factor B, C1 inhibitor, C4b-binding protein, mannose-binding protein
Coagulation system	fibrinogen, plasminogen, urokinase, protein S, vitronectin, plasminogen-activator inhibitor 1
Antiproteases	α1-protease inhibitor, α1-antichymotrypsin, pancreatic secretory trypsin inhibitor, Inter-α- trypsin inhibitors
Transport proteins	ceruloplasmin, haptoglobin, hemopexin
Participants involved in inflammatory response	secreted phospholipase A2, lipopolysaccharide-binding protein, granulocyte colony-stimulating factor, interleukin-1-receptor antagonist
Others	C-reactive protein, serum amyloid A, α1-acid glycoprotein, fibronectin, ferritin, angiotensinogen
Negative Acute-Phase Proteins	
human serum albumin, transferrin, transthyretin, α2-HS-glycoprotein, α-fetoprotein, thyroxine-binding protein, insulin-like growth factor I, factor XII	

The changes in the concentrations of APPs are largely due to changes in their production by hepatocytes [Ceciliani et al. 2007]. By this means, NAPs are down-regulated in plasma during the acute-phase response to allow an increase in the capacity of the liver to synthesize the induced APPs. Hence, it is logical to presume that the down-regulated plasma proteins that are not required for host defense satisfies the need of diverting enough available amino acids to the production of other APPs [Gabay et al. 1999].

1.3.1.2 Cytokines

Sepsis syndrome often is accompanied by overwhelming systemic inflammation which is caused by excessive release of cytokines into the systemic circulation [Blackwell et al. 1996]. Cytokines are low-molecular-weight polypeptides or glycoproteins that regulate numerous cellular functions and allow both autocrine and paracrine signaling [Scott et al. 2002]. Cytokines regulate many of the

pathways involved in the host inflammatory response to sepsis. Four cytokines, TNFα, IL-1β, IL-6 and IL-8 have been most strongly associated with sepsis syndrome. TNFα can be induced rapidly by endotoxin and elevated in patients with sepsis, and has been implicated in a large number of infectious and non-infectious inflammatory diseases [Strieter et al. 1993]. IL-1β is produced by endotoxin-stimulated human monocytes and increased in humans after infusion of endotoxin. IL-6 is a 21 kDa glycoprotein that inducts acute phase protein production in the liver, and modulation of haemotopoiesis [Aderka et al. 1989]. The function of IL-8 in sepsis is likely to be recruitment and activation of neutrophils in specific sites which can lead to tissue injury [Blackwell et al. 1996].

However, cytokines that might have acceptable survival predicting capability are not easy to measure in the clinical setting. Because of their short half lifes, they may have already disappeared from the bloodstream when screening is carried out on a daily basis [Oberhoffer et al. 1999].

1.3.1.3 Systemic inflammatory cascade

A systemic inflammatory cascade is activated by the local release of bacteria, toxins, or other inflammatory mediators. The inflammatory cascade is a complex process that involves humoral and cellular responses, complement, and cytokine cascades [Griffiths et al. 2009]. The cytokines TNFα and IL-1β are released first and initiate several cascades. The release of IL-1β and TNFα leads to cleavage of NF-κB inhibitor. Once the inhibitor is removed, NF-κB is able to initiate the production of mRNA, which induces the production other proinflammatory cytokines [Burdette et al. 2010].

These proinflammatory cytokines can act directly to affect organ function or they may act indirectly through secondary mediators, including nitric oxide, thromboxanes, leukotrienes, platelet-activating factor, prostaglandins, and complement. Then these primary and secondary mediators cause the activation of the coagulation cascade, the complement cascade and the production of

prostaglandins and leukotrienes [Venu 2008]. Clots lodge in the blood vessels which lowers profusion of the organs and can lead to multiple organ system failure. In time this activation of the coagulation cascade depletes the patient's ability to make clot resulting in disseminated intravascular coagulation (DIC) [Levi et al. 1999]. The cumulative effect of this cascade is an unbalanced state, with inflammation dominant over anti-inflammation and coagulation dominant over fibrinolysis, resulting microvascular thrombosis, hypoperfusion, and tissue injury. Severe sepsis, septic shock, and multiple organ dysfunctions may occur, leading to death [Venu 2008].

1.3.2 Mediators and markers involved in sepsis

1.3.2.1 Inflammatory mediators in sepsis

A mediator can be defined as an event, state, substance, or process that causes a disease and that is present during some or all of the clinical expression of the disease [Marschall et al. 2000]. The mediator must be present in all patients with the disease. Furthermore, its neutralization before the onset of the disease must completely prevent the development of the manifestations of the disease as well as after the onset of the disease must attenuate the severity of the disease.

Administration of the putative mediator to an experimental animal must produce the clinical manifestations of the disease. Both endotoxin and TNFα evoke in humans a response with many of the characteristics of sepsis [Michie et al. 1988; Suffredini et al. 1989]. That neither reproduces the entire spectrum of abnormalities of sepsis may reflect the dose or suggest that neither alone is responsible for all aspects of the clinical syndrome. Conversely, the disease that might be treated by neutralization of TNFα or endotoxin can only be the spectrum of abnormalities produced by experimental administration of either.

1.3.2.2 Markers used in sepsis diagnosis

A marker is a measure that identifies a normal biologic state or that predicts the presence or severity of a pathologic process or disease. A marker can serve for

either establishing a diagnosis, or quantifying the severity of that disease, or measuring the response to therapy [Marschall et al. 2000]. Immunological monitoring of the systemic inflammation and its response to therapy is currently widely practiced by measurements of CRP, IL-6, IL-8 and PCT that can be performed routinely in the diagnostic laboratory [Kolb-Bachofen 1991; Koch et al. 1992; Wang et al. 2000; Luzzani et al. 2003; Herzum et al. 2008].

PCT derives from pre-procalcitonin, as a 13 kDa peptide of 116 amino acids. It was suggested that PCT is a secondary mediator that might augment and amplify but does not initiate the septic response [Nijsten et al. 2000; Wang et al. 2000]. CRP is a major acute-phase protein that stimulated by cytokines [Steinwald et al. 1999; Kolb-Bachofen 1991]. PCT and CRP concentrations might discriminate the infectious systemic inflammatory response syndrome (SIRS) from those who are not infected [Brunkhorst et al. 1999]. IL-6 and IL-8 are proinflammatory cytokines indicating the severity of the inflammatory response, but are not specific for bacterial infection [Borden et al. 1994].

However, among the used biomarkers of sepsis, all of them fulfill only a fraction of these requirements, such as improved diagnosis of bacterial infection or a better assessment of the severity of the host response to infection [Meisner 2005]. At present, such aforementioned measurements have therefore generally not proven effective in predicting which individual patients will survive or respond to therapy.

1.4 Proteomics and Human Plasma Proteome

1.4.1 Proteomics

Proteomics is often defined as the systematic study of proteins that constitute a biologic system [Hanash 2003]. Unlike classical protein chemistry techniques that elucidate the structure and function of a single or a small group of proteins, proteomics allows examination of the behavior of numerous proteins in a single experiment [Reddy et al. 2004]. The goals of proteomics are following: to identify

all the proteins in a given cell, tissue or organism; to determine how these proteins interact; finally, to understand the mechanism of the function of these proteins. An ultimate objective of proteomics is the understanding of complex biological systems, which can lead to new diagnostics and therapy [Simonian et al. 2003]. One strategy, known as protein global proteomics, aims to characterize all proteins in a given system by protein mapping or profiling. The other strategy, known as differential proteomics, is used to identify different patterns of protein-expression between two or more groups of samples. Typically, this is considered the discovery phase of proteomics and involves the comparison of different states of a cell or tissue, such as diseased vs. normal, mature vs. immature, or drug-treated vs. non-treated [Simonian et al. 2003]. Unless specific proteins are targeted, the approaches are largely discovery driven and typically rely on finding proteins that are more abundant in plasma obtained from disease-afflicted individuals than in healthy controls.

While the development of faster and more sensitive mass spectrometers has obviously had a major impact on the ability to conduct plasma proteomics, sample preparation and detection methods such as high abundance protein depletion, chromatography, and mass spectroscopy have been notably improved in the past decades [Pieper et al. 2003; Giorgianni et al. 2003; Omenn et al. 2005; Lee et al. 2006; Fröhlich et al. 2006]. It must be pointed out that, currently no single proteomics technology has sufficient analytical power to allow for the detection of an entire proteome of plasma [Ishihama 2005; McDonald et al. 2006]. Approach that can be used to expand proteome coverage is the use of multiple separation technologies. The next major challenge to overcome is to find intelligent solutions to determine which proteins idnetified in a comparative analysis have the greatest likelihood of being validated as useful biomarkers [Issaq et al. 2007].

1.4.2 The human plasma proteome

The human body possesses over 60,000 miles of veins, arteries, and capillaries. Approximately five liters of blood travels continuously through the body by way of

the circulation system. Blood carries oxygen and nutrients to cells and transports carbon dioxide and waste products excreted from cells. It possesses such a richness of information concerning the overall pathophysiology of the patient [Issaq et al. 2007]. Blood is not only the most studied biological fluid, but also the primary material for disease diagnosis in routine which is an extremely popular source for proteomic analysis leading to the identification of biomarkers. Blood samples are reasonably easy to obtain when compared with procedures such as tissue biopsy, the samples are technically and psychologically easy to collect and process [Veenstra et al. 2005], and samples are mostly considered homogeneous when compared to saliva or urine both of which are somewhat compositionally dependent on fluid flow rates [Lundblad 2005].

The global composition of proteins in the blood plasma represents the plasma proteome. Perfusion of blood through the different organs and tissues can result in the addition of new proteins, removal of some proteins, or modification of existing proteins, which may vary according to specific physiological or pathological conditions [Lathrop et al. 2003].

It is logical to expect correlation between the proteomic profiles of normal plasma with the specific physiological or pathological states. Unlike the relatively unchanging genome, the dynamic proteome changes from minute to minute in response to tens of thousands of intra- and extracellular environmental signals. A recent extensive compilation of human plasma proteins indicated that most of the major categories of proteins in the human body were represented in the blood plasma [Anderson et al. 2004]. Thus, the plasma is an ideal source of diagnostic markers and therapeutic targets for many human diseases.

1.4.3 The qualitative and quantitative analytical challenge within plasma

Plasma is the liquid component of blood, in which the blood cells including red blood cells, leukocytes, and platelets are suspended [Thadikkaran et al. 2005]. It is composed of mostly water with approximately 90% by volume, and contains

dissolved proteins, glucose, clotting factors, mineral ions, hormones and carbon dioxide. Given an average blood volume of 4.5 liters in a 70 kg male and an average volume proportion of plasma in blood of 55%, there are about 2.5 liters of plasma in the average person, containing roughly 250 g of plasma protein [Anderson et al. 2002]. An estimate of the number of proteins in blood plasma is at least 10,000, but the actual number of distinct proteins may be several orders of magnitude higher [Anderson et al. 2002]. This is because each protein has a potential for a variety of post-translational and metabolic modifications [Mann et al. 2003; Walsh et al. 2006], both in normal and diseased cells.

Biomarker discovery in plasma is challenging since it involves searching for extremely low abundance proteins (ng/mL range), which comprise less than 1% of the total plasma proteome, whereas the 22 most highly abundant proteins represent over 99% of the total (Figure 1-3).

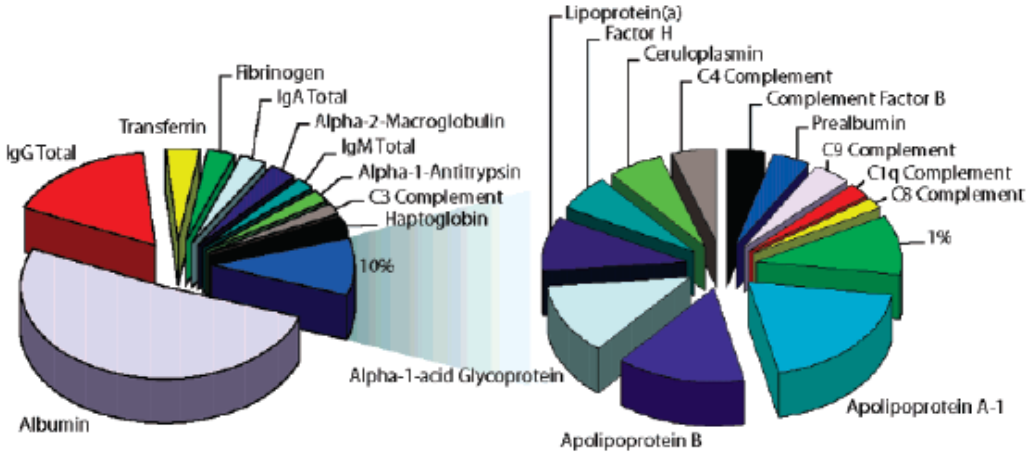

Figure 1-3: The dynamic range of protein concentrations in human plasma [Issaq et al. 2009]. The 22 most highly abundant proteins represent over 99% of plasma by mass.

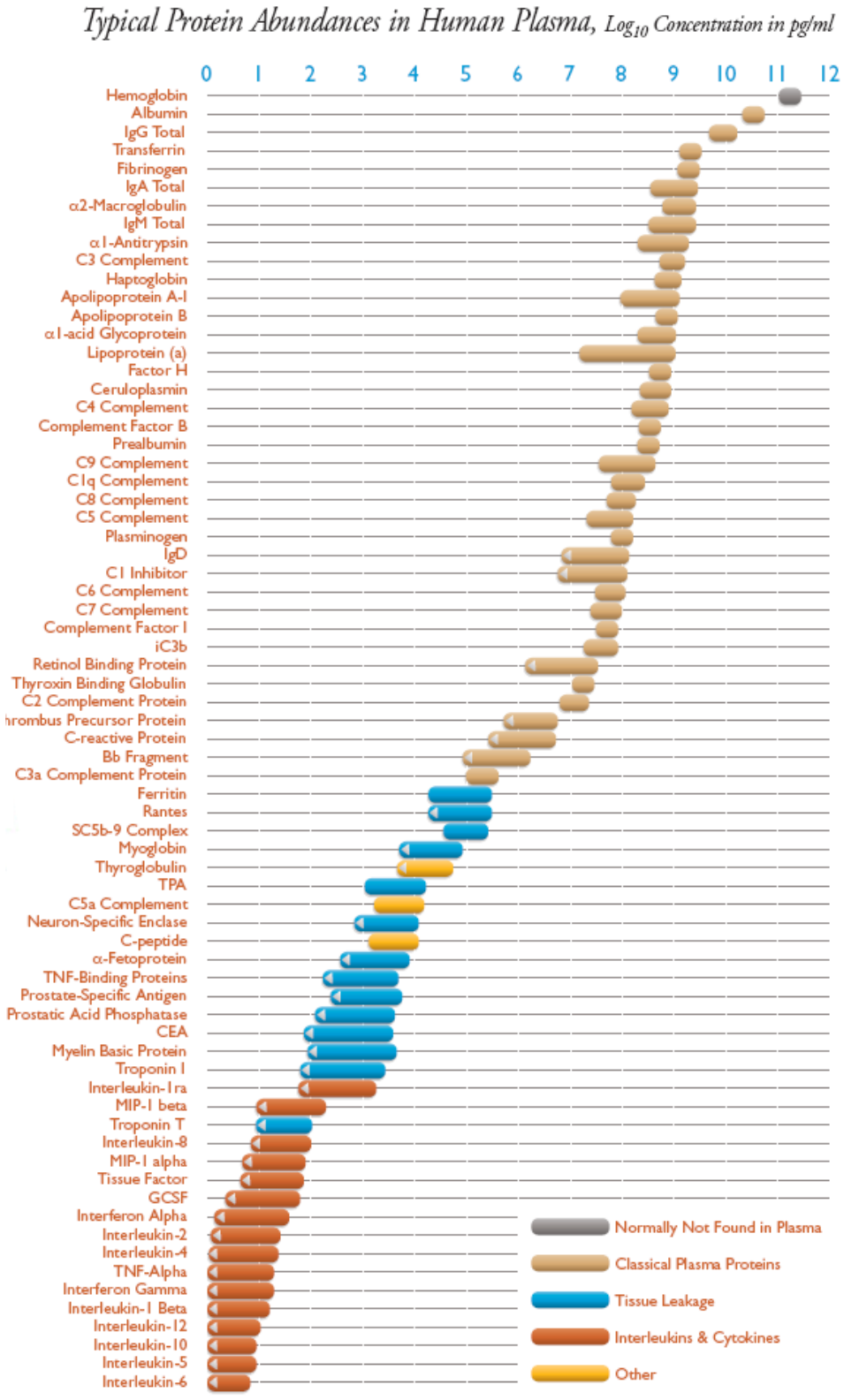

Figure 1-4: Reference intervals for 70 proteins in plasma. Figure obtained from Beckmann Coulter Report BR-9976A.

Figure 1-4 shows the reference intervals for 70 proteins in human plasma. Abundance is plotted on a log scale spanning 12 orders of magnitude. The classical plasma proteins are clustered to the left (high abundance), the tissue leakage markers are clustered in the centre, and cytokines are clustered to the right (low abundance).

In consequence, potential biomarkers are masked by the overwhelming abundance of relatively few proteins. Human serum albumin (HSA) and total immunoglobulin G (IgG) are the two most highly abundance proteins in human plasma, accounting for about 55% and 18% of the total protein, respectively. Taken together, the HSA and total IgG represent approximately 73% of the total plasma protein and are present at 45-60 mg/mL concentration. In contrast, most of the potential biomarkers are secreted into the blood stream at very low copy number [Lathrop et al. 2005; Thadikkaran et al. 2005], especially in the early onset of diseases [Anderson et al. 2002]. For example, the cytokines and the prostate specific antigen (PSA) are present in the low pg/mL levels. Based on this wide dynamic range, to get a qualitative and/or quantitative outcome of all proteins simultaneously in a single assay is enormously difficult. The more abundant proteins will certainly mask the detection of the very low abundance proteins.

This large dynamic range exceeds the analytical capabilities of traditional proteomic methods, making the detection of lower abundance plasma proteins extremely challenging. In biomarker discovery, it is necessary to maximize the observation of the plasma proteome to detect proteins with low abundance. The reduction of sample complexity and dynamic range is thus an essential first step in the analysis of the plasma proteome [Sheng et al. 2005]. This can be achieved by optimization of protein separation methods as well as selective depletion of the highly abundant, non-diagnostic proteins from the raw plasma [Liu et al. 2006; Tirumalai et al. 2003].

1.4.4 Removal of high abundance proteins in plasma

In order to remove high abundance proteins and thereby enrich low abundance proteins there are several possibilities according to their chemical affinity, antibody affinity, and molecular weight properties. Accordingly, several approaches using chromatographic absorbents, immunoaffinity methods, and ultrafiltration have been employed to overcome the presence of these highly abundant proteins. Compared with other strategies, immunoaffinity methods have the advantage of high efficiency and high specificity depletion of target proteins. Several immunoaffinity columns are commercially available for the purpose of the removal of multiple high abundance proteins from human plasma [Lee et al. 2006]. Beckman Coulter is developing ProteomeLab^{TM} IgY-12 proteome partitioning systems for proteomic sample preparation using polyclonal IgY antibodies immobilized to microbeads packed in liquid chromatography columns to deplete 12 of the most highly abundant proteins from plasma that collectively constitute up to 96% of the total protein mass in plasma, resulting in a maximum of 25-fold increase of sensitivity over non-depleted samples.

An ideal depletion method would completely remove high abundance proteins but leave those peptides and proteins behind. However, it is known that high abundance proteins such as serum albumin can function as a carrier and transporter of proteins within the blood, binding physiologically important protein species. One of the potential drawbacks of plasma protein immunoaffinity subtraction methodologies is thus that it may concomitantly remove low abundance proteins of interest by non-specific binding [Huang et al. 2005]. Since most proteome studies don’t have a specific target protein, it is not possible to know whether a biomarker of interest is lost during the removal of serum albumin or immunoglobulin [Lundblad 2005]. Although the increased signal to noise ration achieved by immunodepletion can make it easier to detect low abundance proteins, the increase in sensitivity could outweigh the potential loss of proteins, it remains to be tested with analysis of the eluted fractions containing target proteins.

1.4.5 Marburg Sepsis Project

1.4.5.1 The quest of novel biomarkers in sepsis

The clinical signs of sepsis usually are not specific or often are late symptoms and are already associated with organ dysfunction [Meisner 2005]. The trend in immunologic monitoring of patients has been to focus on the concentration of any one marker. At present, proinflammatory cytokines (such as IL-6 and IL-8), acute-phase proteins (such as CRP), and Procalcitonin are markers routinely used in the laboratory for sepsis diagnosis. However, prognostic studies conducted over the past 20 years have clearly shown that the measurement of any single plasma analyte generally lacks the sensitivity or specificity to predict which individual patients will survive or respond to therapy [Feezor et al. 2005]. Consequently, there is a demand for novel biomarkers of sepsis for clinical applications.

A previous study on several active immunologic markers in septic patients was performed in the intensive care unit (ICU) of the University Hospital of Marburg. More than 120 adult patients with manifest sepsis, severe sepsis and septic shock according to the modified criteria of the ACCP/SCCM Consensus Conference were included. The current project “The quest of novel diagnostic biomarkers in Sepsis” is based on this patient’s population.

1.4.5.2 Aim of the Study

Sepsis proteome analysis by the combination of immunodepletion, two-dimensional HPLC and nanoLC-MS/MS will be developed in this study. To generate a normal plasma proteome and as sequence to find out novel sepsis biomarkers by means of the survey of the difference as well as association between sepsis related proteomes and normal proteome for diagnosis and prognosis of sepsis are the major goal of the project.

2 Materials and methods

2.1 Study protocol

The study in the ICU of the University hospital of Marburg was approved by the Ethical Committee at the University hospital of Marburg. More than 120 adult patients with manifest sepsis, severe sepsis and septic shock according to the modified criteria of the ACCP/SCCM Consensus Conference were included. Those who were less than 18 years old or were pregnant at that time or had congenital disruption in coagulation were excluded in the previous study. The current project “The quest for novel diagnostic biomarkers in Sepsis” is based on this patient’s population.

Those who were less than 18 years old or were pregnant at that time or had congenital disruption in coagulation were excluded in the previous study. The female septic patients and those male septic patients who were less than 70 years old or had congenital disruption in coagulation at the time for previous study were excluded in the current study.

Table 2-1: Characteristics of five selected patients. SIP, study inclusion period.

Patient Nr.	Age	Gender	SIP (days)	Outcome
1	79	male	19	survivor
2	76	male	14	survivor
3	81	male	14	survivor
4	76	male	23	non-survivor
5	70	male	19	non-survivor

Five male patients with 76.4 years old on average from all those 120 patients with a clinically similar cause of sepsis and underlying diseases were selected (Table 2-1). Those male volunteers who had chronic sickness or their sepsis diagnosis related measurements were out of reference value were excluded in the current study. Three patients survived and two died from sepsis. The study

inclusion period in ICU was between 14 and 23 days, which began with the diagnosis of sepsis and ended with the diagnosis of healing for patients 1, 2, and 3 or with the death for patients 4 and 5, respectively. Citrated plasma samples from patients were drawn at the first as well as the last ICU day for further analysis.

Table 2-2: Results of sepsis diagnosis related measurements at the first ICU day.

Patient Nr.	Leukocytes (G/L)	Neutrophils (%)	CRP (mg/L)	PCT (µg/L)	IL-6 (ng/L)
1	30.4	96.3	102	2.6	345
2	23.9	83.7	170	10.6	31
3	18.2	87.9	204	17.7	438
4	25.9	90.3	43	1.3	124
5	10.4	91.9	207	2.2	443
Ref. Value	4.3 - 10	55 - 70	< 5	< 0.5	< 3.3

Five sepsis diagnosis related measurements, particularly the amount of white blood cells (Leukocytes), the quotient of neutrophils in the whole white blood cells, and the plasma concentration of some sepsis related proteins (CRP, PCT, and IL-6), were analyzed. Table 2-2 shows the results of the five measurements at the first ICU day. Obviously, all these measurements exceeded reference value, guaranteeing the reliability of the sepsis diagnosis.

Table 2-3 shows the results of the five measurements at the last ICU day. Some measurements returned to reference value, for instance, the PCT concentration from samples in all of three survived patients. Otherwise, the measurements in the non-survived patients still exceeded reference value largely and were even worse in contrast to the corresponding measurements at the first ICU day. It is therefore believed that the proteomic analysis of these samples could provide valuable information for sepsis diagnosis or prognosis.

Table 2-3: Results of sepsis diagnosis related measurements at the last ICU day.

Patient Nr.	Leukocytes (G/L)	Neutrophils (%)	CRP (mg/L)	PCT (µg/L)	IL-6 (ng/L)
1	19.3	N/A	267	0.5	15
2	26.9	N/A	29	0.1	20
3	9.4	N/A	116	< 0.1	21
4	42.0	43	223	18.1	563
5	15.6	N/A	233	4.0	536
Ref. Value	4.3 – 10	55 - 70	< 5	< 0.5	< 3.3

Citrated plasma samples (0.5 ml of 106 mM sodium-citrate + 4.5 ml venous blood) from three age matched healthy male individuals stored identically as the patient samples were used as control. The sepsis diagnosis related measurements in samples from healthy volunteers in Table 2-4 provided a reliable proteomic comparison between patient and control samples.

Table 2-4: Results of sepsis diagnosis related measurements in volunteers.

	Leukocytes (G/L)	Neutrophils (%)	CRP (mg/L)	PCT (µg/L)	IL-6 (ng/L)
Volunteers	4.9 - 7.4	55 - 66	< 5	< 0.1	< 2
Ref. Value	4.3 – 10	55 - 70	< 5	< 0.5	< 3.3

2.2 Identification of potential sepsis biomarkers

Differential proteomics is used to identify differentially expressed proteins between normal and sepsis-related samples. Figure 2-1 shows the flow sheet of sepsis biomarker discovery strategy using immunoaffinity subtraction chromatography (IgY12), two-dimensional protein separation (PF2D) and protein identification (nanoLC-MS/MS).

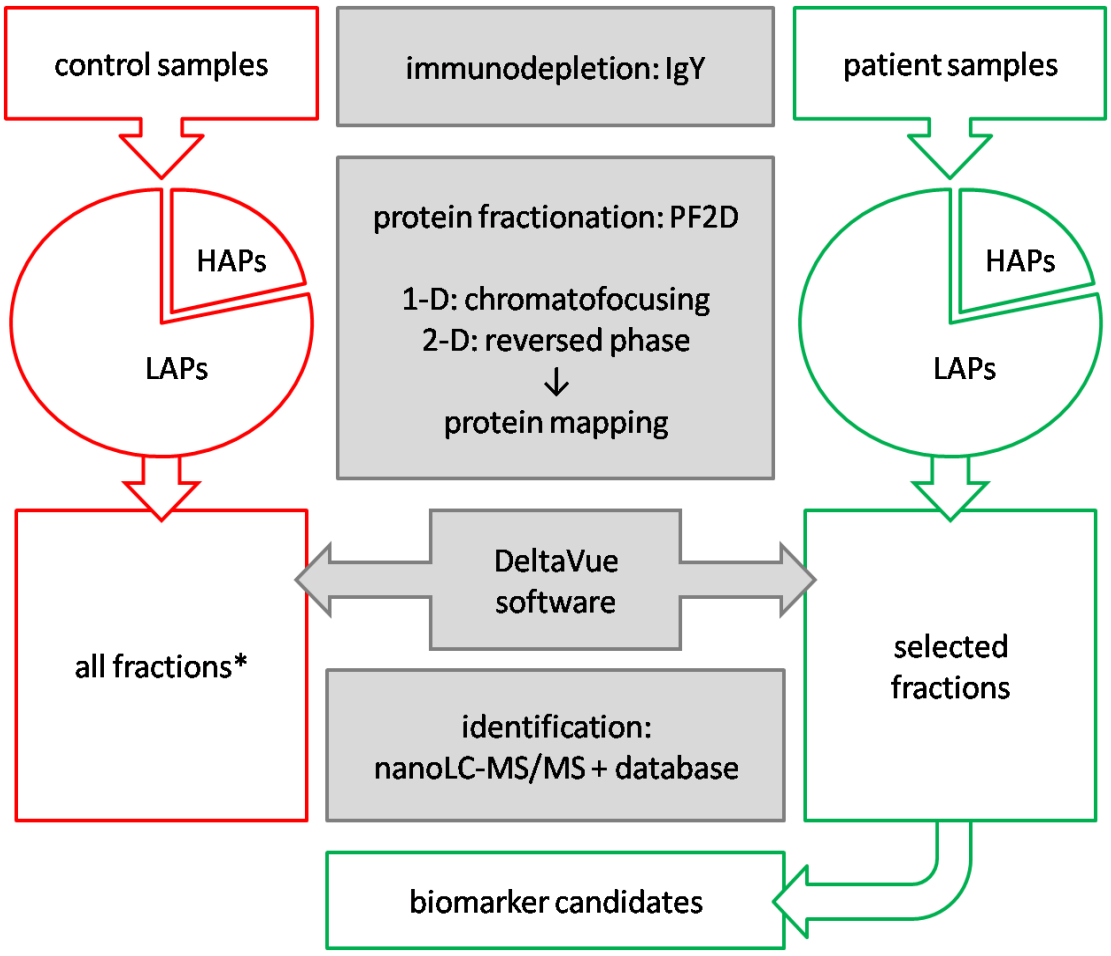

Figure 2-1: Biomarker discovery strategy using 2D HPLC and nanoLC-MS/MS. LAPs, low abundance proteins; HAPs, high abundance proteins. * Identification of all proteins in all fractions by mass spectrometry.

Plasma samples are subtracted using immunoaffinity chromatography at first. The low abundance proteins are pooled and then fractionated into around 600 fractions using chromatofocusing at 1D separation and subsequently reversed-phase chromatography at 2D separation to generate proteome mapping. Proteins in those peaks that are interesting for biomarker discovery are digested with trypsin. Tryptic peptide mixtures are separated by nanoLC, and sequences of the peptides are obtained by MS/MS. The peptide sequence data are used to identify the proteins through database searches using MSDB. In order to identify new biomarkers for sepsis diagnosis and prognosis, the immunodepleted plasma samples from both healthy individuals and patients

were loaded onto the PF2D system to generate protein maps for further analysis. To achieve the maximum resolution and reproducibility in PF2D system 3.5 mg of total plasma protein in a volume of 5 mL were be parallel injected.

The plasma samples from three healthy individuals were analyzed. The common proteins were regarded as reference plasma proteome named Proteome R. The plasma samples from three survived and two non-survived patients at the first as well as the last ICU day were analyzed to detect the differentially expressed proteins with comparison to Proteome R, generating corresponding Proteome S1, S2, N1, and N2 (Table 2-5).

Table 2-5: Experimental plan for generation of sepsis related proteome in four different states according to the timing of study and the treatment outcome.

Timing	**Treatment outcome**	
	survivor	**non-survivor**
the first ICU day	Proteome S1	Proteome N1
the last ICU day	Proteome S2	Proteome N2

The comparison between sepsis related Proteome S1, S2, N1, and N2 and Proteome R as well as the comparison among Proteome S1, S2, N1, and N2 could offer opportunities to generate novel biomarker candidates in sepsis, providing proteome difference between individuals with and without sepsis and between those who survive or die from sepsis, and ultimately finding clinical applications of one or more of the three issues: diagnosis, prognosis, and early detection of sepsis, that can predict which individual patients will survive or respond to therapy.

2.3 Human plasma preparation

The procedure used for sample preparation is an important parameter that can drastically affect reproducibility and is particularly important in the comparison of a differential proteomic study. It is suggested that the immediate separation of plasma from the cellular elements provide optimal analyte stability [Boyanton et al. 2002]. The time between venipuncture and freezing, process/storage containers, centrifugation speed, and the temperature of storage are the most critical variables for control of sample homogeneity in plasma [Lundblad 2005].

To prepare plasma from septic patients and healthy individuals, blood is withdrawn using venipuncture in the presence of citrate. 15 mL of blood were drawn from healthy male adults. The blood samples were collected into tubes containing citrate and centrifuged at 1000 xg for 10 min at 8°C until all of the blood cells fall to the bottom of the tube. The citrated plasma is then carefully removed, distributed into 2 mL aliquots, and frozen immediately at -80°C for further analysis. To ensure a reliable proteomic comparison between septic patients and healthy individuals all the plasma samples are allowed of freeze and thaw just for once.

2.4 Determination of Protein Concentration

The plasma protein concentration in different range was measured using UniCel^{TM} DxC 800 Systems Total Protein Assay (Beckman Coulter, USA) and SYNCHRON^{TM} LX20 Systems Micro Total Protein Assay (Beckman Coulter, USA).

UniCel^{TM} DxC 800 Systems Total Protein Assay (Beckman Coulter, USA) was used for the quantitative determination of total protein concentration in human

plasma in range of 30 to 120 mg/mL by a timed-endpoint biuret method. In the reaction, the protein sample bind to cupric ions in an alkaline medium to form colored protein-copper complexes. The system automatically proportions the plasma sample and cupric reagent with a ratio of 1:50 into a cuvette. The System monitors the change in absorbance at 560 nm. This change in absorbance is directly proportional to the concentration of Total Protein in the sample and is used by the System to calculate and express the Total Protein concentration.

SYNCHRON^{TM} LX20 System Micro Total Protein Assay (Beckman Coulter, USA) was used for the quantitative determination of total protein in plasma at low protein concentration by fixed time-endpoint method. Such measurements are limited to the concentration range of 0.06 to 3.0 mg/mL. Plasma protein in the sample reacts with the Pyrogallol Red-Molybdate complex to form a purple color that has a maximal absorbance at 600 nm. The system automatically apportions the sample and the complex reagent with a ration of 1:60 into a cuvette. The system monitors the change in absorbance at 600 nm at a fixed-time interval. The change in absorbance is directly proportional to the concentration of protein in the sample and is used by the system to calculate and express the protein concentration.

2.5 Immunoaffinity subtraction chromatography: IgY-12

In biomarker discovery using plasma sample, the presence of very high abundance proteins and the complexity of plasma proteins present formidable challenges. Twelve of the most highly abundant proteins comprise up to 96% of the total protein mass from human plasma, with serum albumin comprising approximately 40–50% of protein. It is thus necessary to maximize the concentration of the plasma proteome to detect proteins at low abundance. This can be achieved by optimization of protein separation methods as well as

selective depletion of the high abundance proteins. Antibodies IgG have been used successfully in various immunoassays. There is another class of immunoglobulins called IgY, which can be isolated from egg yolks of the lower vertebrates, such as birds, reptiles and amphibia. There are several attractive advantages of using chickens as the immunization host and their eggs as the sources for antibody isolation, such as remarkable immune responsiveness to mammalian antigens [Zhang 2003].

A commercial products ProteomeLab^{TM} IgY-12 LC2 Partitioning Kits (Beckman Coulter, USA) addresses this issue by reversibly capturing 12 of the most highly abundant proteins from human plasma, in particular serum albumin, total immunoglobulins G (IgG), transferrin, fibrinogen, total immunoglobulins A (IgA), α2-macroglobulin, total immunoglobulins M (IgM), α1-antitrypsin, haptoglobin, apolipoprotein A-I, apolipoprotein A-II, and α1-acid glycoprotein, yielding an enriched pool of low abundance proteins for further studies (Figure 2-2). The removal of target proteins by the immunoaffinity subtraction system and the overall process was reported to be highly reproducible [Huang et al. 2005; Liu et al. 2006].

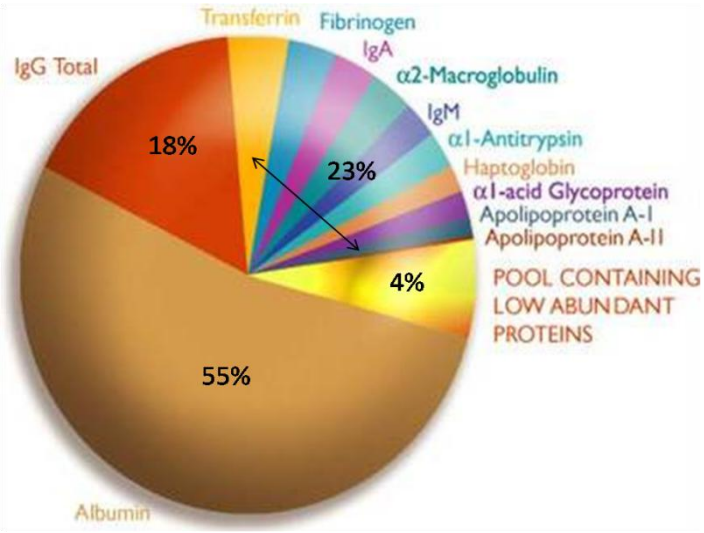

Figure 2-2: 12 high abundance proteins comprise up to 96 % of the protein mass in plasma. Low abundance proteins are pooled after immunodepletion for biomarker discovery. Figure obtained from Beckmann Coulter Report BR-9976A.

The IgY-12 Partitioning kits are based on affinity columns using avian antibody -antigen interactions and optimized buffers for sample loading, eluting, and regenerating. This technology enables removal of the 12 high abundance proteins from human plasma in a single step. The low abundance proteins in the flow-through fractions and the high abundance proteins in the bound fractions can be collected and further fractionated. One caveat of immunodepletion is that potential biomarkers that bind to serum albumin or high abundance proteins may also be completely or partially depleted from plasma samples through protein-protein interactions. However, this possibility can be evaluated with further analyses upon elution of the adherent protein fraction.

The technology uses physiological buffers for binding and washing, and avoids urea and other chaotropic agents for elution that can precipitate at low temperature. The enriched proteome, which includes medium and low abundance proteins, is the primary target for discovery and validation of biomarkers. The IgY-12 High Capacity LC12 affinity column (6.4 x 63 mm, affinity-purified chicken IgY polyclonal antibodies to 12 high abundance proteins are covalently conjugated through their Fc portion to 60 µm polymeric microbeads) requires liquid chromatography equipment with UV detector at 280 nm and has a capacity of 50 µL human plasma per cycle. The expected yield of a sample partitioned of the 12 high abundance proteins is about 400 µg. Under proper conditions of sample preparation and affinity chromatography, each column is capable of 100 cycles before replacement is needed. The expected volume of the flow-through fraction is 2.5-3.0 mL. The expected volume of the bound fraction is 3.5-4.5 mL. The applied method in detail: 50 µL plasma samples were diluted with 75 µL of Dilution Buffer (0.1 M Tris-HCl, 1.5 M NaCl, pH 7.4) to get a final volume of 125 µL. Any sample particulates and aggregates were removed by filtration through a 0.45 µm spin filter at 9200 xg for 1 min followed by injection of the diluted sample onto the column. After the enriched flow through fractions containing low abundance

proteins were collected, the bound and high abundance proteins were eluted with Stripping Buffer (0.1 M Glycine-HCl, pH 2.5). The column was then neutralized with Neutralization Buffer (0.1 M Tris-HCl, pH 8.0). Finally, the column was re-equilibrated with dilution buffer at a flow rate of 2 mL/min. Collected bound fractions were neutralized with neutralization buffer. The flow-through and eluted fractions were collected and stored at -80°C until further analysis. Concentration of the flow-through protein samples was performed with Amicon Ultra-4 centrifugal filter units with a cut-off of 5 kDa. After concentrating the flow-through protein samples to a minimum volume, ProteomeLab™ PF2D Stock Denaturing Buffer (7.5 M Urea, 2.5 M Thiourea, 12.5% Glycerol, 62.5 mM Tris-HCl, 2.5% (w/v) n-octylglucoside.) was added to give a final volume of 4.0 mL and samples were concentrated again. Finally, ProteomeLab™ PF2D Start Buffer (see Section 4) was added up to a final volume of 5.0 mL. Now the samples were ready for fractionation.

2.6 Two-dimensional protein fraction chromatography: PF2D

The ProteomeLab™ PF2D system (Beckman Coulter, USA) uses two-dimensional liquid chromatography, which separates proteins in the first dimension using chromatofocusing followed by in line reversed phase chromatography in the second dimension, thereby separating intact proteins based on their p*I* in the first dimension (1D) and on hydrophobicity in the second dimension (2D). The 32 Karat™ Software (Beckman Coulter, USA) was used for data processing and calculation of peak areas and heights. This two-dimensional approach was used to compare the plasma protein proteome from septic patients and healthy individuals and then determine if there were any qualitative and/or quantitative differences between these proteomes using the integrated DeltaVue™ software.

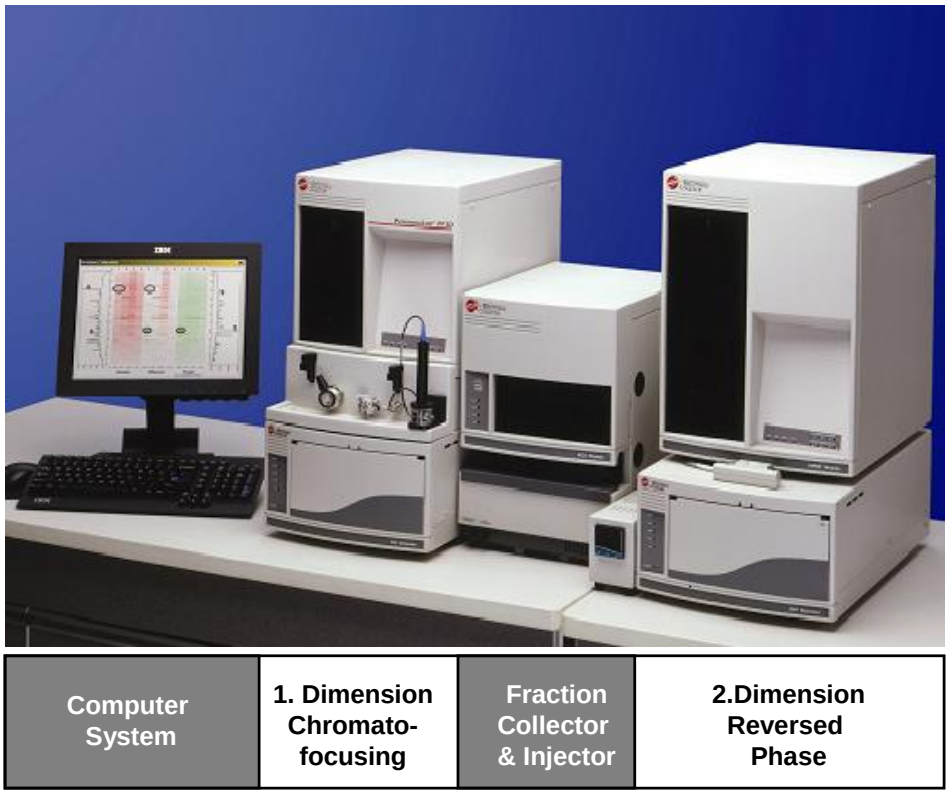

Figure 2-3: Beckman Coulter ProteomeLab™ PF2D System.

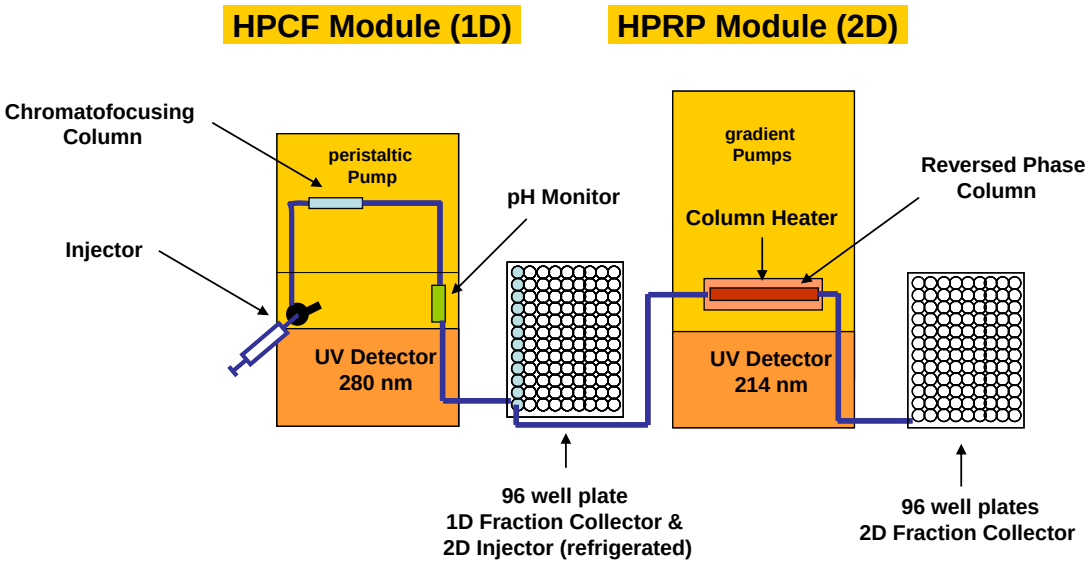

Figure 2-4: Schematic representation of the sample flow through the PF2D.

Figure 2-4 represents the sample flow through the ProteomeLab™ PF2D system beginning with a manual injection. For chromatofocusing in the first dimension a pH-gradient ranging from pH 4.0 to 8.5 was applied using Start Buffer (6M urea/ 0.2% octyl-glycoside/ 25 mM triethanolamine that is adjusted to pH 8.5 with saturated iminodiacetic acid) and Elute Buffer (6M urea/ 0.2% octyl-glycoside/ 10% Polybuffer™ 74 (GE Healthcare) that is prepared to pH of 4.0).

Proteins with p*I* values above 8.5 pass through the HPCF column (250 mm x 2.1 mm, 30 nm porous silica, Beckman Coulter), and proteins with p*I* values below 4.0 are eluted as fractions at the end using a high ionic wash buffer containing 1 M NaCl in 30% n-propanol and 70% water. Fractions covering 0.3 pH units are collected together in a 96 well polypropylene plate. Typically 30 fractions were produced in one run.

Each fraction from the first dimension is then separated by reversed phase using a C18 HPRP column (4.6 x 33 mm, 1.5 µm monomeric non-porous silica, Beckman Coulter) in the second dimension, with elution at 0.75 ml/min by a gradient of water (A) and acetonitrile (B) containing TFA of 0.1% and 0.08%, respectively. The gradient elution program was set as follows: 0%-0% B (0-2 min), 0%-100% (2-32 min), 100%-100% (32-36 min), 100%-0% (36-37 min). Detection was performed at room temperature by UV absorbance at 280 nm in the first dimension and at 50°C in a heated column jacket by UV absorbance at 214 nm in the second dimension.

A saturated iminodiacetic acid or ammoniac solvent was used for pH adjustment if required. Online pH measurement was performed as the eluent eluted from the column and before fraction collection using a pH electrode (Lazar Research, USA) where the separation was monitored at 280 nm using a Beckman 166 model UV detector (Beckman Coulter, USA).

2.6.1 1st Dimension separation, chromatofocusing

The chemistry components consist of the HPCF chromatofocusing column and four solvents, Start Buffer (pH 8.5), Eluent Buffer (pH 4.0), high ionic wash buffer (1 M NaCl in 30% n-propanol and 70% water), and water.The first dimension separation was done at ambient temperature with a flow rate of 0.2 mL/min, and absorbance of the column effluent was monitored at 280 nm by a UV detector, principally due to the presence of aromatic amino acids (tryptophan, tyrosine, and phenylalanine) and disulfide bonds.

Using the Direct Control mode of the software, the column was first equilibrated with 30 volumes (130 minutes) of Start Buffer. The method was then started with the injection of 3.5 mg of protein sample. 20 minutes after the sample was injected and the 280 nm absorbance baseline was achieved, the pH gradient was generated by starting the Eluent Buffer, which was done by the programmed switching of the solvent selector valve in the HPCF Module. When the effluent reached pH 4.0 at 140 minutes after the injection of sample, the column was washed with 10 volumes of high ionic wash buffer (45 minutes) followed by 10 volumes of water (45 minutes). These washes were programmed to take effect with the switching of the HPCF Module's solvent selector valve. During the pH gradient portion of the run, fractions at 0.3 pH intervals were collected as detected by the pH monitor, which controlled the fraction collection by the FC/I Module. During other portions of the run, fractions were collected by time at 8.5 min/fraction. The first dimension liquid fractions can be used immediately in the second dimension separation or stored at -80°C for later analysis.

2.6.2 2nd Dimension separation, reversed-phase

In the second dimension elution was monitored at 214 nm to increase the sensitivity of peptide and protein detection. The HPRP reversed-phase column was used with 0.1% TFA in water (Solvent A) and 0.08% TFA in acetonitrile

(Solvent B). The second dimension separation was done at 50°C with a flow rate of 0.75 mL/min and absorbance of the column effluent was measured at 214 nm by a UV detector, the necessary wavelength to detect the amide bond.

The column was first equilibrated with 10 volumes (8 minutes) of 100% Solvent A prior to each injection. From each 1D fraction, 250 µL were injected and, 2 minutes after injection, the column was eluted with a gradient of 0-100% Solvent B over 30 minutes. At the conclusion of this gradient, 100% Solvent B was maintained for five column volumes (4 minutes) prior to re-equilibration to 100% Solvent A. The second dimension liquid fractions can be used immediately for mass spectrometry or stored at -80°C for later analysis.

2.6.3 Proteome map representation by ProteoVue™ software

The second-dimension results can be imported into integrated ProteoVue™ software. It allows representation of second-dimension runs for one sample in a banded map display. Normally, the pH elution in 1D generates 30 fractions. All of these fractions were injected into the non-porous reversed phase column to separate proteins based on hydrophobicity by an increasing acetonitrile concentration. In consequence, in 2D, 30 RP chromatographic traces were obtained for a sample. The two dimensional ProteoVue profile organizes the RP chromatographic traces according to decreasing p*I* range on the horizontal axis versus retention time on the vertical axis, which from bottom to top describes increasing hydrophobicity of proteins. Each lane represents the relative absorbance intensity based on UV detection at 214 nm of the second-dimension separation of respective CF fraction collected in 1D. Each stripe represents a peak on the corresponding chromatographic trace in 2D. Taken together, stripes in protein map two-dimensionally demonstrate the p*I* as well as retention time, intensity and width of peaks in the whole run. Stripes shade from red into blue in terms of decreasing intensity, whereas the background is shaded purple.

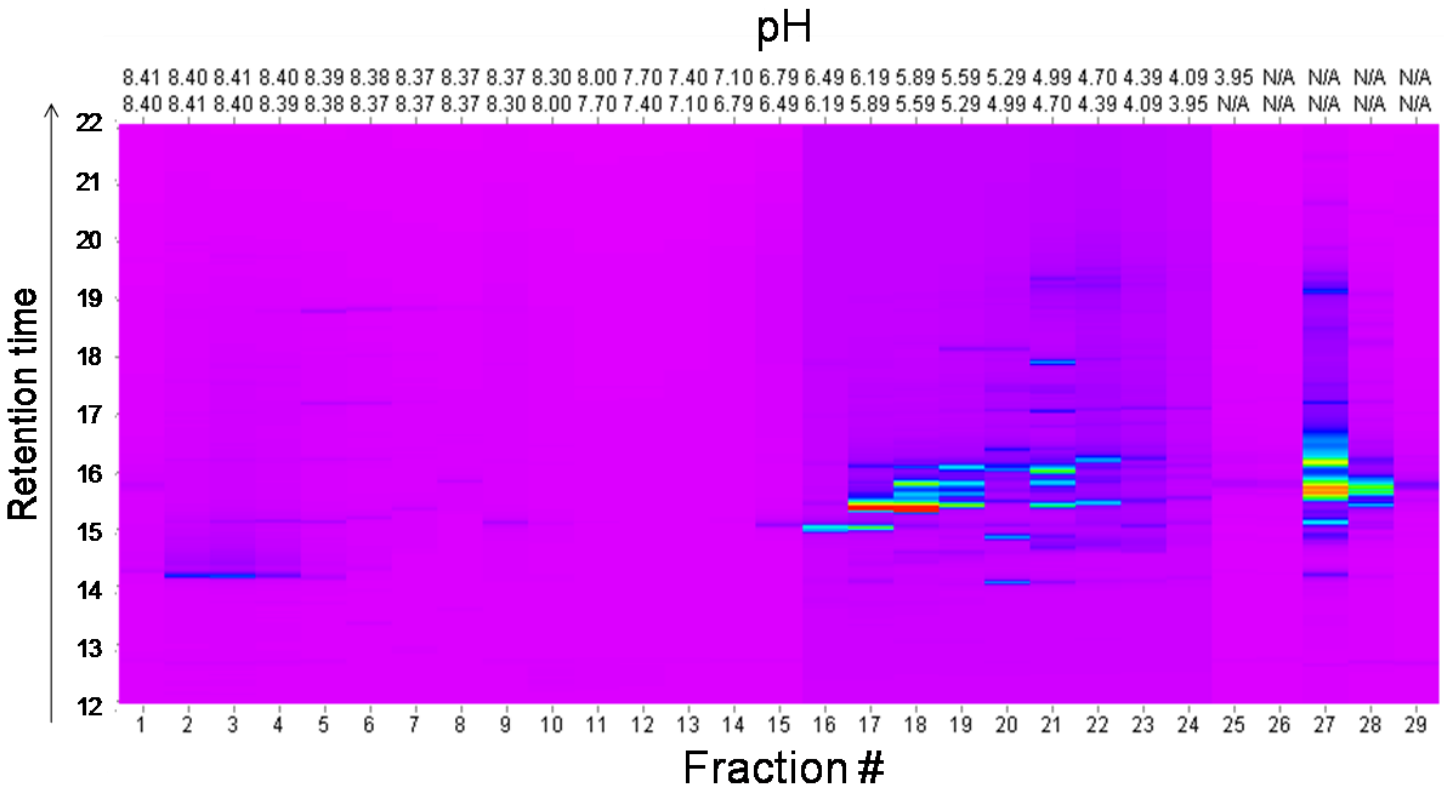

Figure 2-5: Representation of a typical ProteoVue imagination.

2.6.4 Differential image analysis by DeltaVue™ software

DeltaVue™ software compares two ProteoVue profiles of multiple second-dimension runs from two respective samples. DeltaVue allows side-by-side viewing of the second-dimension runs to show the difference map between the corresponding p*I* lanes in the middle. The lanes in the middle display in red or green, indicating whether the corresponding peaks from left or right samples are higher, respectively.

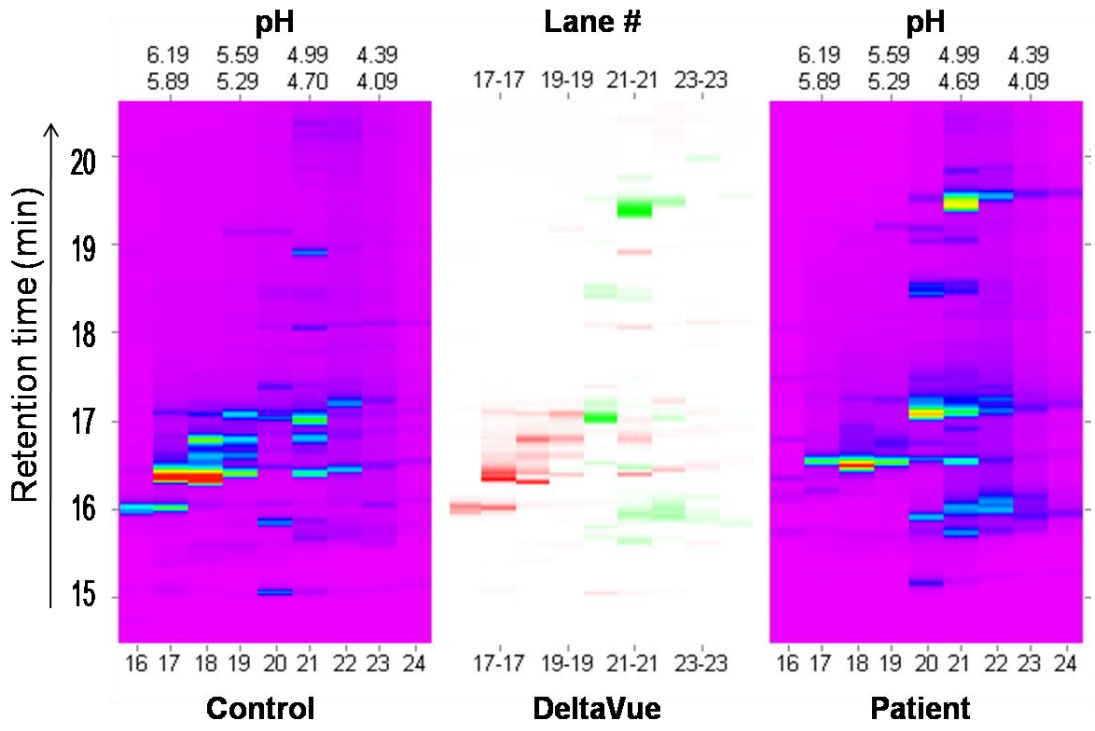

Figure 2-6: Representation of a typical DeltaVue interface between two individual ProteoVue profiles, typically Control (left, red) and Patient (right, green) samples.

2.6.5 High throughput comparison by MultiVue™ software

Since only two ProteoVue profiles can be imported into DeltaVue at the same time, the comparison among more than three individual ProteoVue profiles becomes fussy and complicated. This gab is supplied by MultiVue™ software, which allows comparison in term of exact pI value among up to 10 individual ProteoVue profiles at one time, exhibiting excellent throughput capacity.

MultiVue organizes 2D chromatograms at given p*I* range from different ProteoVue profiles in parallel without differential imagination like DeltaVue feature. The other shortcoming of the MultiVue feature is that only the fractions located in pH gradient are able to be imported in. Thus, comparison among the fractions before and behind pH gradient can only be performed using DeltaVue™ software as described above.

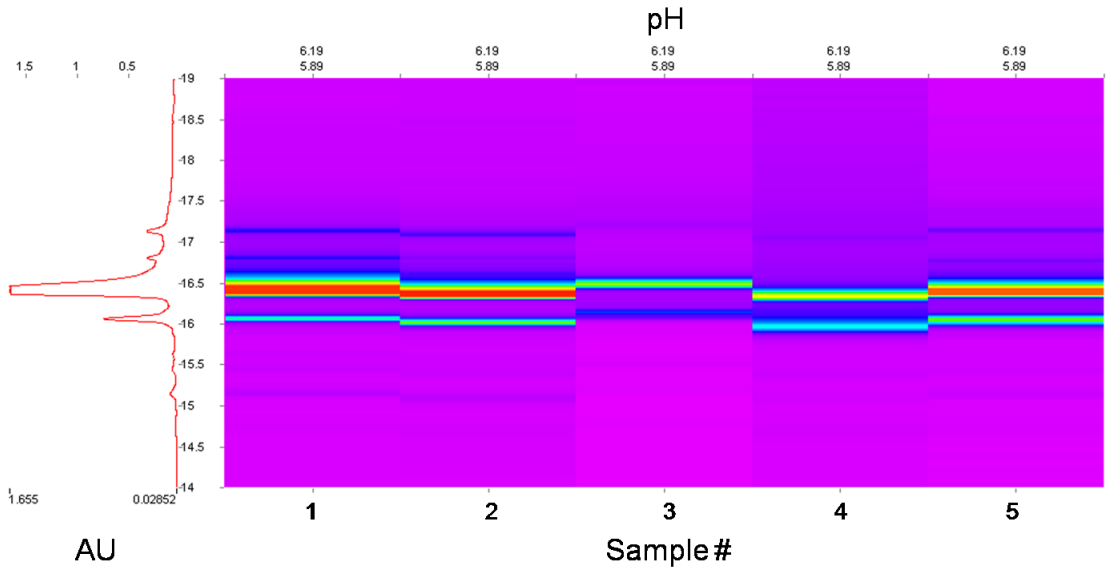

Figure 2-7: Representation of a typical MultiVue interface from five individual ProteoVue profiles at given p*I* range.

2.7 Sample preparation for MS analysis

Fractions of interest were transferred to a polypropylene microfuge tube for subsequent digestions. The microwell was rinsed with an equal volume of 95% acetonitrile - 5% water and combined with the fraction in the microfuge tube. Using a speed-vacuum centrifuge, samples were evaporated to a final volume of 10 µL. Subsequently, 17 µL of ammonium bicarbonate and 8.5 µL of DTT were added. Samples were placed in a water bath at 60°C for 1 hour after vortexing for 15 seconds. 3.5 µL of trypsin were added after cooling down the samples to room temperature. Capped samples were placed in a water bath at 37°C for 14-16 hours. Afterwards, samples were sonicated for 5 seconds and another 3.5 µL of trypsin were added. After vortexing for 5 seconds and centrifuging for 5 seconds sample vials were placed again in the 37°C water bath for another 8-10 hours. To stop the reaction, formic acid was added to a final concentration of 0.1%. At this point the samples could be stored at - 80°C till MS analysis.

2.8 nanoLC-MS/MS and data analysis

The mass spectrometric analysis of the samples was performed using a API QSTAR^{TM} Pulsar QqTOF instrument (Applied Biosystems, Germany). An Ultimate nano-HPLC system (Dionex, Germany), equipped with a nano C18 RP column (75 µm inner diameter, 150 mm length, Pep-Map C18 beads, 5 µm, 100 Å pore size) was connected on-line to the mass spectrometer through a Protana nanospray source. Injection of 20 µL tryptic digest was done by a Famos autosampler (Dionex, Germany). Automated trapping of the sample was performed at a flow rate of 30 µL using a Switchos module (Dionex, Germany).

Separation of the tryptic peptides was achieved with a 50 min 5%-50% buffer

B (80% acetonitrile/ 0.045% formic acid) gradient. Solvent A was water with 0.05% formic acid. The gradient was applied with a flow rate of 200 nL/min. The column was connected to a nanoemitter (New Objective, USA) and the eluent sprayed towards the orifice of the mass spectrometer using a potential of 2800 volte. A survey scan was combined with two data dependent MS/MS scans utilizing dynamic exclusion for 20 seconds. Tandem mass spectra were obtained using nitrogen as CID gas at collision energies that were set automatically depending on the mass and the charge of the precursor ion.

The sequences of the peptides were obtained after transfer of the MS/MS data to the MASCOT software. Searches were performed in human protein database (MSDB), which is a comprehensive, non-identical protein sequence database maintained by the Proteomics Department at the Hammersmith Campus of Imperial College London (MSDB release 20063108). The standard search parameters for MASCOT search engine were the following: MS/MS ion search; trypsin; monoisotopic; unrestricted protein mass; 200 ppm peptide mass tolerance; 0.15 Da fragment mass tolerance; maximal one missed cleavage; instrument type ESI-Quad-TOF. Each charge state of a peptide was considered as a unique identification. MS/MS spectra of proteins identified with less than two peptides were confirmed by manual data interpretation using Analyst QS. Output results were combined together using customized software to yield protein list and to delete keratins, titins and the redundant proteins.

Large scale shotgun proteomics projects routinely generate thousands to millions of tandem mass spectra. Efficient, sensitive and specific algorithms are required to correlate these spectra to peptide sequences in protein databases. A number of algorithms have been published and they can be sorted into three major categories: descriptive, interpretative and probability-based models. SEQUEST and MASCOT are the most widely used search engines and they are representatives of descriptive and

probability-based modes, respectively. MASCOT search algorithm uses a probability-based MOWSE scoring algorithm that uses mass spectrometry data to calculate and report probability-based Ions score for each peptide and to identify proteins from primary sequence databases. Probability is calculated based on the match between observed experimental data and the database sequence and that it is a random event. The significance of this match is calculated based on the size of the sequence database.

The experimental mass values are then compared with calculated peptide mass or fragment ion mass values, obtained by applying cleavage rules to the entries in a comprehensive primary sequence database. By using an appropriate scoring algorithm, the closest match or matches can be identified. If the “unknown” proteins in the sequence database, then the aim is to pull out that precise entry. If the sequence database does not contain the unknown protein, then the aim is to pull out those entries which exhibit the closest homology, often equivalent proteins from related species.

3 Results

3.1 Plasma sample immunodepletion using IgY-12

ProteomeLab™ IgY-12 LC2 immunoaffinity chromatography based on IgY-12 technology was used to selectively remove 12 of the high abundance proteins in human plasma. 50 µL of plasma sample was processed during one chromatographic cycle. Total protein content yields from the flow-through fractions were around 350 µg for normal plasma samples and around 250 µg for sepsis diseased samples, respectively. Accordingly, it took at least 10 cycles for the former and 15 cycles for the latter, achieving the maximum resolution in protein fractionation using the PF2D system that 3.5 mg of immunodepleted plasma proteins were routinely used for biomarker discovery.

One caveat of immunodepletion is that potential biomarkers that bind to serum albumin or other high abundance proteins may also be completely or partially depleted through protein-protein interactions. This potential for co-depleting non-target proteins was evaluated with MS analyses upon the flow-through and bound fractions of IgY-12 chromatography and to determine the specificity of protein separation.

Furthermore, the sepsis diseased plasma samples exhibit quite different protein content against the normal condition, which could introduce new interference upon the current IgY-12 technology. Consequently, a feasibility study concerning IgY-12 column performance on 1) the recovery of the low abundance proteins, and 2) binding of non-target proteins to the column in two different conditions were validated.

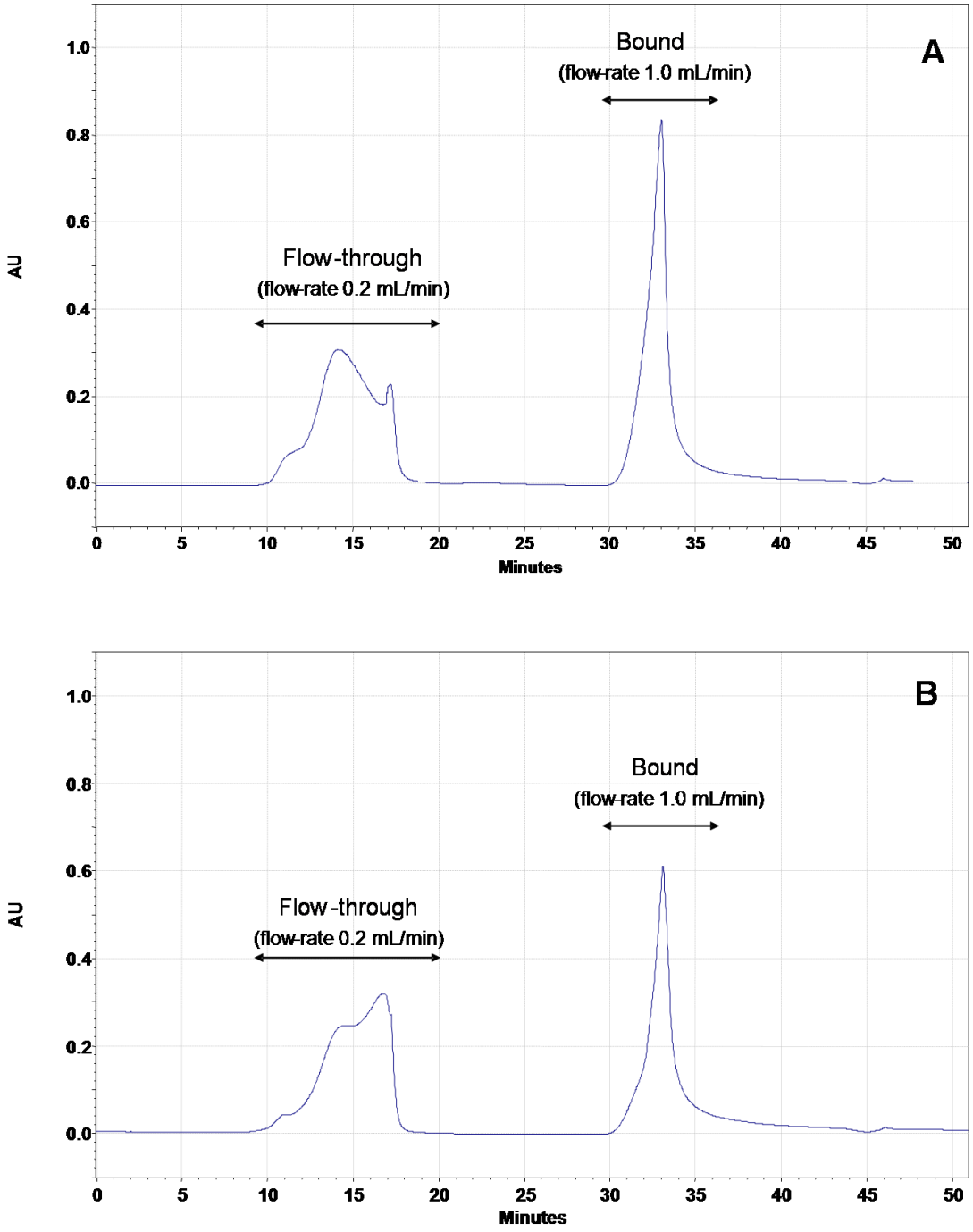

Figure 3-1: Chromatography of immunodepletion of normal (A) and sepsis diseased (B) plasma samples using ProteomeLab™ IgY-12 LC2 kit. 50 µL of human plasma was partitioned at an absorbance of 280 nm. The Flow-through (10-18 min) as well as Bound (30-35 min) were collected and used for further analysis with PF2D.

3.1.1 Estimation of recovery of the low abundance proteins

Plasma samples of three healthy individuals and five patients were subjected to ProteomeLab™ IgY-12 LC2 column from 13 times to 18 times in consideration of achieving 3.5 mg total plasma protein for maximum resolution in the PF2D system. The raw plasma protein concentration was measured using UniCel™ DxC 800 Systems Total Protein Assay (Beckman Coulter, USA) and the protein content of the flow-through was estimated using SYNCHRON™ LX20 Systems Micro Total Protein Assay (Beckman Coulter, USA), according to the different concentration range.

Table 3-1: Validation of ProteomeLab™ IgY-12 LC2 chromatography based on estimation of protein recovery of the flow-through fractions. Three normal plasma samples Control 1-3 and five diseased plasma samples Patient 1-5 were analyzed. 50 µL of each sample were injected into the IgY-12 column. The protein content of samples and their respective flow-through (FT) were measured. The values are expressed as mean ± standard deviation.

Sample ID	Protein Conc. (µg/µL)	Total protein loaded (µg)	Protein in FT (µg)	Percentage of load in FT (%)	Repeated cycles (times)	Protein pooled from FT (mg)
Control 1	65.7	3285	368±8.5	11.2±0.3	13	4.8
Control 2	68.3	3415	356±33.5	10.4 ± 1.0	13	4.6
Control 3	67.1	3355	302±6.4	9.0 ± 0.2	15	4.5
Patient 1	41.6	2080	281±18.1	13.5± 0.9	18	5.0
Patient 2	40.1	2005	255 ± 8.8	12.7 ± 0.4	18	4.6
Patient 3	38.7	1935	277±19.7	14.3 ± 1.0	18	5.0
Patient 4	40.8	2040	255±13.9	12.5 ± 0.7	18	4.6
Patient 5	35.2	1760	231±10.0	13.1 ± 0.6	18	4.2

Even though these samples were run not sequentially, very similar protein recovery was constantly found in the flow-through fractions, 10% for control

samples and 13% for patient samples, respectively. Importantly, the mean percentage recovery of protein in the flow-through of each sample was very reproducible with only a 2% difference not only for the normal samples but also for the diseased samples: from 9% for the lowest Control 3 to 11.2% for the highest Control 1 as well as from 12.5% for the lowest Patient 4 to 14.3% for the highest Patient 3. As expected, protein content of the flow-through decreased as the amount of protein loaded for the chromatography decreased, showing approximately from 1.5 to 2-fold difference between Control and Patient samples, which corresponded well to their difference in raw plasma protein concentration.

3.1.2 Binding of non-target proteins on IgY-12 column

To investigate the extent of potential binding of non-target proteins to the IgY-12 column in detail, 3.5 mg of total plasma protein in a volume of 5 mL from bound fraction of normal and diseased samples were individually injected into PF2D to separate proteins according to their p*I* and hydrophobicity, nanoLC-MS/MS was used to analyze all of the protein peaks. Two important criteria used to obtain positive protein identifications were (1) each charge state of a peptide was considered as a unique identification and (2) MS/MS spectra of proteins identified with less than two peptides.

The bound fractions from two normal samples (Control 1 and Control 3) and two diseased samples (Patient 1 and Patient 5) were analyzed, respectively. Figure 3-2 exhibited the ProteoVue map of bound fraction from sample Control 1. All of the peaks/strips were trypticly digested for the further protein identification process using nanoLC-MS/MS. Proteins identified in the bound fraction demonstrated that they exclusively consisted of the 12 targeted abundance proteins, in addition to 8 non-target proteins: complement C3, zinc-α2-glycoprotein, apolipoprotein D, serum amyloid protein P, transthyretin, hemopexin, clusterin, and α2-HS-glycoprotein. These 20 proteins were identified in all of the other three samples under the same conditions and listed in Table 3-2.

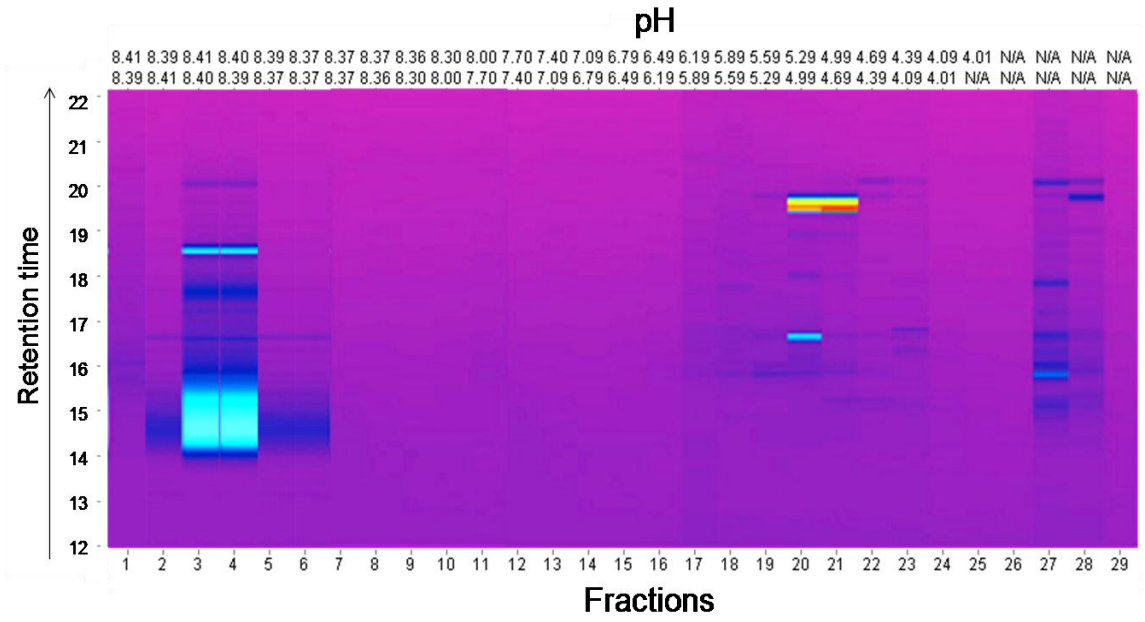

Figure 3-2: Representative 2D ProteoVue protein map of bound fraction from sample Control 1. 3.5 mg of protein from bound fraction were fractionated using ProteomeLab^{TM} PF2D system.

As example Figure 3-2 shows the most highly abundant immunoglobulins (IgG and IgM) that eluted immediately from the column were concentrated in fraction 1-6 during the basic wash (pH 8.5). It was shown that only the heavy and light IgG/IgM chains were detected in this region of alkaline p*I*.

As expected, most of the immunodepletion targeted proteins appeared in fraction 16-23 and 27-28 corresponding to the range of pH 6.5 to 4.0. As the most highly abundant protein in plasma, serum albumin spread a wider pH distribution because of different subunits and most of them were concentrated in the fraction 20 and 21 with the retention time of 19.8 min in RP chromatography. Importantly, it acts as a plasma carrier by non-specifically binding several hydrophobic steroid hormones and as a transport protein for hemin and fatty acids. This point might be the reason that a number of non-target proteins were bound onto serum albumin and simultaneously eluted during immunodepletion.

Remarkably, the most target and non-target proteins were eluted in RP chromatography between 15 and 20 min. Some of them exhibited identical or close retention times. Most of peaks in fact composed of a mixture of proteins, which could be 5 to 10 or even more proteins, indicating that most of the peaks are not well resolved in these complex chromatograms.

However, one important finding from this set of analyses for both normal and diseased samples is that, 8 non-target proteins were observed to bind to the IgY-12 column at similar levels, so that the fraction of binding for non-target protein to the column appeared to be reproducible. By doing replicate experiments of similar concentrations of plasma proteins, the column was also validated for its performance in real situations where every individual plasma sample differ in their protein content. No carry-over of proteins was detected in the flow-through of Patient 1 when followed by the chromatography of Control 5, which possessed much more protein content.

It was also observed no trace of proteins in the flow-through of injections that were run blank without samples followed by a few of the plasma sample runs. This shows the efficacy of the column reagents in the complete removal of all the highly abundant plasma proteins before the next sample injection and lack of cross contamination from run to run. This feature is critical for sequential depletion of clinical samples like plasma.

Table 3-2: Identification of 12 target proteins and 8 non-target proteins in bound fraction, which was demonstrated by the location in 1D fraction and the retention time of their dominating 2D fraction.

Protein name	1D Fraction Nr.	Retention time (min)
serum albumin	19/20/21/22/23/27/28	18/19/19.8
IgG*	2/3/4/5/6/27/28	15/17.6/18.5
transferrin	19/20/27	15.8
fibrinogen	22/27/28	16
IgA*	20/23/28	16.5/18
α2-macroglobulin	20/27	17.9
IgM*	2/3/4/5/6/27	14.5/17.2/20
α1-antitrypsin	22/23/27/28	20
haptoglobin	20/23/27/28	19.8
apolipoprotein A-I	18/20/27	16.3
apolipoprotein A-II	23/27	16.8
α1-acid glycoprotein	27/28	16
complement C3	22/23	16.8
zinc-α2-glycoprotein	20/21/22	15.8
apolipoprotein-D	28	15
serum amyloid protein P	23/27	16.2
transthyretin	20/21/23/27	14.8
hemopexin	21/22/23	19.8
clusterin	20/21	18
α2-HS-glycoprotein	23/27/28	16.2

* Proteins indentified in RP fractions with broad retention time distribution because of various heavy and light chains.

3.2 Two-dimensional Protein Fractionation using PF2D

The ProteomeLab^{TM} PF2D system separates peptides and proteins according to their p*I*s in the first dimension and hydrophobicity in the second dimension. The chromatographic profiles of identical pH fractions are then compared between control and diseased samples to detect protein expression differences. This approach requires that the formation of the pH gradient during the chromatofocusing elution step be highly reproducible from run to run. Attention must therefore be paid to the careful calibration of the on-line pH monitor and the pH adjustments of the start and elution buffers, ideally with standardized pH calibration buffers.

In order to achieve the maximum resolution and reproducibility in the first-dimension 3.5 mg of total plasma protein in a volume of 5 mL were routinely injected. This is about 1.5 mg of protein less than the specified binding capacity of the chromatofocusing column.

3.2.1 Reproducibility of PF2D system

The reproducibility of the first dimension separation was evaluated in terms of pH gradient formation. The second dimension separation was evaluated in terms of peak retention times on the reversed-phase column. It was found that in three consecutive chromatofocusing separations that the pH gradient differed by less than 0.1 pH units at any time during the elution step. Second dimension retention times of peaks from identical pH fractions differed by less than 6 sec in three consecutive separations. Using semi-automated software for peak-to-peak comparison between 2D-LC chromatograms, it was demonstrated that the peak concordance is very high. The rates of concordance were higher in the second dimension repeatability tests, indicating that the limiting factors for 2D-LC reproducibility rely on the p*I* fractionation and sample preparation steps. The reproducibility between maps was closely related to pH curves similarities, further stressing the need of careful pH adjustment and precise electrode calibration.

3.2.1.1 Reproducibility in terms of pH gradient formation in 1st dimension

The reproducibility in terms of pH gradient formation in 1st dimension (1D) of the PF2D system was tested by injecting diluted plasma samples three times onto the chromatofocusing column. The pH traces of three independent 1D runs detected by UV absorption at 280 nm are displayed in Figure 3-3. It demonstrates that in these consecutive separations during a period of 6 days the pH value of the elution gradient shifted scarcely in the range of pH 8.3 to 5.5 (70–115 min). Otherwise, relatively evident differences in the gradient were observed during the later part of the elution at pH values of less than 5.5 (115–150 min). But the shifts in the gradient less than 0.1 pH units were measured. It is not clear whether these small shifts were due to minor temperature differences between runs that were performed several days apart.

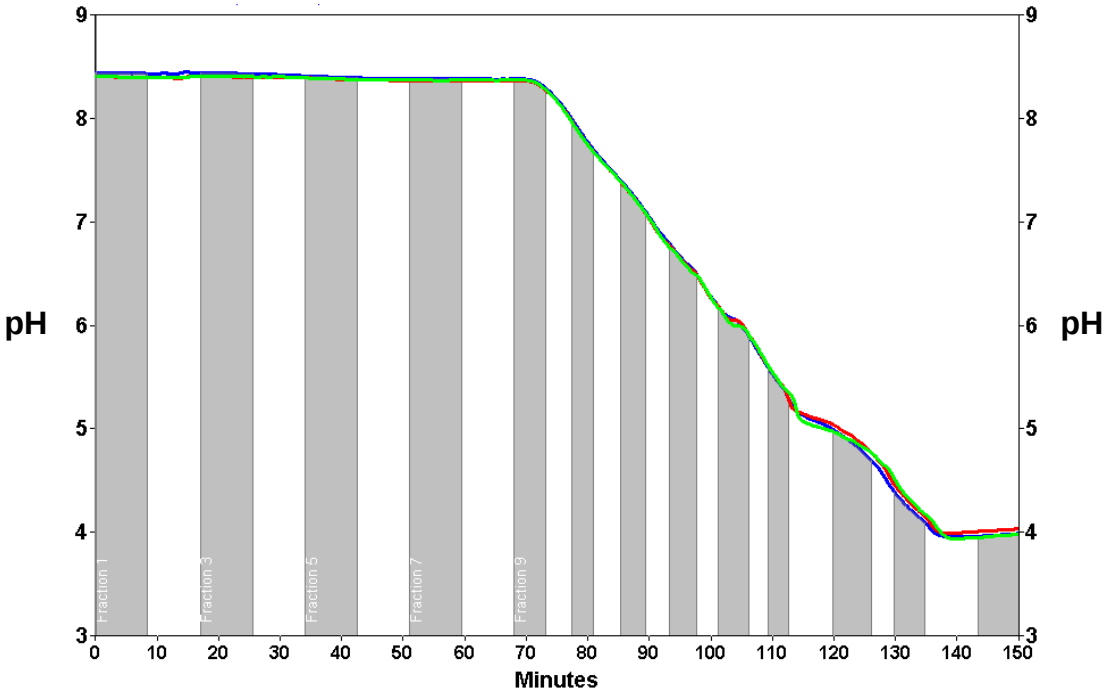

Figure 3-3: Reproducibility of the pH gradients in the first dimension separation process. pH gradients from three independent experiments (shown in red, green, and blue) generated during the chromatofocusing step. Gray-white strips represent the fractions limits, which start at pH 8.3 and end at pH 4.0.

It was consented that the reproducibility between runs was closely related to pH gradient similarities. No significant shift (< 0.1 pH unit) was found among those pH traces that overlapped together excellently. As conclusion, no pronounced effect on protein separation according to p*I* values from run to run should be taken into account. It is clear that protein separation based on chromatofocusing in the first dimension among these different samples is well performed and thus ensures the proteomic comparison in combination with further separation based on hydrophobicity in the second dimension and mass spectrometric identification.

3.2.1.2 Reproducibility in terms of peak retention time in 2nd dimension

To test for the 2nd dimension (2D) reproducibility, the respective 1D fractions in the range of pH 4.99-4.69 of the three independent experiments were used for a 2D fractionation. For a quantitative evaluation, four peaks of each run were selected based on variable peak height (Figure 3-4). Two highly abundant protein peaks (1 and 2) with intensities more than or near 0.5 AU as well as two lowly abundant protein peaks (3 and 4) with intensities less than or near 0.1 AU were analyzed with the MultiVue™ software. Table 4-3 indicates that peak retention times in the 2D differed by less than 0.06 min for both high and low abundance proteins. Differential protein expression profiling with the PF2D platform is based on peak height as well as peak area comparisons with the MultiVue™ software.

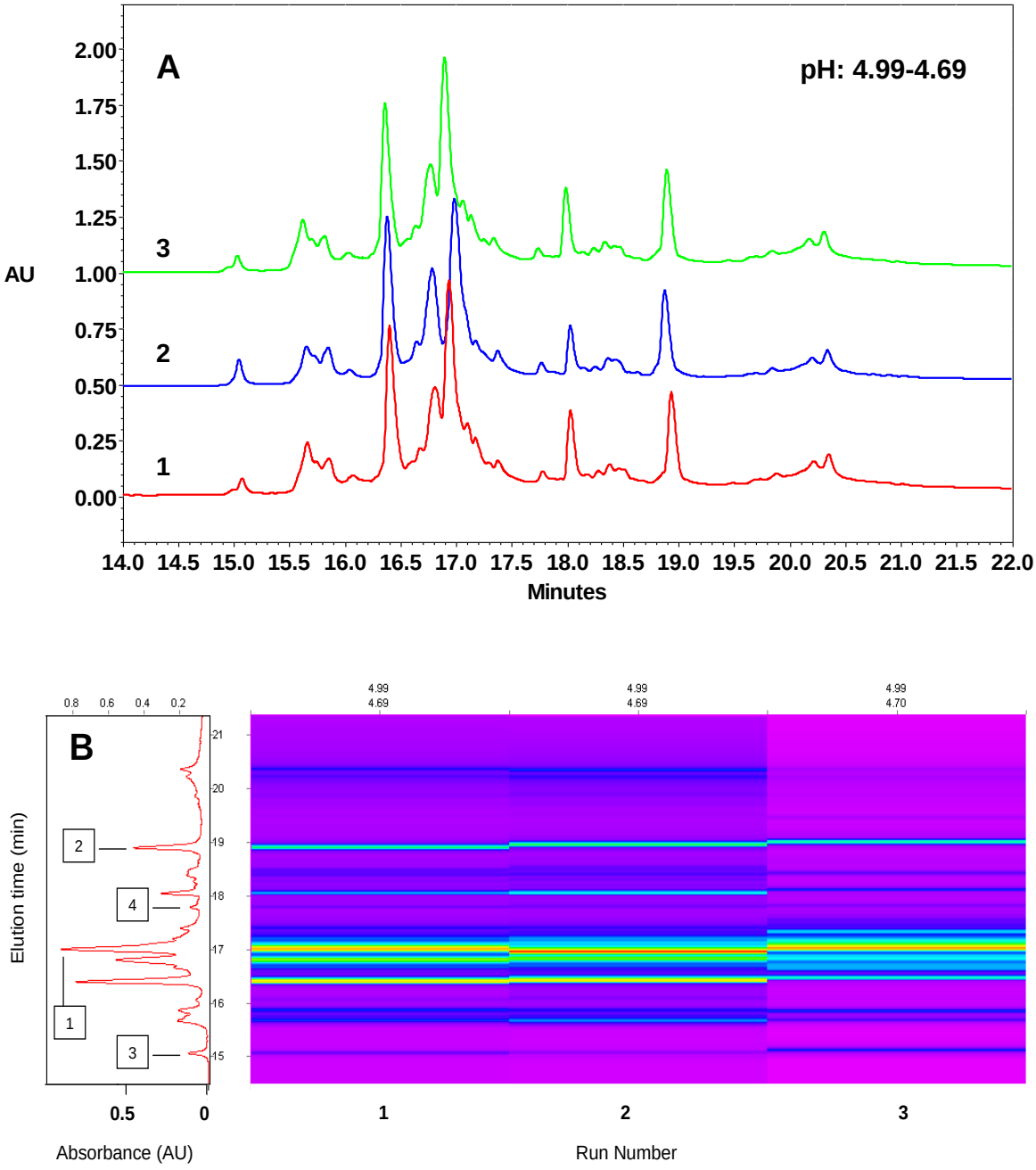

Figure 3-4: Reproducibility of the 2D separation method for p*I* fraction 4.99-4.69. (A) Three independent RP traces have been offset by 0.5 AU for clarity and (B) their respective 2D chromatograms were generated from second dimension separations. Identical p*I* fractions were imported for display into MultiVue^{TM} software for side by side comparison. Four peaks were selected based on variable peak height.

Table 3-3: Quantitative analysis of selected 2D chromatography peaks from p*I* fraction 4.99-4.69. Peaks were analyzed with the integration tools provided in the MultiVue™ software.

Peak No.	Run No.	Retention time (min)	Peak height (AU)	Peak area
1	1	17.0	0.822	7.003
	2	16.94	0.951	6.836
	3	17.06	0.904	7.711
Mean	-	17.0	0.892	7.183
Standard deviation	-	0.04	0.047	0.352
Coefficient of variation (%)	-	0.24	5.3	4.9
2	1	18.89	0.407	2.882
	2	18.94	0.441	3.388
	3	19.04	0.461	3.651
Mean	-	18.96	0.436	3.307
Standard deviation	-	0.06	0.019	0.283
Coefficient of variation (%)	-	0.32	4.4	8.6
3	1	15.06	0.114	0.624
	2	15.08	0.083	0.543
	3	15.16	0.125	0.693
Mean	-	15.10	0.107	0.62
Standard deviation	-	0.04	0.016	0.051
Coefficient of variation (%)	-	0.26	14.9	8.2
4	1	17.78	0.089	0.840
	2	17.78	0.094	1.012
	3	17.86	0.116	1.071
Mean	-	17.81	0.1	0.974
Standard deviation	-	0.04	0.011	0.090
Coefficient of variation (%)	-	0.22	11	9.2

Table 3-3 indicates that the coefficients of variation of height for highly abundant protein peaks (1 and 2) were found to be less than 6%, whereas lowly abundant protein peaks (3 and 4) had coefficients of variation between 10% and 15%. Similar outcome was obtained for quantitative analysis of the respective peak area. These values indicate that protein expression differences between normal and diseased samples should be at least 30%, which corresponds to a double value of the inherent variation, in order to be reliably detected with this approach. Furthermore, MS analysis of these peaks has shown that identical proteins/peptides were identified from the three respective RP fractions. In conclusion, the results indicate that the second dimension is repeatable enough to detect small changes in peak intensities.

3.3 Normal plasma Proteome R as control

Plasma samples from three healthy individuals were analyzed by IgY-PF2D-nanoLC-MS/MS approach, the common proteins were regarded as normal plasma proteome as reference (Proteome R). Figure 3-5 shows the chromatofocusing profiles of three distinct normal plasma samples and the pH trace. Protein elution is monitored by absorbance at 280 nm using a UV detector in the first dimension, principally due to the presence of aromatic amino acids (tryptophan, tyrosine and phenylalanine) in proteins. As consequence, only high abundance proteins that contain a large number of aromatic residues such as serum albumin, total immunoglobulins and Transferrin were detected, resulting in chromatograms in the first dimension with a limited number of peaks. As shown in Figure 3-5, the pH trace composes of three stages, which was done by the programmed switching of the solvent selector valve in the first dimension. The first stable baseline (0-70 min) is generated using Start Buffer (pH 8.5) for column equilibration. The pH gradient (70-135 min) ranging from 8.5 to 4.0 was established by starting the Eluent Buffer (pH 4.0). When the pH 4.00 at 135 min

was reached, the column was washed with high ionic solvent to elute all the tightly bound proteins inside the column during basic and gradient wash. According to this pH elution strategy the plasma proteins were correspondingly eluted into three major regions. As described in the previous section, all of the immunoglobulins, located in the first region between 0 to 40 min, which should be up to 95% depleted using IgY immunoaffinity subtraction chromatography according to the manufacturer´s evaluation. The faint peak in the first 40 min of chromatofocusing profile indicated the presence of such non-depleted remnant. Next is the region between 90 to 140 min, where the presence of numerous peaks clearly demonstrated the separation based on p*I*s. At the end of the profile from 165 to 180 min the most intense peaks are located, which were eluted into two fractions.

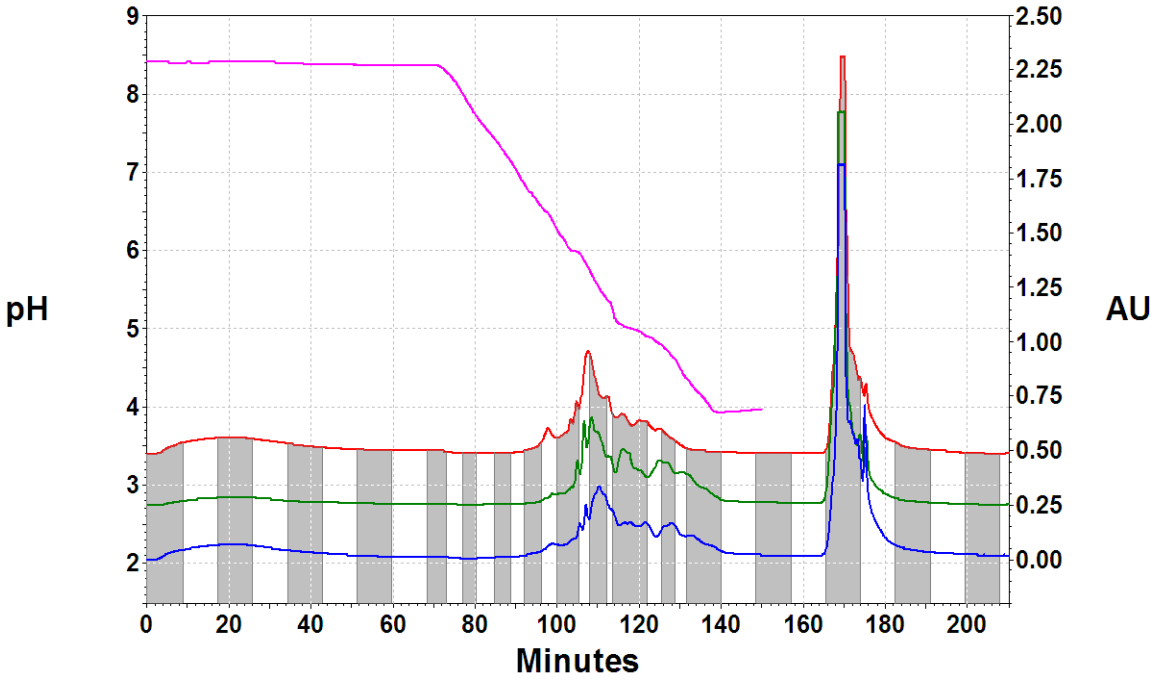

Figure 3-5: Representation of chromatofocusing profiles of three normal plasma samples detected by UV absorbance at 280 nm and pH trace in the first dimension. The chromatograms have been offset by 0.25 AU for clarity. All the fractions are viewed in gray and white stripes one after the other.

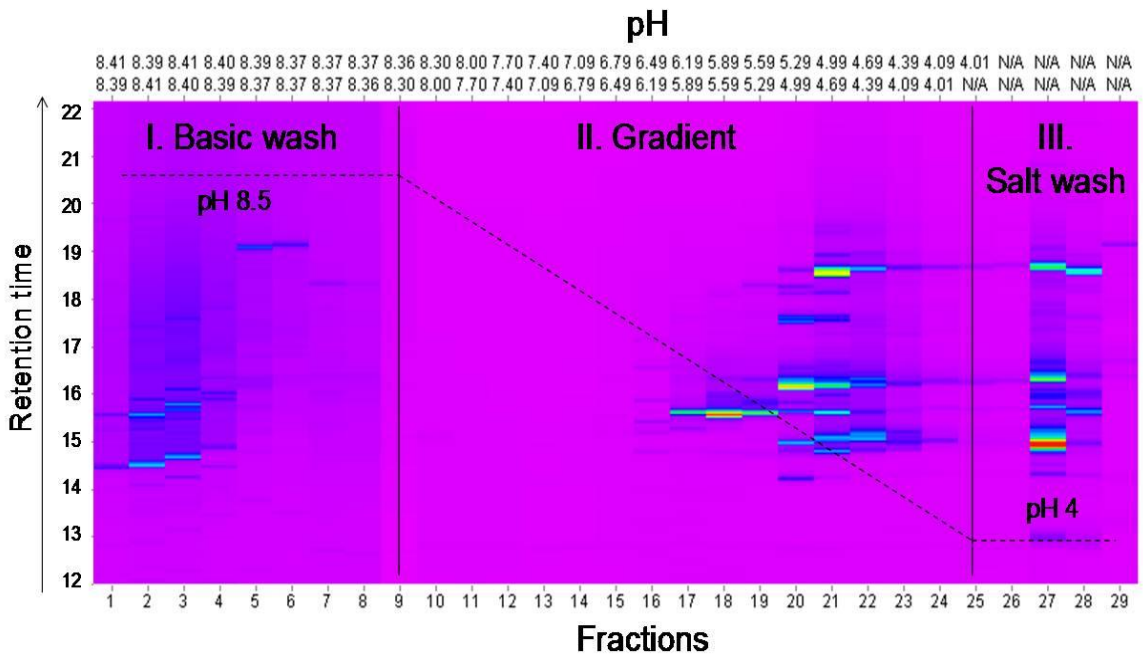

Figure 3-6: Representative 2D ProteoVue profile of a normal plasma sample (Control 2) with depletion of high abundance proteins as example. At the top of each lane is the starting and ending pH of each the first dimension fraction. N/A means that the exact pH of fractions during salt wash is not available and was thus generally considered as pH 4.0.

Figure 3-6 shows a two-dimensional immunodepleted plasma protein map of a healthy volunteer utilized as control. According to the chromatographic traces in Figure 3-5, the display of the proteome consists correspondingly of 3 regions. Each lane represents the relative absorbance intensity based on UV detection at 214 nm of the second-dimension separation of each fraction collected in the first dimension (stripe shades from red into blue in terms of decreasing intensity and purple as background). The first one is the basic wash period, where the separation of the extreme basic proteins on the first dimension. Next is the region of the pH gradient, where the separations by p*I* revealed a superior resolution demonstrated by the presence of numerous strips. Some strips are observed with identical elution times in adjacent lanes, which may indicate the separation of fractions for the first dimension splits an individual protein between two fractions. The third is the salt wash period, which also presents a very complex set of two major fractions indicative of minimal separation in the first dimension. Figure 3-6

also shows that most plasma proteins eluted between 15 to 21 min, corresponding to acetonitrile concentrations between 40% and 60% (v/v). This reflects the narrow range of hydrophobicity among plasma proteins.

Full scan analysis of these protein maps was performed by nanoLC-MS/MS after tryptic digestion. As expected, a great number of plasma proteins were identified using the combination of tandem MS and database searching. Most proteins were detected based on correlations of the MS/MS data for multiple unique peptides to the protein sequence, such matches were considered as valid identifications. In addition, the database searches also retrieved proteins for which less than three peptides were matched. To confirm or to rule out the identification, these peptides matches were examined manually using Analyst QS according to the following criteria: (i) a good-quality MS/MS spectrum with most of the abundant product ions assigned; (ii) a continuous stretch of the peptide sequence covered by either the y- or b-ion series; (iii) intense y-ions corresponding to a proline residue (if Pro was present in the sequence); (iv) approximately similar values of p*I* estimated from chromatofocusing (1D) and the theoretical p*I* (variation less than 2 pH units).

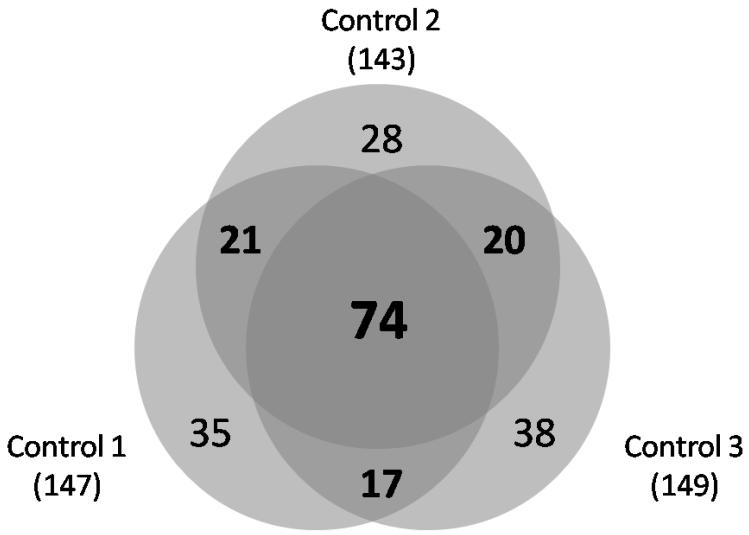

Figure 3-7: Diagram of proteins identified in immunodepleted plasma samples from three healthy individuals. All overlaps are shown (2-way in moderate grey and 3-way in dark grey) for full scan of all three plasma samples. Numbers represent the number of shared accessions in the respective overlapping areas.

A total of 233 distinct proteins were identified in plasma samples from three healthy individuals according to the above analysis criteria, as totalized in Figure 3-7. In particular, 74 proteins of them (32%) existed in all of the three full scan analyses, and 58 proteins (25%) were merely found in every two of the three individuals. Otherwise, altogether 101 proteins (43%) were respectively identified without overlapping to any other analysis.

On the other hand, around 145 distinct proteins were identified in each full scan analysis (147 proteins in Control 1, 143 proteins in Control 2, and 149 proteins in Control 3). Nearly 50% of the identified proteins in each analysis were also found in the other two independent analyses, leading to a triple overlapping. If the proteins with double overlapping were also taken into account, 76%, 80%, and 74% of proteins were identified by at least two independent analyses in Control 1, Control 2, and Control 3, respectively.

As consequence, 132 proteins from three healthy individuals were identified by double and/or triple determination with high reliability, which were regarded as the superior protocol of Proteome R. The other 101 proteins identified by simple determination were used as inferior protocol because of low data reliability. All these 233 proteins were arranged in increased alphabetic order in Supplemental Table 1. For the identical proteins with 2-way or 3-way overlapping, only the one with highest Mowse Score was listed.

3.4 Comparison of proteome between normal and diseased states

The differential proteomics strategy was adopted to identify different states of protein-expression between normal and diseased states. The approach based on ProteomeLab^{TM} PF2D system is typically rely on finding proteins that are more abundant in plasma obtained from disease-afflicted individuals than in healthy controls. In general, only those peaks which imaged with significantly increased expression in DeltaVue^{TM} software were noted, such peaks located fractions were analyzed using nanoLC-MS/MS in succession. According to the outcome of the treatment in patients, plasma samples from three survivors and two non-survivors at the first ICU day as well as at the last ICU day were analyzed, respectively (see section 2.2). Results from the healthy male individuals (controls) used as reference were summarized as Proteome R and significant differential protein-expression between patients and controls were summarized to generate sepsis-related subproteomes S1 (survivors, samples from day 1), S2 (survivors, samples from last day), N1 (non-survivors, samples from day 1) and N2 (non-survivors, samples from last day), respectively.

3.4.1 Difference between normal and diseased plasma at first ICU day

3.4.1.1 Generation of differential Proteome S1

The plasma samples at the first ICU day from Patient 1, 2, and 3 who finally survived were injected into PF2D after immunodepletion to generate ProteoVue profiles, respectively. The comparison of these diseased proteome profiles to control proteome was done with the DeltaVue^{TM} software for differential analysis.

To interpret the analysis process concisely, DeltaVue comparison of fractions 16 to 28 for Control 2 and Patient 1 was shown in Figure 3-8 and more detailed comparison at a given pH range 5.59-5.29 was shown in Figure 3-9 and

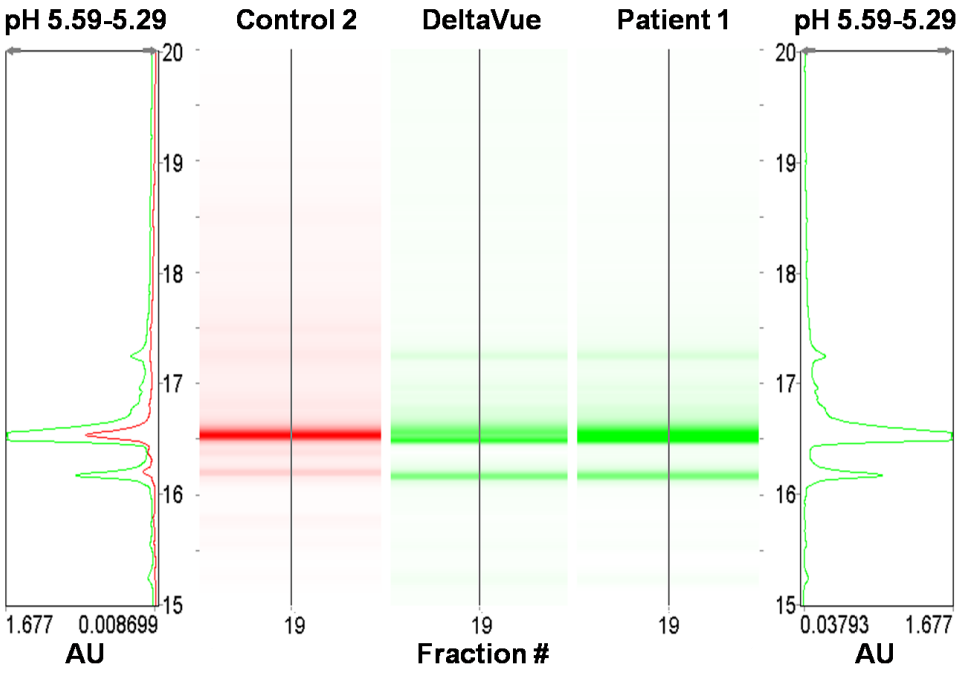

Figure 3-10 as example.

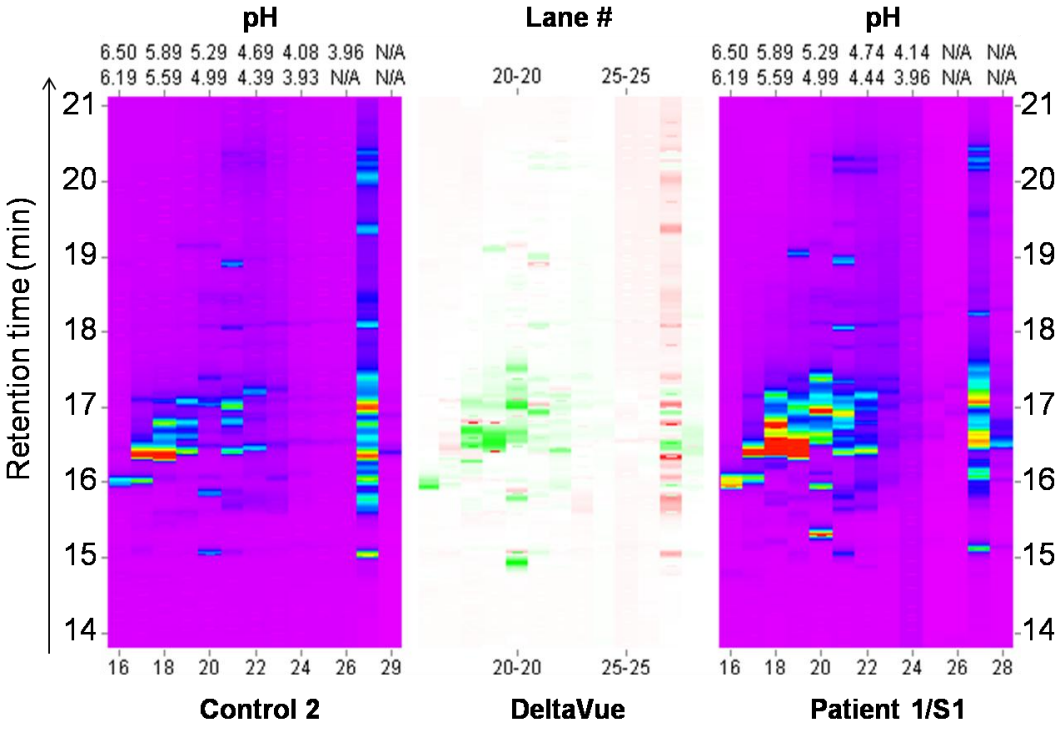

Figure 3-8: DeltaVue comparison of two-dimensional maps within fractions 16 to 24 for Control 2 and Patient 3 at the first ICU day.

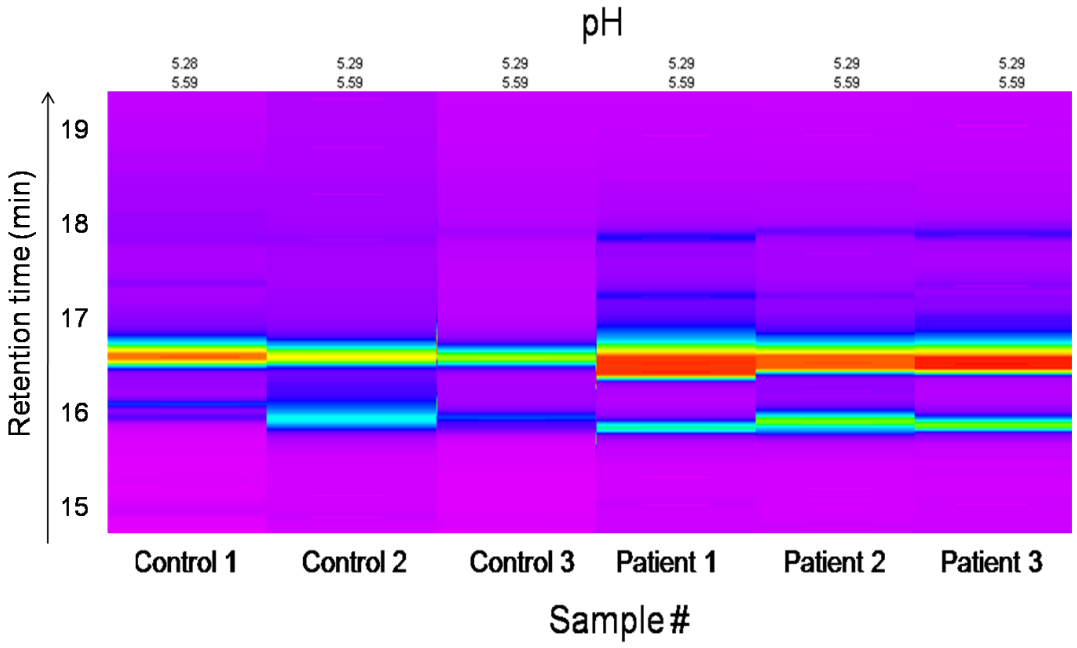

Figure 3-9: Significant difference in protein expression among Control samples and Patient samples 1, 2, 3 in pH fraction 5.59-5.29 displayed by MultiVue™ software.

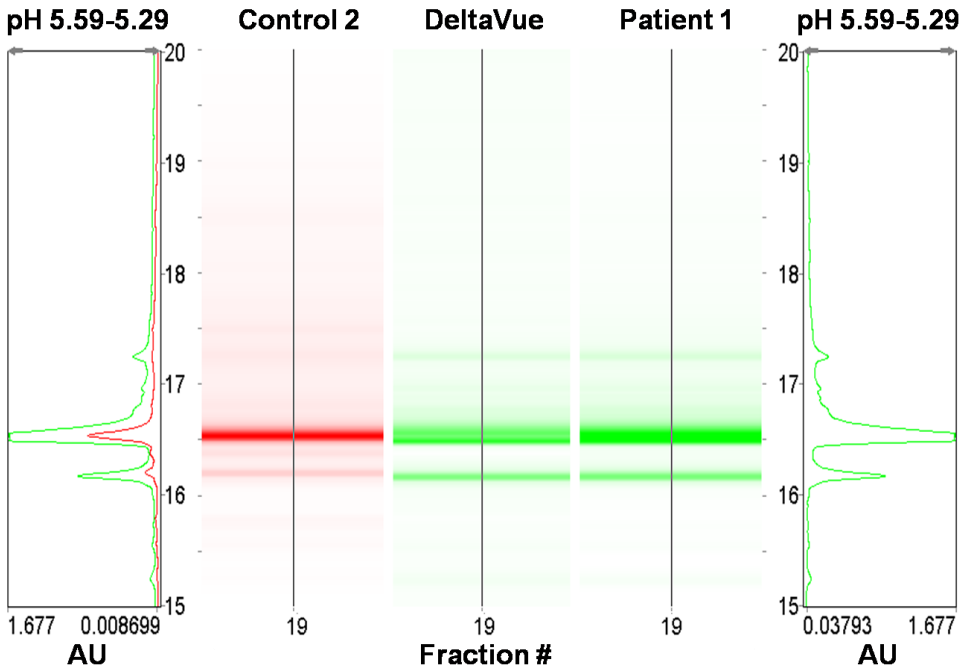

Figure 3-10: DeltaVue comparison of 2D profiles for Control 2 (red, left) and Patient 1 (green, right) in pH fraction 5.59-5.29, which corresponds to Lane 19. The right chromatographic view was overlaid in left graph display in order to demonstrate the difference between control and patient patterns more comparatively.

With the zoom feature enabled in DeltaVue^{TM} software, several significant differences can be observed between the two states of the plasma proteome in the middle panel in Figure 3-8. These significant differences located p*I* fractions were chosen for further fraction-by-fraction comparison such as lane 19, this corresponds to p*I* fraction between pH 5.59-5.29 and 2D retention time at 16.5 min.

According to the above described process, a total of 15 significantly increased peaks in all of the three diseased samples were analyzed with nanoLC-MS/MS, resulting in differential Proteome S1. A total of 64 distinct proteins in diseased samples were identified. As the result of comparison with Proteome R, 48 distinct proteins (75%) were cancelled out because of their presence in control samples. As a result, there are 16 distinct proteins that were only detected in diseased samples, considering at least two peptides hits for high evidence involved in all of the three diseased samples.

3.4.1.2 Generation of differential Proteome N1

The plasma samples at the first ICU day from Patient 4 and 5 who finally died were injected into PF2D after immunodepletion to generate ProteoVue profiles, respectively. The comparison of these diseased proteome profiles to control proteome was done with the DeltaVue^{TM} software.

As the same as the generation of differential Proteome S1 described in former section, a total of 11 significantly increased peaks in both diseased samples were analyzed with nanoLC-MS/MS, resulting in incomplete human plasma Proteome S2 based on differential proteomics. A total of 64 distinct proteins in diseased samples were identified. As the result of comparison with Proteome R, 50 distinct proteins (78%) were cancelled out because of their presence in control samples. As a result, there are 14 distinct proteins that were only detected in diseased samples, considering at least two peptides matched for high evidence involved in both diseased samples.

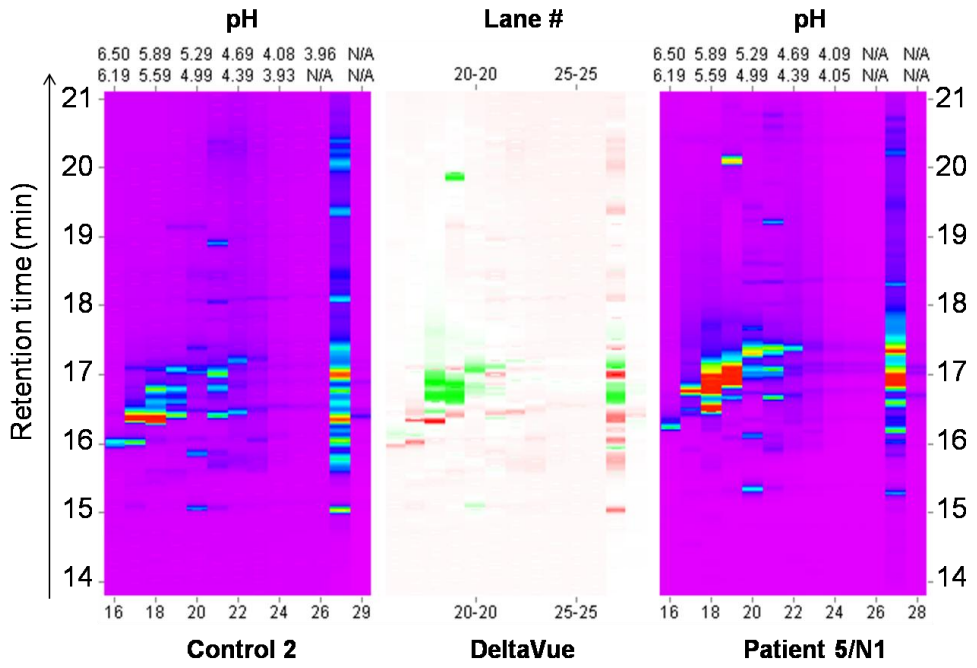

Figure 3-11: DeltaVue comparison of two-dimensional maps within fractions 16 to 28 from Control 2 and Patient 5 at the first ICU day.

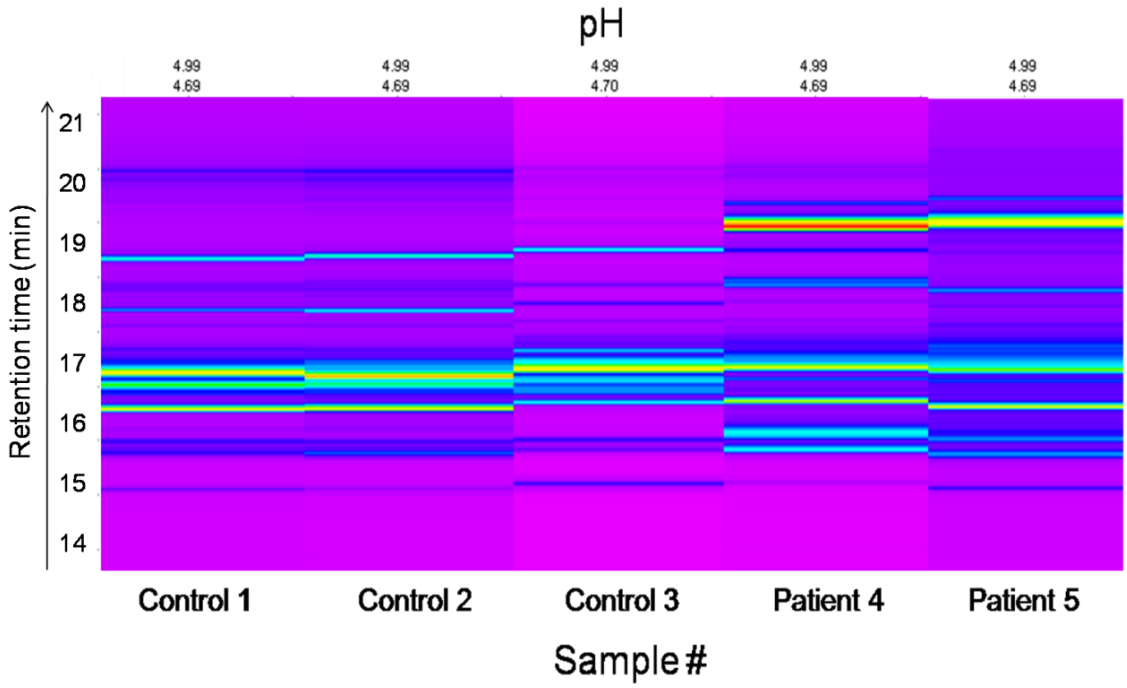

Figure 3-12: Significant difference in protein expression among Control samples and Patient samples 4, 5 in pH fraction 4.99-4.69 displayed by MultiVue^{TM} software.

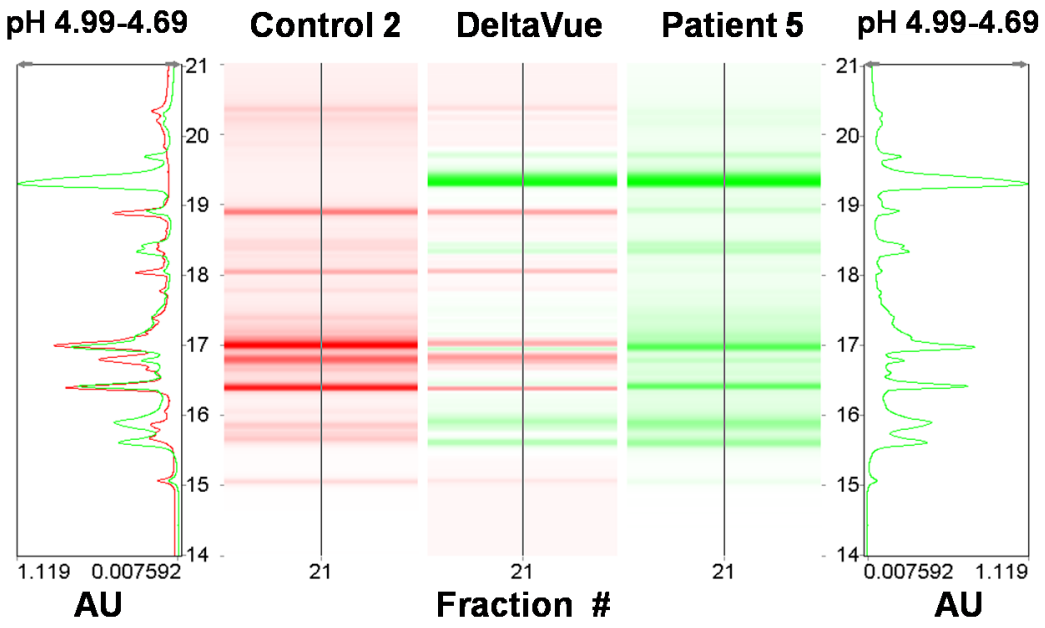

Figure 3-13: DeltaVue comparison of 2D profiles for Control 2 (red, left) and Patient 5 (green, right) in pH fraction 4.99-4.69, which corresponds to Lane 21. The right chromatographic view was overlaid in left graph display in order to demonstrate the difference between control and patient patterns more comparatively.

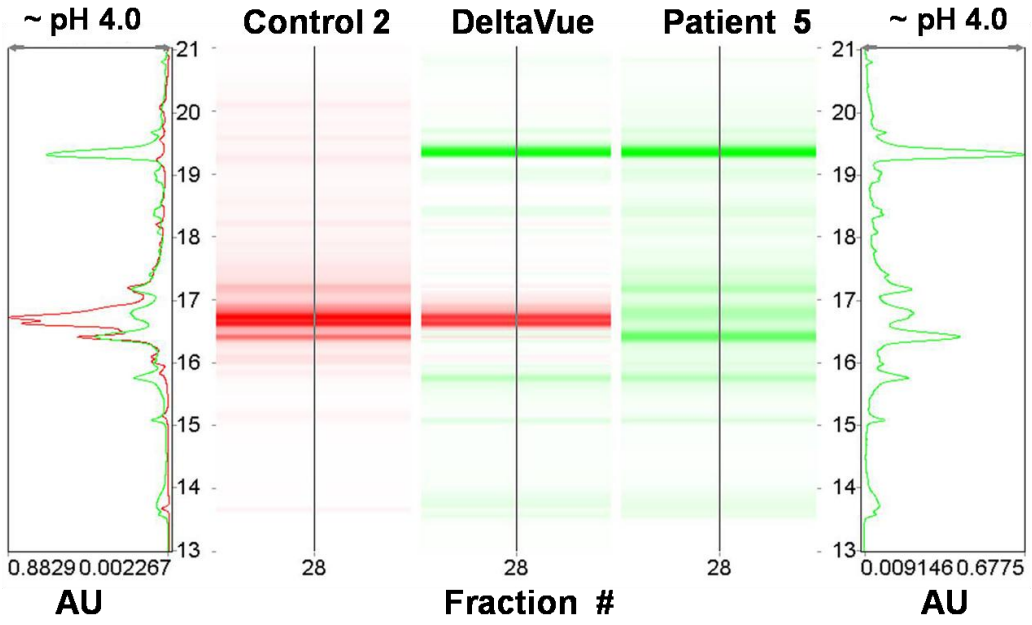

Figure 3-14: DeltaVue comparison of 2D profiles for Control 2 (red, left) and Patient 5 (green, right) in Lane 28.

3.4.2 Difference between normal and diseased plasma at last ICU day

3.4.2.1 Generation of differential Proteome S2

The plasma samples at the last ICU day from Patient 1, 2, and 3 who have diagnostically healed with the treatment were injected into PF2D after immunodepletion to generate ProteoVue profiles, respectively. The comparison of these diseased proteome profiles to control proteome was done with the DeltaVue™ software.

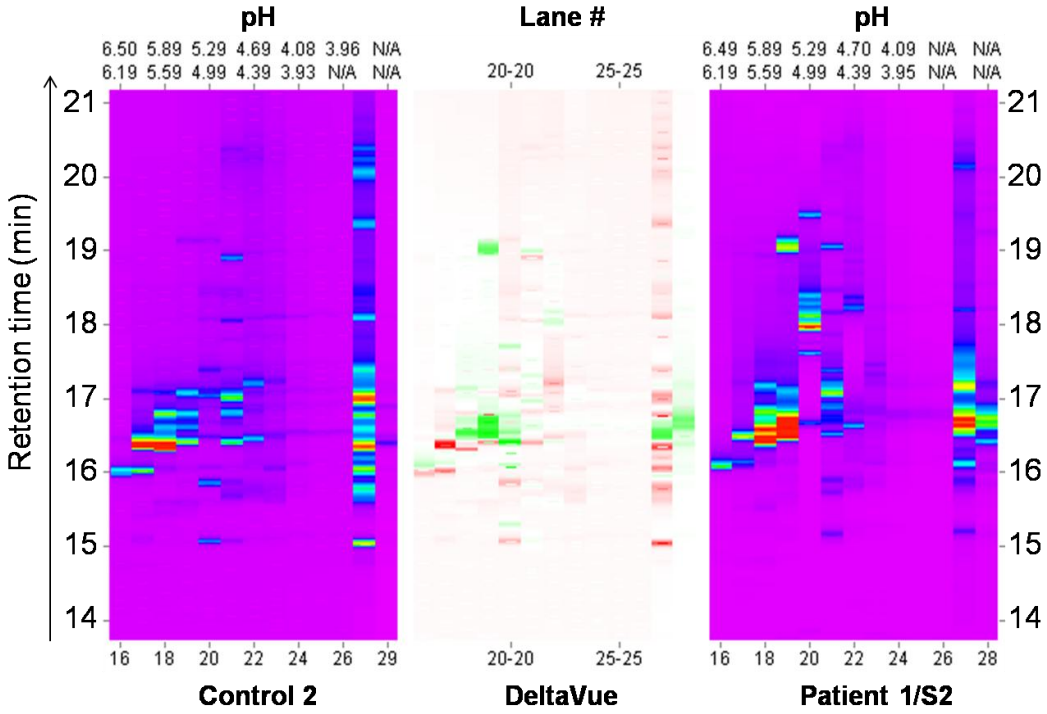

Figure 3-15: DeltaVue comparison of two-dimensional maps within fractions 15 to 29 from Control 2 and Patient 3 at the last ICU day.

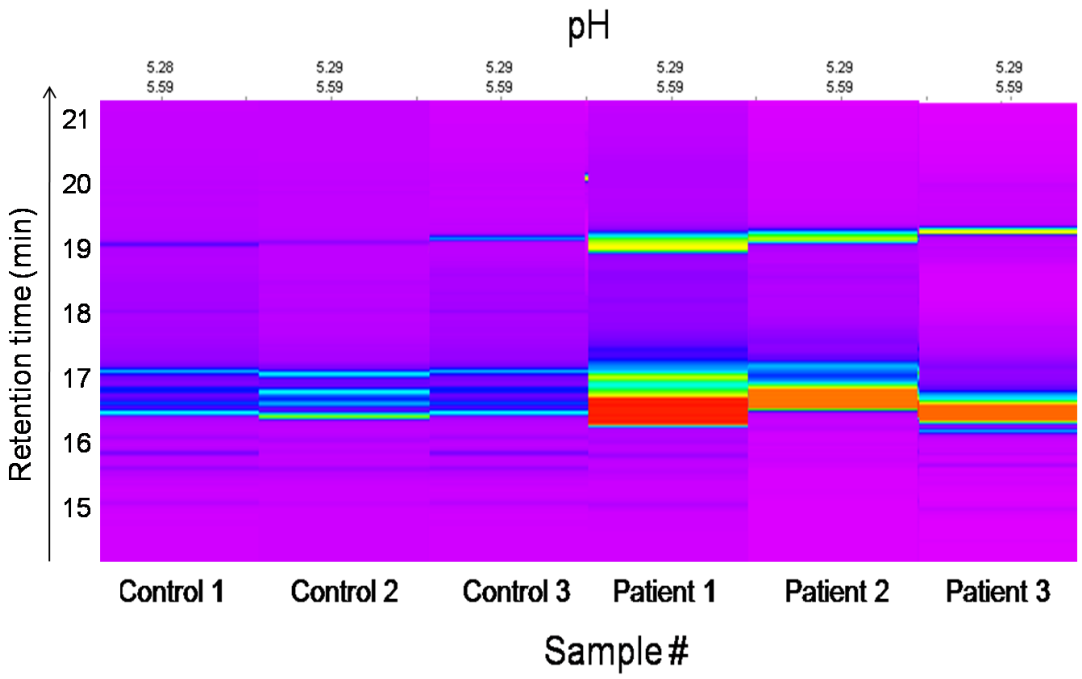

Figure 3-16: Significant difference in protein expression among Control samples and Patient samples 1, 2, 3 in pH fraction 5.59-5.29 displayed by MultiVue™ software.

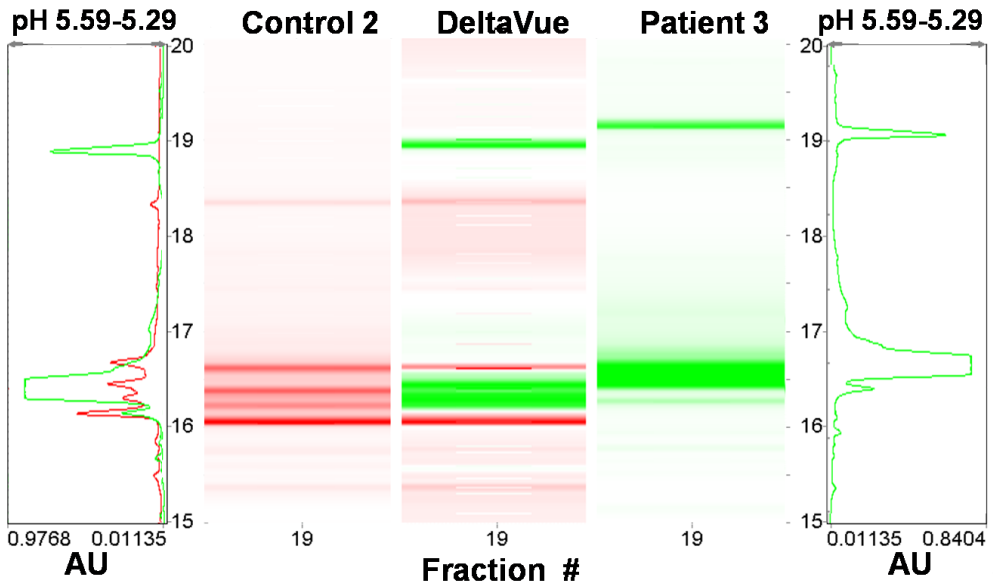

Figure 3-17: DeltaVue comparison of 2D profiles for Control 2 (red, left) and Patient 3 (green, right) in Lane 28.

According to the above described process, a total of 9 significantly increased

peaks in all of the three diseased samples were analyzed with nanoLC-MS/MS, resulting in incomplete human plasma Proteome S2 based on differential proteomics. A total of 68 distinct proteins in diseased samples were identified. As the result of comparison with Proteome R, 63 distinct proteins (93%) were cancelled out because of their presence in control samples. As a result, there are 5 distinct proteins that were only detected in diseased samples, considering at least two peptides matched for high evidence involved in all of the three diseased samples.

3.4.2.2 Generation of differential Proteome N2

Patient 4 and 5 were finally not response to the therapy despite treatment in ICU. The plasma samples at the last ICU day were injected into PF2D after immunodepletion to generate ProteoVue profiles, respectively. The comparison of these diseased proteome profiles to control proteome was done with the DeltaVue™ software.

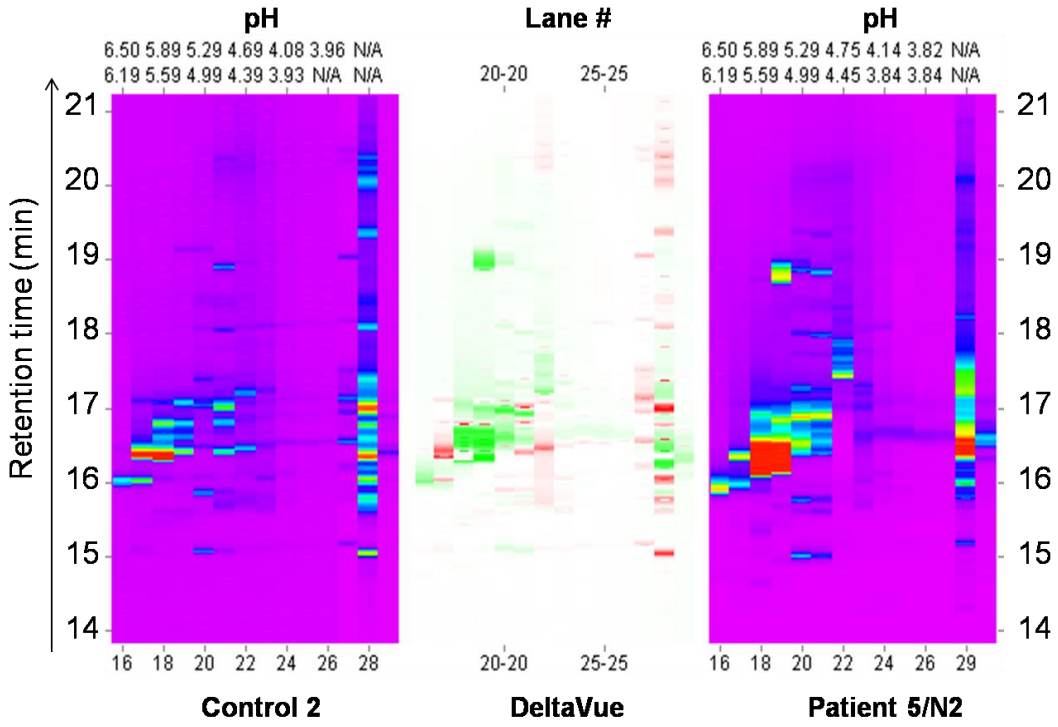

Figure 3-18: DeltaVue comparison of two-dimensional maps within fractions 14 to 28 from Control 3 and Patient 5 at the last ICU day.

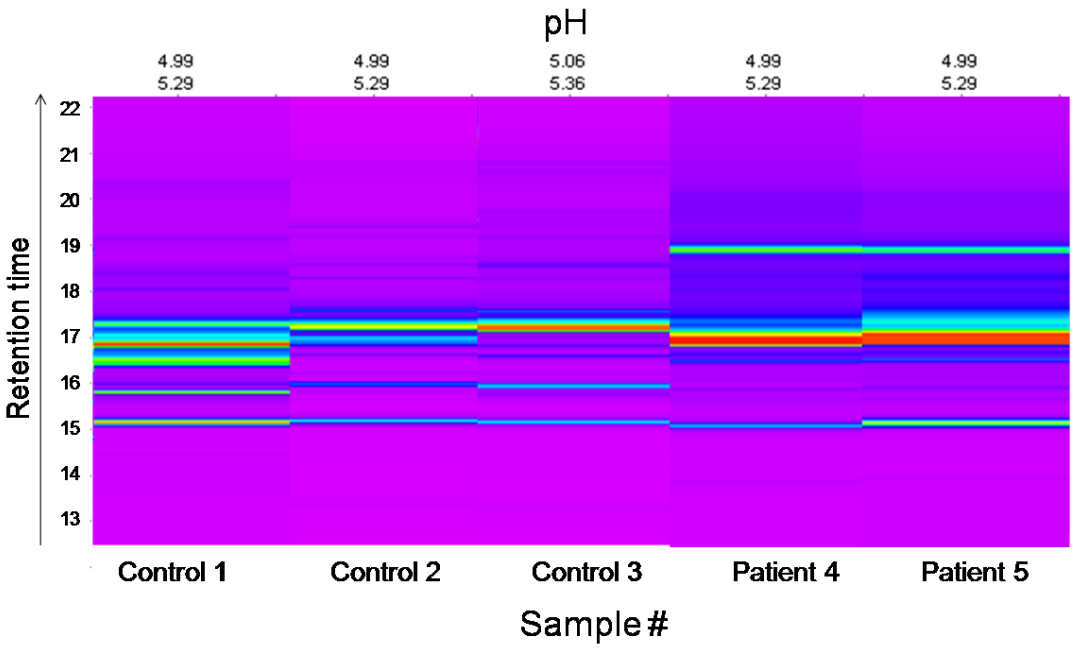

Figure 3-19: Significant difference in protein expression among Control samples and Patient samples in pH fraction 5.29-4.99 displayed by MultiVue™ software.

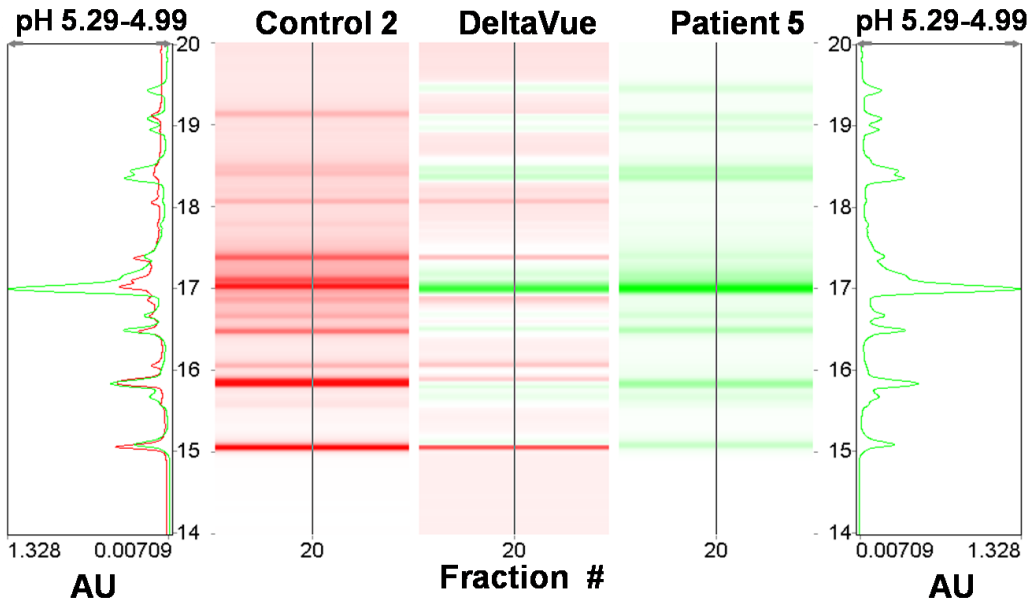

Figure 3-20: DeltaVue comparison of 2D profiles for Control 2 (red, left) and Patient 5 (green, right) pH fractions 5.29-4.99, which corresponds to Lane 20.

As the same as the generation of Proteome S1 described in former section, a total of 14 significantly increased peaks in both diseased samples were analyzed with nanoLC-MS/MS, resulting in incomplete human plasma Proteome N2 based on differential proteomics. A total of 63 distinct proteins in diseased samples were identified. As the result of comparison with Proteome R, 53 distinct proteins (84%) were cancelled out because of their presence in control samples. As a result, there are 11 distinct proteins that were not detected in Proteome R, considering at least two peptides matched for high evidence involved in both diseased samples.

3.5 Comparison of sepsis related proteome

The sepsis-related incomplete plasma Proteome S1, S2, N1, and N2 were generated from the inter-assay investigation as described above. To find out the association as well as difference among these proteomes is the essential aim of this study, which offers a thorough understanding for the meaning of biomarker candidates in different clinical stage. According to the timing of study and the outcome of patients, the biomarker candidates were classified, providing information to early detection, diagnosis and prognosis of sepsis, that can predict which individual patients will survive or respond to therapeutics.

3.5.1 Difference between Proteome S1 and Proteome S2

Patient 1, 2, and 3 responded to the therapeutics. Thus, the difference in protein expression among these patients at different clinical phase offers the opportunities to predict which sepsis patients will survival with molecular diagnostics or find out new target proteins for drug development or prognostic indicators.

Intra-assay in samples from Patient 1 at the first as well as the last ICU day was performed using DeltaVue^{TM} Software. As expected, Figure 3-21 shows that peaks in Patient 1/S1 were generally up expressed in contrast to Patient 1/S2, leading to more red strips were shown in DeltaVue panel in the middle, implying

that the plasma proteome at the last ICU day is regressing to the normal level.

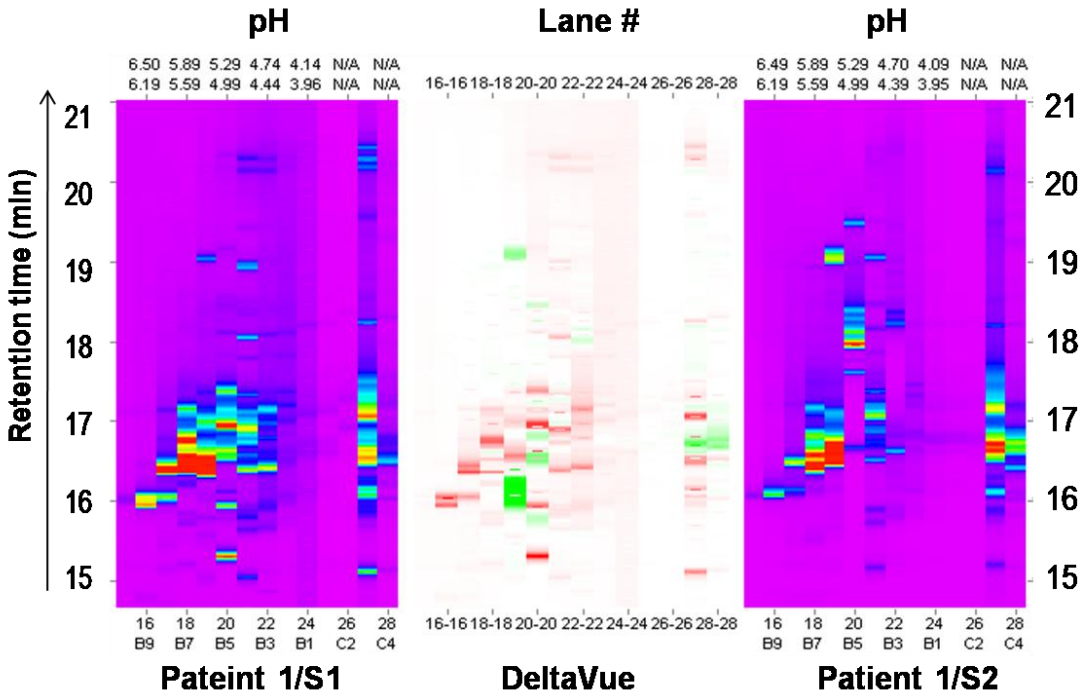

Figure 3-21: DeltaVue comparison of two-dimensional maps within fractions 15 to 28 from sample Patient 1 at the first (Proteome S1) and last ICU day (Proteome S2).

7 significantly up-expressed protein peaks in Patient 1/S1 and the corresponding peaks in Patient 1/S2 were analyzed with nanoLC-MS/MS. The results confirmed the prediction, some acute phase proteins like SAA and CRP are only detected in Patient 1/S1.

3.5.2 Difference between Proteome N1 and Proteome N2

Samples from Patient 4 and 5 presented two sepsis stages: SIRS and its progression MODS. The difference in protein expression between these two stages is very valuable information for sepsis prognosis, monitoring, and prediction. Intra-assay among these corresponding four ProteoVue maps was performed with MultiVue^{TM} software.

Only 1 p*I* fraction exhibited two peaks in the second dimension whose peak height in both samples at the last ICU day (Patient 4/N2 and 5/N2) differed significantly in

both at the first ICU day (Patient 4/N1 and Patient 5/N1). Figure 3-23 shows that the peaks eluting at 14.5 min and 16.3 min in p*I* fraction 4.69-4.36 were increased in the samples at the last ICU day.

The related fractions from Patient 4/N2 and Patient 5/N2 were analyzed by nanoLC-MS/MS. To cancel out the proteins that may also present in the samples at the first ICU day, the corresponding fractions from Patient 4/N1 and Patient 5/N1 were taken into MS analysis. The comparison of MS results revealed the presence of two proteins ferritin and cationic trypsinogen within retention time 14.5 min and 16.3 min, respectively.

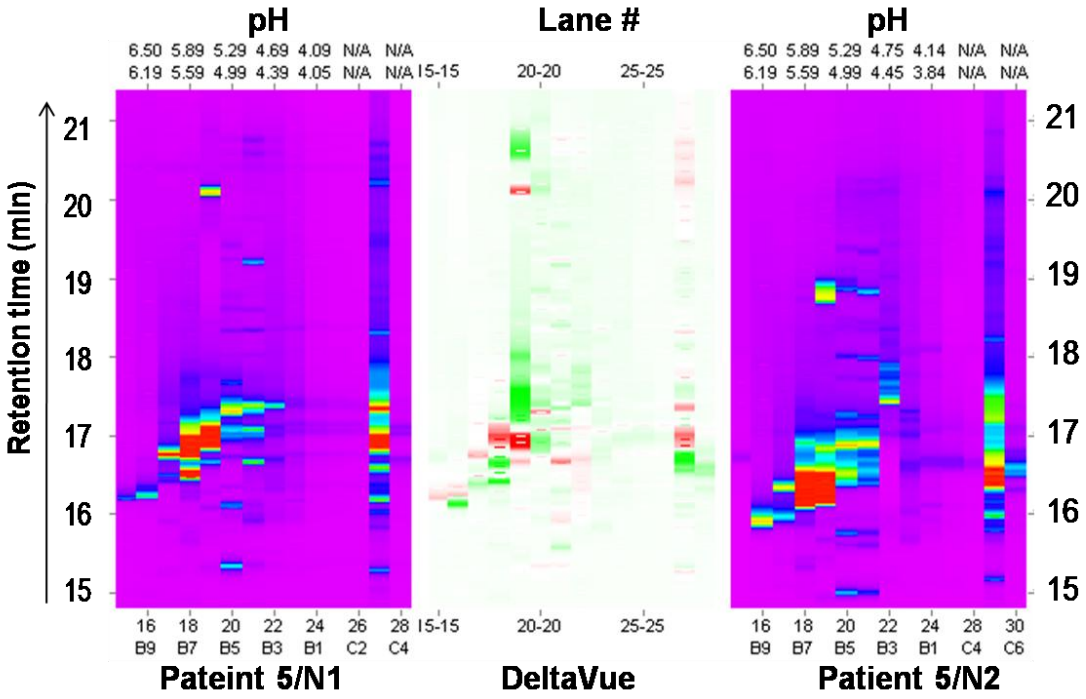

Figure 3-22: DeltaVue comparison of two-dimensional maps within fractions 15 to 28 from sample Patient 5 at the first (Proteome N1) and last ICU day (Proteome N2).

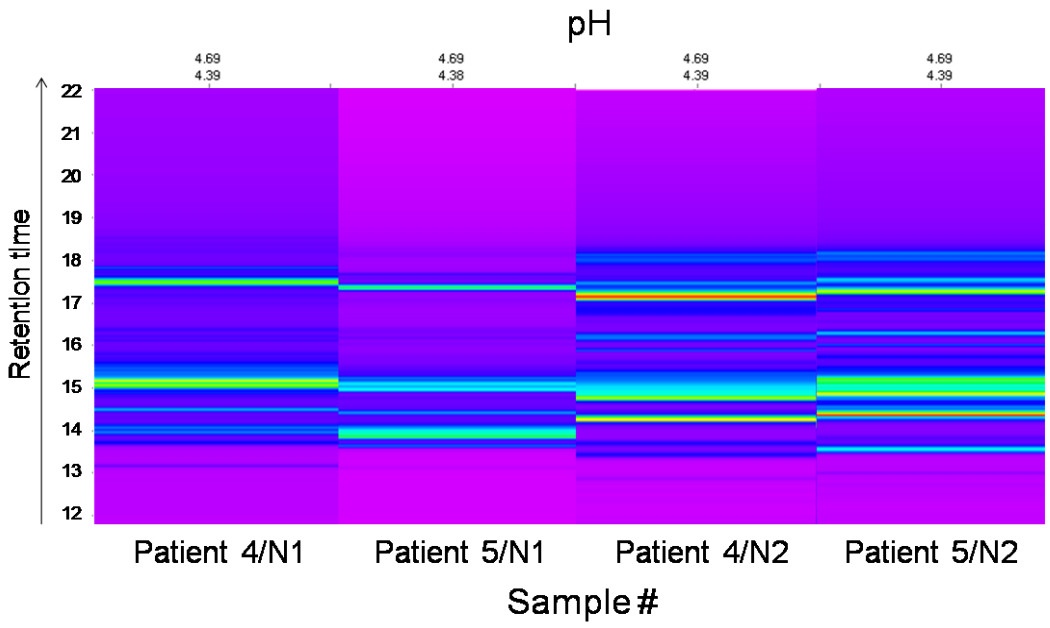

Figure 3-23: Significant difference in protein expression among samples from Patient 4 and 5 at the first ICU day (Proteome N1) and the last ICU day (Proteome N2) in pH fraction 4.69-4.39 displayed by MultiVue^{TM} software.

4 Discussion

4.1 Sample Preparation

Plasma is easily obtained with fewer restrictions in contrast to other sample types such as cerebrospinal fluid and tissue biopsy. It is therefore the most commonly tested clinical material for diagnostics. The most valuable biomarkers are highly sensitive, specific, reproducible and predictable, and the majority of FDA approved biomarkers are plasma-derived single proteins [Lee et al. 2006].

However, biomarker discovery in plasma is a great analytical challenge that requires a series of proteomic approaches such as fractionation, peptide identification and data handling. In addition, factors utilized in the preparation of plasma, such as the anticoagulant used, the clotting time allowed, the length of the time period before centrifugation, and repeated freeze/thaw cycles, had a significant effect on the sensitivity and reproducibility of the plasma proteome profile. A Standard operating procedure (SOP) should be established for the process of obtaining a plasma sample and should be very strictly documented, in order to assure reproducibility of samples and to allow some rationale comparison of data from various laboratories.

The most commonly used anticoagulants include EDTA or sodium citrate. Both prevent coagulation by chelating calcium ions. The use of plasma with sodium citrate for anticoagulation was recommended for biomarker discovery from human blood [Omenn et al. 2005]. It is recommended that the plasma should be carefully separated from cells within half hour after blood collection. If assays are not completed immediately, plasma sample should be stored at -80°C for minimum alteration. Frozen samples should be thawed only once to avoid analyte deterioration, which may occur in samples that are repeatedly frozen and thawed.

4.2 Advantages and Disadvantages of Approaches

4.2.1 Detection Limit of IgY-PF2D-nanoLC-MS/MS Strategy

The toughest challenge with the use of plasma sample for proteomic analysis is the dynamic qualitative and quantitative range of proteins. It is out of dispute that the dynamic range of protein concentration in plasma is nearly 12 orders of magnitude. The analytical challenge may emerge when the very low concentrations of potential biomarker proteins that present at pg/mL to ng/mL level in plasma are beyond the detection limit of most analytical instruments. Theoretically, the resolution of low abundance proteins (1% of plasma protein content) in immunodepleted sample gains a maximum 100-fold increase over a non-depleted sample. In fact, the removal of target proteins in this case got approximately 10% of protein content in depleted samples leading to 10-fold increase in resolution.

In addition, the use of a C18 non-porous reversed phase column in association to a UV detector at 214 nm (2D) enables the detection of proteins in nanogram up to microgram range [Daulty et al. 2006]. For this reason the 2D chromatograms were analyzed with a dynamic range of 3 orders of magnitude. Furthermore, the mass spectrometry (MS) represents the most sophisticated and sensitive analytical tool at present, the current dynamic range of detection is just about 3 orders of magnitude when analyzed in a single spectrum [Aebersold et al. 2003]. Even when MS is combined with an on-line separation such as HPLC, enhancement of the dynamic range will only be in the range of 4 to 6 orders of magnitude. Taken together, the analytical capabilities of proteomics technology used in this study quotes a dynamic range of approximate 9 orders of magnitude. In the other words, the concentrations of proteins in plasma at ng/mL level are theoretically able to be detected. Accordingly, proteins from tissue leakage, interleukins, and cytokines that exist at pg/mL level in plasma are in principle not detectable.

4.2.2 Immunoaffinity subtraction

Supplemental Table 3 shows the distribution of the remnant 12 target proteins for both control and patient samples in corresponding proteomes, which was demonstrated by the distribution in chromatofocusing (1D). Obviously, serum albumin and transferrin, which are known as negative acute-phase proteins [Steel et al. 1994; Ceciliani et al. 2007] could be detected with a decreased absorbance in reversed phase chromatography (2D) in patient samples contrasting with control samples or were not detectable in the former. On the contrary, those proteins who addressed as acute-phase proteins [Ceciliani et al. 2007], in particular fibrinogen, α1-antitrypsin, haptoglobin, and α1-acid glycoprotein, processed not only an increased UV absorbance in patient samples but also spanned broader p*I* fractions because more protein amount makes their heterogeneity more detectable and evident. It could be speculated that the IgY-12 column capacity was designed for specific removal of 12 high abundance target proteins from normal human plasma without taking a possible increase in plasma concentration under abnormal situation, e.g. inflammatory response, into account. According to the manufacturer protocol the specific removal of 12 high abundance proteins partitions up to 96% of total protein from human plasma, but it could not be as efficient as reported. Moreover, the acute-phase proteins are those whose plasma concentration increases at least 50% during acute-phase reaction. Taken together, the plasma concentration of the acute-phase proteins might largely exceed the limit of the designed IgY-12 column capacity and it leads to their more extensive distribution in Chromatofocusing (1D) in contrast to the normal pattern. Otherwise, antibodies (total IgG, IgA, and IgM), and α2-macroglobin show an equal result after depletion in both patterns, either are not detectable or exist in similar p*I* fractions.

This feature of IgY-12 immunoaffinity subtraction strategy is seemingly very advantageous and practical, since it significantly reduces the number of proteins of little interest in human plasma proteomics and consequently makes biomarker

discovery readily achievable. However, to the understanding of acute-phase response, the plasma concentrations of some high abundance proteins like α1-antitrypsin and haptoglobin increase largely during sepsis and maybe exceed the IgY column capacity for each specific protein as discussed above. In the case of depleting sepsis diseased plasma, the efficiency of IgY subtraction strategy could not be equal to its designed ambition. On the other hand, there is evidence that the removal of serum albumin and IgG may remove other bound proteins as well. For instance, serum albumin is known to act as a carrier and transport protein within blood and therefore is likely to bind many species of interest such as peptide hormones, cytokines, and chemokines [Burtis et al. 2001].

However, the increase in sensitivity outweighs the potential loss of other proteins. Table 3 demonstrates that a substantial number of heterogeneous sequences of the high abundance proteins remained in plasma samples even following immunodepletion with IgY-12 LC2 column. According to the manufacturer's protocol the specific removal of 12 high abundance proteins partitions up to 96% of total protein from human plasma. In fact, if serum albumin could be removed to 99.9% from the plasma sample, the remaining albumin would still be present at 50 µg/mL which corresponds to a 50,000-fold higher concentration in comparison with known concentration of tumor markers such as the prostate-specific antigen [Zolg et al. 2004]. MS identification results from fractions containing such high abundance proteins may therefore be dominated by them, in particular by serum albumin and various immunoglobulins because of their several isoforms with various p*I* values.

In consequence, the flow-through fractions were not shown to be deeply cleaned of the 12 high abundance proteins except α2-macroglobulin and haptoglobin within samples from healthy individuals, a mass of serum albumin, Fibrinogen, and immunoglobins were detected in broad p*I* range. However, the succeeding MS identification results suggest that the removal of target proteins by the immunoaffinity subtraction system was highly reproducible. The eight non-target

proteins were also observed to be eluted in bound fractions in a reproducible manner.

4.2.3 Peak Complexity in 2D Separation

MS analysis of peaks in 2D separation has shown that most of the peaks are in fact composed of a mixture of multiple peptides and proteins, between 10 to 16 proteins were detected in some large peaks. In addition, many high abundance plasma proteins like serum albumin and various immunoglobulins appeared in multiple peaks spanning a broad p*I* range. These are anticipated since many proteins exist as isoforms or are post-translationally modified in plasma, resulting in a great deal of different p*I* values. Quantitative analysis of these peaks was therefore too complicated to get an exact observation of different expression of a particular protein. It must be pointed out that MS is not a quantitative technique. It is therefore only possible to show which proteins was detected, yet unable to offer a quantitative consequence of how much these proteins differently expressed. In general, differences in peak height cannot be attributed to a particular protein in the sample. Under these conditions, additional separation and validation steps will be required to identify the differentially expressed proteins.

4.2.4 Concordance of Chromatogram Comparison

A limited number of peaks were detected in 1D chromatograms, it is attributed to the present of proteins that contain aromatic residues. It was thus speculated that detection at 280 nm was not sensitive enough to observe the impact that the shift in the pH gradient may have had on less abundance proteins. Therefore, the concordance of chromatograms may be chiefly influenced due to following factors in 2D separation. First, most of the 2D peaks are composed of a mixture of proteins. A different integration of the same peak between two chromatograms may therefore due to a small change in a shoulder slope. Second, slight variations in the ACN gradient between experiments can be responsible for local deformations of the chromatograms. It might not globally affect the

chromatograms, this nevertheless impacts the resolution of peaks located at corresponding retention time. In addition, the reproducibility of PF2D certainly also depends on the reproducibility of the sample preparation, sample storage, and the desalting/gel filtration prior to each fractionation experiment, in which these parameters are mandatory and could be responsible for a decrease in reproducibility.

The ProteomeLab^{TM} PF2D system demonstrates a reliable reproducibility not only in terms of pH gradient formation during chromatofocusing in the first dimension but also in terms of peak retention time in reversed-phase chromatography in the second dimension. Furthermore, the protein content inside the paired peaks that possess identical retention times and shape from different 2D fractions were also taken into consideration, some strips was selected and its corresponding fraction was analyzed by nanoLC-MS/MS to identify the proteins. The chromatograms can be marked using the retention time of identified proteins as control. MS analysis of these peaks impacted concordance of the two-dimensional chromatographic fractionation strategy. The reproducible feature of PF2D in thus validated to measure the differential expression between the control and disease specimens under its limit of detection.

4.2.5 Robustness of Liquid Based Proteomics

The traditional proteomics including protein mapping and comparison has been accomplished by two-dimensional gel electrophoresis (2-DE), which suffers from some significant shortcomings and limitations. Problems associated with 2-DE include poor reproducibility and limited resolving power for proteins with highly basic p*I*s, high molecular weight or low abundance [Shin et al. 2006]. Furthermore, as the most common visualization technique silver staining is protein dependent and has a short dynamic range [Hamler et al. 2004].

Some significant advantages of the PF2D versus 2-DE includes: (1) the proteome is fractionated in a contamination-free liquid flow path resulting liquid fractions,

which makes in-solution digestion without further extraction or solubilization of the sample possible, hence presents excellent compatibility with various MS systems; (2) high loading capacity and visualization of protein bands using integrated software increase the efficiency of biomarker discovery; (3) improved detection low molecular weight proteins with high reproducibility. Moreover, liquid-phase chromatofocusing in 1D separation provides p*I* information that offers sufficient sensitivity to detect post-translational modifications and separate proteins isoforms [Linke et al. 2006]. As a consequence, the liquid based ProteomLab^{TM} PF2D system offers a new platform tool for plasma fractionation in clinical setting.

4.3 Protein Identification

4.3.1 2D protein map of calculated molecular weights versus p*I*

A total of 233 distinct proteins were identified with nanoLC-MS/MS analysis in the Proteome R (Supplemental Table 1). Base on calculated MW and p*I* value in MSDB, a 2D map of these proteins was developed to demonstrate the biochemical characters of plasma proteins. The MS analysis revealed the identification of 233 plasma proteins with MW ranging from 8.1 kDa (Apolipoprotein C-II precursor) to 670 kDa (Microtubule-actin crosslinking factor 1). Many proteins in plasma with MW less than 15 kDa were able to be detected in PF2D pattern, extending the proteome discovery range beyond the traditional 2D gel approach. Figure 4-1 presents that most plasma proteins have a p*I* value between pH 5 to 7 and MW less than 200 kDa, on the other hand, demonstrating PF2D has a high resolution for proteins locating in this region.

In must be pointed out that the identification of 233 proteins is relatively a small portion in contrast to the estimated amount of plasma proteins that could reach up to several thousand [Saha et al. 2008]. Despite the detection limit of the used strategy, it might due to the presence of the remnant of high abundance proteins and to their high heterogeneity.

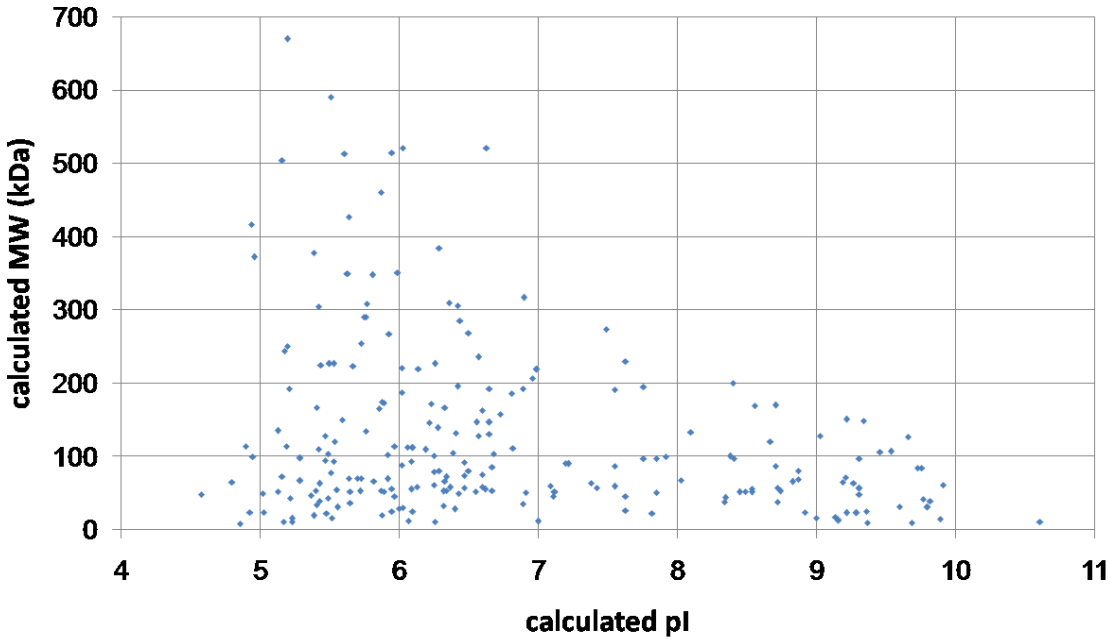

Figure 4-1: Two-dimensional map of calculated molecular weight versus p*I* for 233 proteins in Proteome R. Each spot represents a protein mass and p*I* signal that was detected by nanoLC-MS/MS coupled with MSDB.

Supplemental Table 3 demonstrated that a substantial number of heterogeneous sequences of the high abundance proteins remain in plasma samples even following immunodepletion with IgY-12. Especially, serum albumin and immunoglobulins were represented by eight and nine multiple forms, respectively. Actually, a redundant Proteome R comprises more than 300 observable protein subunits before the consolidation of multiple forms into a single entry. For instance, four immunoglobulin chains (λ and κ light chains, α and γ heavy chains) were united into one accession due to their sequence similarity. As a consequence, excluding database redundancies and considering the heterogeneous sequences as one protein, the number of the identified proteins reduced to 233, obtaining a non-redundant Proteome R.

4.3.2 Post-translational modifications of proteins

Figure 4-2 exhibited the correlation between calculated p*I* for those 74 proteins which identified with 3-way overlapping in Proteome R and their corresponding

measured pH. A linear regression was applied to fit the data and a slope of 1.052 and correlation coefficient (R2) of 0.604 were observed. The measured pH value describes the average value of pH range of 1D fraction. For instance, proteins detected in fraction with the pH range of 5.29-4.99 had p*I* 4.85. Proteins eluted before and after pH gradient had generally p*I* 8.3 and p*I* 4.0, respectively. It was found that the difference in measured and calculated p*I* value was nearly 1 to 2 pH units for most proteins, resulting that the measured p*I* did not match the database exactly.

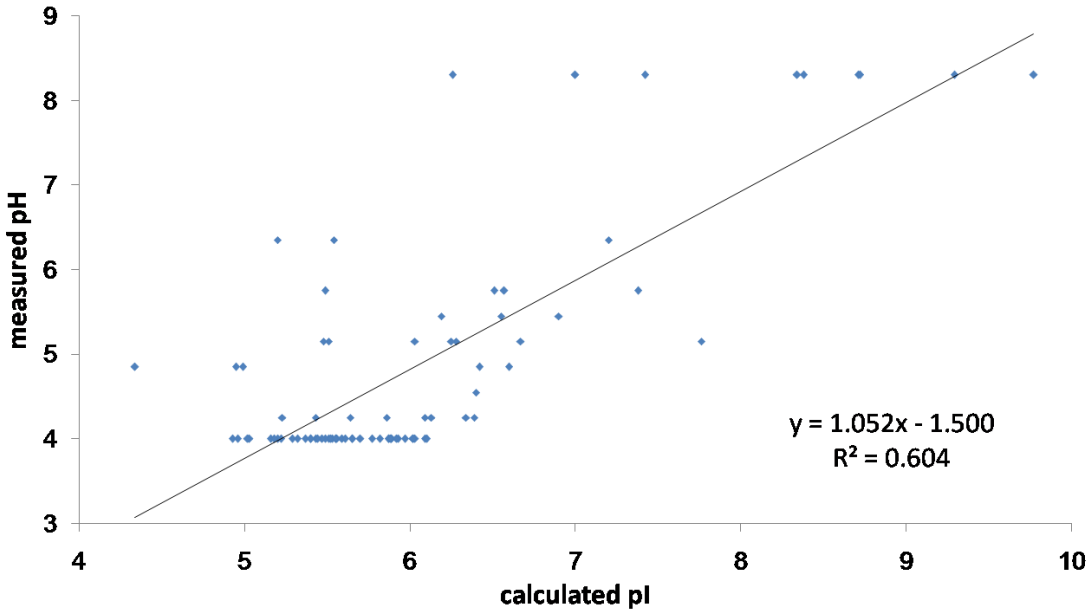

Figure 4-2: Correlation between calculated p*I* and corresponding pH in chromatofocusing period for 74 identified proteins in control specimens.

Some of the p*I* shifts might result from the interaction of a partial protein sequence with the stationary phase, since chromatofocusing is in principle a charge exchange technique and not truly electrophoretic focusing [Shin et al. 2005]. However, most protein p*I* shifts are related to post-translational modifications (PTMs) that shift the chromatographic properties of particular proteins [Zhu et al. 2005]. Many theoretical protein p*I*s in databases are calculated from amino acid

sequences translated directly from gene sequences, which would be post-translationally modified into functional proteins. It was reported that one phosphorylation may decrease the p*I* by 1-2 units [Yamataga et al. 2002]. Post-translational truncation could also change the total number of basic and acidic residues in a protein, resulting in a negative or positive shift of the theoretical p*I*. In fact, more than 20 proteins were identified in more than two non-sequential fractions in both 1D and 2D separation in redundant Proteome R, suggesting that these proteins may have potential PTMs.

In addition, PTMs affect the protein p*I* as well as increase the protein molecular weight, such as acetylation and phosphorylation, or decrease it per truncation [Hamler et al. 2004], resulting in heterogeneous forms of proteins.

4.3.3 Differential expression of classical plasma proteins in sepsis

Since mass spectrometry detection is concentration-dependent, such concentration increase is effectively translated into the increase of MS signal. Consequently, the number of peptide counts from the results of LC-MS/MS analysis seems to be useful for semi-quantitative comparison of changes in plasma protein concentration between different states. A list of 37 classical plasma proteins (Supplemental Table 4) along with their typical concentrations in plasma documented in the previous study [Qian et al. 2005] was used to evaluate the speculation. Figure 4-3 shows that there is a general correlation between peptide counts and protein concentration; by and large protein concentration is approximately in direct proportion to peptide hits. However, pronounced variation in peptide hits for some given protein concentration is also observed. This variation was expected since the number of peptide hits is dependent on the size and exact sequence of the protein. Therefore, the speculation upon differential expression for a given protein based on peptide hits could be used as a rule of thumb in limited spectrum.

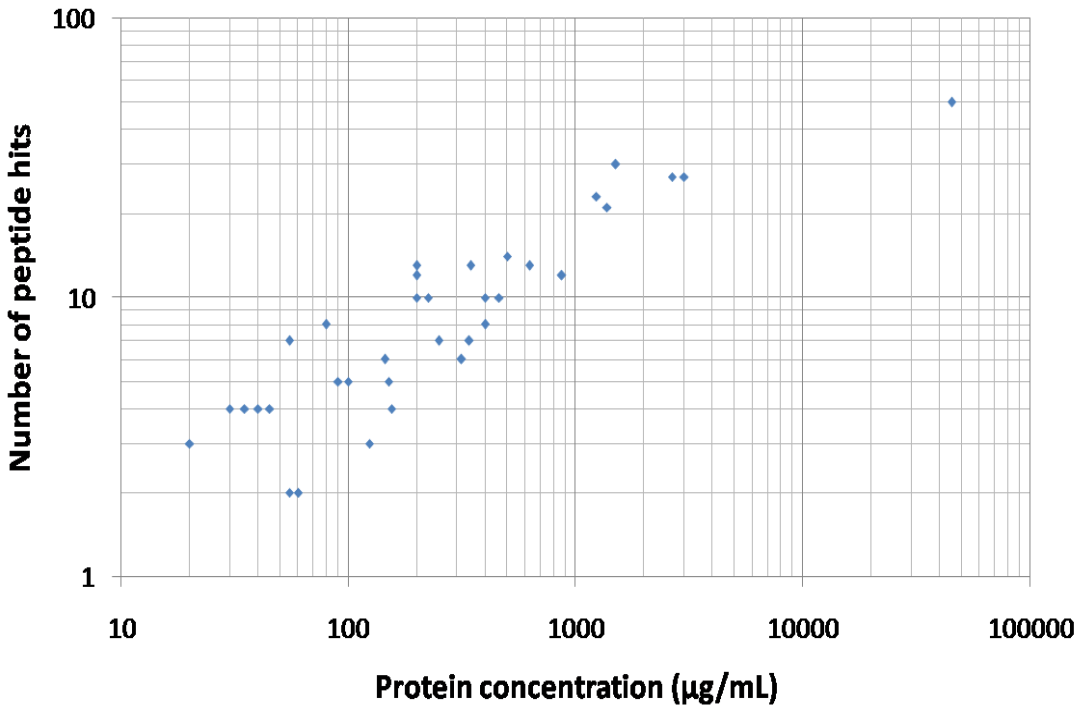

Figure 4-3: Correlation between peptide counts for 36 classical plasma proteins and their plasma concentration in normal state documented in previous study [Qian et al. 2005]. The plasma protein concentrations and peptide hits for the selected proteins are listed in Supplemental Table 4.

Interestingly, 21 out of the 37 classical plasma proteins are previously reported to response to acute-phase reaction (see section 1.3.1.1), resulting in change of the protein concentrations in plasma. In an attempt to determine whether the differential expression between normal and sepsis diseased states for these proteins could be reflected by the change of MS signal, the number of peptide hits for each protein from both states was compared and demonstrated in Supplemental Table 4. It was found that the relative change of peptide hits for all of the negative acute-phase proteins and most acute-phase proteins agreed with the acute-phase response they should have, except C4b-binding protein as well as other three acute-phase proteins that exhibited minor variation in peptide hits. Hence, it is believed that such approach for comparing relative changes of expression between two states is more efficient for those proteins in which at least 2-fold change in peptide hits was found. According to this speculation, a set of

proteins that are not yet reported to response to acute phase reaction and thus are potentially involved in inflammatory response were demonstrated in this analysis. Prothrombin was observed to be up-expressed, which is reported as a key pro-coagulant protein, but not an inflammation-sensitive protein in previous study [Tracy 2003]. Contrarily, several proteins were observed to be significantly down-expressed, including complement factor H, apolipoprotein A-I/II/E, vitamin D-binding protein, and retinol binding protein. Since it is practically difficult to determine the quantitative change of down-expressed proteins in clinical routine, they are generally not considered as sepsis markers.

4.4 New Sepsis Biomarker Candidates

A total of 17 biomarker candidates were identified using nanoLC-MS/MS coupled with human protein database MSDB, which only observed in patient samples and the number of peptide hits was at least 3 (Supplemental Table 2). In particular, 5 proteins (alpha-1-antichymotrypsin precursor, inter-alpha-trypsin inhibitor precursor, Urinary protease inhibitor, V-myb myeloblastosis viral oncogene, and Lumican) were present in all of the sepsis-related proteome. It was known, except V-myb myeloblastosis viral oncogene the other four proteins are involving in inflammatory cascade. 4 proteins (serum amyloid A protein precursor, nuclear mitotic apparatus protein, obscurin, and apolipoprotein B-100) were only detected in the early sepsis stage, corresponding to Proteome S1 and Proteome N1 at the first ICU day. 4 proteins (SNC66 protein, Leucine-rich alpha-2-glycoprotein, C-reactive protein precursor, and HDL-binding protein) existed in Proteome S1, N1, and N2 at the same time. 2 proteins (protein tyrosine phosphatase 1B and Lactoferrin) were just detected in Proteome S1. 2 proteins (ferritin and cationic trypsinogen) were only able to be detected in Proteome N2. These proteins were considered biomarker candidates for sepsis diagnosis which have not been previously reported except CRP.

These potential sepsis biomarkers are not yet taken into a validation phase. However, by means of literature searching might reveal whether these candidates have relation to inflammation, in respect that the inflammatory cascade offers a large number of opportunities for development of molecular models that describe various aspects of sepsis. PubMed search engine was used to individually search each of these 17 proteins for relevance to inflammatory function and sepsis using the key words “sepsis” or “inflammation”. When searches of protein names returned no results, the anonyms of the corresponding protein names were used. Abstracts or manuscripts were manually selected and relevance of specific proteins to inflammatory pathology was extracted.

Urinary trypsin inhibitor (UTI) is a multivalent Kunitz-type serine protease inhibitor that exists in human urine and blood. UTI is degenerated from inter-alpha-trypsin inhibitors during inflammation [Pratt et al. 1989]. The plasma concentration of UTI is increased in bacterial infections, severe viral infections, acute and chronic inflammation conditions [Pugia et al. 2005]. Recent in vitro studies have demonstrated that serine protease inhibitors may have anti-inflammatory properties beyond their inhibition of neutrophil elastase at the site of inflammation. It was suggested that UTI can protect against systemic inflammatory response and subsequent organ injury induced by bacterial endotoxin through the inhibition of proinflammatory cytokine and chemokine expression [Inoue et al. 2008]. UTI may therefore present an attractive therapeutic option for systemic inflammatory response syndromes such as disseminated intravascular coagulation (DIC) and multiple organ dysfunctions (MODS).

Lumican (LUM) is an extra-cellular matrix protein and is localized in the skin, cornea, and blood vessels, which specifically bind to bacterial endotoxins and regulate inflammatory responses. It was found that lumican-deficient mice are resistant to bacterial toxin-mediated septic shock suggesting that therapeutic methods and agents to modulate lumican activity could regulate inflammatory responses [Wu et al. 2007]. Treatment with lumican based therapies may block a

wide range of inflammatory cytokines activity to provide general immune protection. Lumican is thus considered as potential biomarker candidate for identifying patients with predisposition to sepsis and chronic inflammation, and a target for therapeutic interventions.

Apolipoprotein B-100 (apoB100) is a 550 kDa amphipathic glycoprotein that is secreted from the liver, acting as a transport protein to shuttle hepatic lipid store to peripheral tissues [Banaszak et al. 2008]. It is the major protein component of triglyceride-rich low density lipoprotein. Recent study revealed important link between activation of hepatic inflammatory nuclear factor-κB (NF-κB) signaling cascade and regulation of apoB100 containing lipoproteins [Tsai et al. 2009]. Hepatic inflammation may be an underlying factor in hepatic apoB100 overproduction observed in insulin resistance. It was also reported that apoB100 plays a role in vascular inflammation and coronary endothelial dysfunction [Adibhatla et al. 2008]. More studies will be required to investigate the association between the regulation of apoB100 and systemic inflammation during sepsis.

Leucine-rich α2-glycoprotein (LRG) is a plasma protein purified 32 years ago, in which leucine-rich repeats were first discovered. LRG is known to support neutrophil granulocytic differentiation in humans [O´Donell et al. 2002]. Although the physiological function of LRG is unclear, increases in the plasma level of LRG have been reported in various studies. Norkina et al. demonstrated that gene expression of LRG was significantly increased during intestinal inflammation by quantitative RT-PCR confirmation, associating with elevated systemic inflammation [Norkina et al. 2004]. Current report showed that the induction of LRG by IL-6 was up-regulated synergistically with either IL-1β or TNFα in a pattern similar to those for type 1 acute-phase proteins. LRG was thus speculated to be a secretory acute-phase protein whose expression was up-regulated by the mediator of acute-phase response [Shirai et al. 2009]. The molecular mechanisms underlying LRG in inflammation remains to be investigated.

Lipoproteins were shown to bind and neutralize bacterial lipopolysaccharide (LPS) and other bacterial cell wall components and to exert direct anti-inflammatory actions. High density lipoproteins (HDL) are thus thought to be important regulators of the host immune response during endotoxemia, which may also have the potential of improving the care of patients with Gram-negative sepsis [Wendel et al. 2007]. The protective effects of HDL in sepsis are regarded as possible therapeutic agents for sepsis and conditions associated with local or systemic inflammation. HDL-associated protein may play an important role in promoting cellular cholesterol efflux and removal from sites of inflammation and cell destruction [Van der Westhuyzen et al. 2007]. High density lipoprotein-binding protein, also known as vigilin, is a 110 kDa protein that specifically binds HDL and up-regulated by cholesterol loading of cells [Fidge 1999]. It may function in the removal of excess cellular cholesterol, but its physiological significance remains unknown. Protein tyrosine phosphatase 1B (PTP1B) is the prototype for the superfamily of protein tyrosine phosphatases (PTPs) and has been implicated in cellular signaling within and between cells [Edwards et al. 2001]. PTPs remove phosphates from substrate tyrosines (dephosphorylation) to regulate protein function in response to a variety of signals, including hormones, mitogens, and oncogenes. Recently, it was shown that PTP1B overexpression in multiple tissues in obesity and diabetes is regulated by inflammation and that PTP1B may be a target of anti-inflammatory therapies [Zabolotny et al. 2008]. Continued investigation into the involvement of PTP1B in inflammation is needed.

Lactoferrin (LAC) is a 78 kDa iron-binding glycoprotein and is found especially in milk and many other body fluids. LAC is a prominent component of the mucosal defense system whose expression is upregulated in response to inflammatory stimuli. It contributes to mammalian host defense by acting as both an antibacterial and anti-inflammatory agent. The anti-inflammatory activity occurs through inhibition of binding of lipopolysaccharide endotoxin to inflammatory cells, as well as through interaction with epithelial cells at local sites of inflammation to inhibit inflammatory cytokine production [Conneely 2001]. LAC has been shown to

reduce inflammation both in the skin and in the gut by inhibiting the production of the cytokine mediators. It has also been shown to upregulate the proliferation of polymorphonuclear cells, which are the first responders to inflammation and are responsible for clearing up any exudates associated with inflammation [Gonzalez-Chavez et al. 2009].

Cationic trypsinogen (CTG) is the most abundant isoform of the total trypsinogen in the human pancreatic juice and secreted into the blood circulation by the pancreas [Chen et al. 2009]. The plasma level of CTG is increased during acute pancreatitis, which relates to inappropriate activation of trypsinogen to trypsin. Anti-trypsin protective mechanisms are overwhelmed with further activation of trypsinogen, thereby resulting in pancreatic injury and initiation of a systemic inflammatory response syndrome beyond pancreas [Whitcomb 2006]. Phosphoinositide phospholipase C (PLC) is a family of eukaryotic intracellular enzymes that play an important role in signal transduction processes. PLCs comprise a related group of multidomain phosphodiesterases that cleave the polar head groups from inositol lipids [Rebecchi et al. 2000]. Recently, it was reported that mammalian PLC subtype ε is involved in skin Inflammation as assessed by expression of proinflammatory cytokine IL-1α [Ikuta et al. 2008]. Despite some acute-phase proteins are known as sepsis marker like CRP or as inflammatory mediator like inter-alpha inhibitor protein (IaIp), ferritin, serum amyloid A and alpha-1-antichymotrypsin, they were only detected in patient samples and highlighted here. IaIp inhibits trypsin and plasmin, and lysosomal granulocytic elastase. Its plasma concentrations would be increased under various inflammatory conditions so that it is discussed as an acute phase protein. The inter-alpha inhibitor protein family is a group of plasma-associated serine protease inhibitors. Members of this family are composed of heavy and light polypeptide subunits that are covalently linked by a glycosaminoglycan. The light chain, also called bikunin, is responsible for the serine protease inhibitor activity of the molecules. Plasmin plays an important role in inflammation, and the fact that the anti-plasmin activity of inter-alpha-inhibitor lends further support to the idea

that inter-alpha-inhibitor is an anti-inflammatory agent.

CRP and SAA are the major acute phase reactants predominantly produced and secreted by hepatocytes. Other cells including lymphocytes, monocytes, and macrophages can also produce these proteins. The induction of SAA and CRP synthesis is triggered by a number of cytokines, chiefly IL-6 and TNF predominantly released from macrophages and monocytes at the inflammatory sites [Steel et al. 1994; Takala et al. 2002]. Measurements of CRP can help to differentiate not only inflammatory from non-inflammatory conditions but also bacterial from viral infections [Herzum et al. 2008]; thus it is the most widely used indicator of the response of acute-phase proteins. SAA concentrations usually parallel those of CRP, however, assays for SAA are not widely available in sepsis diagnosis at present [Gabay et al. 1999].

Alpha-1-antichymotrypsin (ACT) is a glycoprotein produced in the liver and is also an acute-phase protein synthesized in response to pro-inflammatory cytokines early in the inflammatory response. ACT is a member of the serine protease inhibitor family that inhibits neutrophilic chymotrypsin from mast cells, protecting tissue from damage by these proteolytic enzymes. ACT contains a reactive centre loop that interacts with cognate proteases, resulting in loop cleavage and a major conformational change. As an acute phase protein, ACT is active in the control of immune and inflammatory responses. Ferritin is a 450 kDa protein complex consisting of 24 protein subunits whose principal role within cells is the storage of iron in a soluble and non-toxic form. Plasma ferritin is also known as an early acute phase reactant and can be increased during inflammation, which suggests that it may play a role in modulating inflammatory effects [Kalantar-Zadeh et al. 2004; Recalcati et al. 2008]. During acute inflammation, the normal control of iron metabolism is reorganized by the cytokines TNFα and IL-6, plasma ferritin concentrations increase rapidly and in parallel with those of CRP during neutropenic sepsis [Feelders et al. 1998].

Some identified proteins which appeared only in patient specimens seem to be not specific to sepsis and may have other causes. Nuclear mitotic apparatus protein (NuMA), as a mitotic centrosomal component, is essential for the organization and stabilization of spindle poles from early mitosis until at least the onset of anaphase [Zeng et al. 2000]. SNC66 protein is an N-linked glycoprotein [Zhou et al. 2009]. SNC66 protein is known as an immunoglobulin-like protein which is down-regulated in colorectal cancer. Obscurin is an 800 kDa protein existing in skeletal muscle and may have a role in organizing the myofibrils and intracellular membranes of striated muscle cells [Kontrogianni-Konstantopoulos et al. 2005]. It must be pointed out that, not only with infections and the immune system, inflammation has also been associated with the basic mechanism available for repair of tissue after an injury and consists of a cascade of cellular and microvascular reactions that serve to remove damaged and generate new tissue. These cell proteins might appear in plasma because of cell destruction in sepsis. While this study actually proceeds to identify the peaks of interest, these proteins are unlikely to have the necessary specificity to diagnose a particular sepsis.

4.5 Biomarker for Sepsis Diagnostics

To find out new sepsis biomarkers, which may play an important role in the early detection and diagnosis of sepsis, is a major goal of biomedical research on sepsis. According to the generally accepted criterion, an ideal diagnostic biomarker for sepsis should possess following characteristics: (1) wide and consistent existence in the circulation system; (2) quantifiable through common biochemical approaches and reproducible between patients and laboratories [Ren et al. 2007; Etzioni et al. 2003]; (3) sepsis specific for early detection, monitoring of the treatment effect, and prediction of the outcome. A total of 17 biomarker candidates were identified, their physiological function or biochemical properties

are different for each other. Such results reflect that the sepsis is multifactorial and its pathogenesis is complex. Sepsis is thus considered not as a one fold inflammation response any more, there is growing evidence that it is a process which consists of systemic inflammation, prothrombotic diathesis, and fibrinolysis disorders. The pathological understanding of the acute inflammation syndromes was effectively improved in the last decade; however, it is believed that using just only a singular biomarker for prediction of mortality is nearly impossible because of the complex cooperation of the multiple factors in sepsis. Otherwise, the ratio of pro- and anti-inflammatory cytokines and the dynamics of alteration in plasma concentration of cell associated and circulated cytokines must be taken into account.

Clinical proteomics allows the broad-scale detection of a number of proteins, rather than the traditional protein-by-protein approach, may provide higher sensitivities and specificities for diagnosis than those that can be afforded with single markers. However, given the current state of technology, there are a lot of cumulative factors that make such discovery extremely difficult. Proteomic results usually do not possess the convincing precision and accuracy found in standardized assays. This deficiency requires a broad range of patients to be analyzed in order to achieve the level of confidence that would be required before even considering taking the potential biomarkers into a validation phase.

5 Conclusion

Sepsis is usually considered as proven infection associated with the systemic inflammatory response to infection. Although the understanding of the pathogenesis of inflammation and sepsis has improved, until recently this has not translated into clinical benefit and sepsis remains the most common cause of death in intensive care units. The continuum of sepsis, severe sepsis, and septic shock is correlated with increasing mortality despite supportive care and therapy. Sepsis could be referred to as a process of malignant intravascular activation of the complex enzyme cascades of haemostasis and inflammation. A complex interaction of cytokines and cytokine-neutralizing molecules probably determines the clinical presentation and course of sepsis. The concentrations of individual cytokines in body fluid alone, therefore, may not reflect the septic status correctly.

To date, some plasma proteins such as procalcitonin (PCT), C-reactive protein (CRP), Interleukin-6 (IL-6), and IL-8 are routinely used as a combination criterion in clinical diagnosis of sepsis. PCT and CRP concentrations might discriminate the infectious systemic inflammatory response syndrome (SIRS) from those who are not infected. IL-6 and IL-8 are proinflammatory cytokines indicating the severity of the inflammatory response, but are not specific for bacterial infection. An ideal diagnostic biomarker for sepsis should sepsis specific for early detection, monitoring of the treatment effect, and prediction of the outcome, i.e., it must be closely related to therapeutic consequences. Among the used biomarkers of sepsis, all of them fulfill only a fraction of these requirements, such as improved diagnosis of bacterial infection or a better assessment of the severity of the host response to infection. At present, such aforementioned measurements have therefore generally not proven effective in predicting which individual patients will survive or respond to therapy. To find out new sepsis biomarkers, which may play an important role in the early detection, diagnosis and prognosis of sepsis, is a major goal of biomedical research on sepsis in this study.

Plasma can be relatively easily obtained from the patient and has a very high protein concentration in the range of about 5%. It seems to be the ideal clinical sample for biomarker discovery; however, twenty-two proteins make up approximately 99% of the protein content of plasma. It is estimated that the protein concentrations in plasma span 12 orders of magnitude, and the specific disease biomarkers for diagnostic and prognostic purposes are most likely within the very low concentration range. In biomarker discovery, it is necessary to maximize the observation of the plasma proteome to detect proteins with low abundance. This can be achieved by optimization of protein separation methods as well as selective depletion of the proteins at high abundance such as serum albumin and various immunoglobulins.

In the present study, a combination of IgY-PF2D-nanoLC/MS/MS approach was used as an alternative approach to traditional technology for identifying novel biomarkers of sepsis. The 12 high abundance plasma proteins would be removed in a single step using ProteomeLab^{TM} IgY-12 immunoaffinity subtraction system (Beckman Coulter, USA). The proteins remaining are pooled for further separation of complex protein mixtures. Traditionally, this profiling has been accomplished by two-dimensional gel electrophoresis (2-DE), which suffers from a number of shortcomings such as lack of reproducibility and unsatisfactory resolution of proteins in the alkaline region.

To parry these problems, a new platform tool for use of proteome fractionation named the ProteomeLab™ PF2D system (Beckman Coulter, USA) has been developed, which features separation by chromatofocusing (CF) in the first dimension, followed by reversed-phase (RP) chromatography in the second dimension. In contrast to traditional profiling it handles samples in liquid form, which lends itself to subsequent MS analysis without further extraction or solubilization of the sample. Separation is monitored by UV detection, allowing comparison of samples to detect changes in the proteome using the integrated DeltaVue^{TM} software. Relevant fractions were then subjected to MS to identify the

potential marker proteins. The analytical capabilities of proteomics technology used in this study quotes a dynamic range of approximate 9 orders of magnitude.

This strategy is sufficient to gain comprehensive coverage of the low abundance proteins within plasma, according to the IgY-12 LC2 column validated performance on the recovery of the low abundance proteins as well as on the binding of non-target proteins to the column. Very similar protein recovery was constantly found in the flow-through fractions per immunodepletion of the 12 high abundance proteins in plasma, 10% for control samples and 13% for patient samples, respectively. Despite the domination of 12 high abundance proteins in the bound fractions, 8 non-target proteins including complement C3, zinc-α2-glycoprotein, apolipoprotein D, serum amyloid protein P, transthyretin, hemopexin, clusterin, and α2-HS-glycoprotein were also detected in these fractions from both control and patient samples. It was expected because non-target proteins were bound onto serum albumin or other high abundance proteins and simultaneously eluted during immunodepletion.

With regard to the protein fractionation step, PF2D provides approximate p*I* value of each protein as viewed in proteome map, which is essential issue for protein identification. The pH gradient formation in the chromatofocusing (1D) and the peak retention times on the column in the reversed-phase separation (2D) were evaluated. It was found that in three consecutive chromatofocusing separations that the pH gradient differed by less than 0.1 pH units at any time during the elution step. Second dimension retention times of peaks from identical p*I* fractions differed by less than 6 sec in three consecutive separations, indicating a high reproducibility from run to run.

Plasma samples from three healthy individuals were analyzed, determining the common proteins which were regarded as normal plasma proteome as reference named Proteome R. Nearly 145 distinct proteins were identified in each parallel full scan analysis. Taken together, the MS analysis revealed the identification of

233 distinct plasma proteins with MW ranging from 8.1 kDa (apolipoprotein C-II precursor) to 670 kDa (microtubule-actin crosslinking factor 1), in which 132 proteins from three healthy individuals were identified by double and/or triple determination with high reliability. Most plasma proteins possess MW less than 200 kDa and a measured p*I* value between 5 to 7, which might shift 1 to 2 pH units from the calculated p*I* value because of post-translational modifications.

According to the timing of study and the treatment outcome, patient samples were divided into four groups. Differential Group-assay was performed between Patient and Control samples, generating sepsis-related differential plasma proteomes (Proteome S1, N1, S2, and N2). A total of 17 biomarker candidates were identified for sepsis using nanoLC-MS/MS coupled with human protein database MSDB, which only observed in patient samples and the number of peptide hits is at least 3, including lumican, urinary protease inhibitor, high density lipoprotein-binding protein, leucine-rich alpha-2-glycoprotein und cationic trypsinogen. Most of them are reportedly related to inflammation or sepsis syndrome. It is necessary, a broad range of patients to be analyzed in order to achieve the level of confidence that would be required before even considering taking the potential biomarkers into a validation phase.

6 Supplement

6.1 Non-redundant reference proteome

Supplemental Table 1: Non-redundant Proteome R including 233 unique proteins that identified in plasma specimens from three healthy individuals with up to 3-way overlap, arranged in alphabetical increased order. Sequence coverage is defined as the ration of number of the explained amino acids to the total number of amino acids of the protein. Probability based Mowse Score describes the significance of the search result based on the significance threshold of 0.05. Only such protein hits have been considered in this study, which showed a Probability based Mowse Score higher than the identity or homology threshold. + and – mean significant up- /down-regulation in relation the septic proteome, respectively. +/- means no significant differential regulation was observed. *marked proteins: cited as regulated in septic patient by Shen et al.

Accession in MSDB	Protein name	theo. p*I*	theo. MW	Mowse Score	Sequence coverage	Peptide counts	Overlap	Regu-lation
CAB41526	ABO glycosyltransferase	9.16	12757	34	4	2	2	/
AAD22767	A-kinase anchoring protein 350	4.94	416855	73	1	8	1	/
OMHU1	alpha-1-acid glycoprotein 1 precursor	4.93	23497	74	13	15	3	+
OMHU2	alpha-1-acid glycoprotein 2 precursor	5.03	23588	120	8	10	3	+
ITHU	alpha-1-antitrypsin precursor	5.37	46707	186	33	23	3	+
OMHU1B	alpha-1-B-glycoprotein	5.65	51908	255	12	10	3	+/-
I59403	alpha-2,8-polysialyltransferase	9.77	41269	28	2	4	2	/
WOHU	alpha-2-HS-glycoprotein precursor	5.43	39300	78	5	13	3	-
S02392	alpha-2-macroglobulin receptor precursor	5.16	504245	49	1	4	1	+/-
A41948	alpha-fetoprotein enhancer-binding protein	6.42	305548	23	1	3	2	/
ALMS1	Alstrom syndrome protein 1	5.87	460655	54	2	6	3	/
ANHU	Angiotensinogen	5.87	53091	68	9	4	3	+
AAR25662	Ankyrin repeat-containing protein	6.57	235521	47	1	3	3	/
AAM46656	Anti-pneumococcal antibody 7C5 light chain	7.82	22192	49	25	8	1	/
XHHU3	Antithrombin III precursor*	6.32	52569	147	11	3	3	-
LPHUA1	Apolipoprotein A-I precursor*	5.56	30759	407	38	21	3	-

LPHUA2	Apolipoprotein A-II precursor*	6.26	11168	72	26	10	3	-
AAA51784	Apolipoprotein A-IV precursor	5.22	43358	722	54	22	3	/
Q6P163	Apolipoprotein C-II precursor	4.86	8141	67	25	4	3	/
LPHUC3	Apolipoprotein C-III precursor	5.23	10846	52	27	3	3	+/-
LPHUE	Apolipoprotein E precursor	5.65	36132	126	17	4	3	-
NBHU	Apolipoprotein H precursor	8.34	38287	109	7	7	3	/
DAHUAL	Arachidonate 5-lipoxygenase	5.51	77933	39	2	2	2	/
A59188	ATP-binding cassette transporter ABC3	7.55	191265	43	1	10	1	/
CAC60121	Axonemal beta heavy chain dynein type 11	6.03	520649	51	1	8	2	/
Q96JB1	Axonemal dynein heavy chain 8	5.95	514485	59	1	9	1	/
Q59HC1	Beige-like protein variant	5.41	166753	56	1	4	1	/
1A6ZB	beta-2-microglobulin	6.07	11724	40	20	2	1	/
CAA26382	beta-2-glycoprotein	6.43	49264	95	6	3	1	/
Q5W026	Breast cancer antigen NY-BR-1	5.86	165770	35	1	5	2	/
AAQ97181	Breast cancer tumor suppressor BRCA2	6.29	383963	75	1	4	1	/
Q7Z7D6	Bromodomain PHD finger transcription factor	5.77	307897	49	1	3	2	/
AAL66061	Bullous pemphigoid antigen 1	5.51	590510	73	1	7	3	/
CAA26617	C4b-binding protein	6.13	58278	138	7	7	3	+/-
Q6NVY0	Calcyclin binding protein	7.63	26166	41	4	2	1	/
Q6IBT3	CCT7 protein	7.55	59291	34	4	8	1	/
A42681	Centromere protein C	9.54	106861	53	5	5	2	/
Q66GS8	Centrosome protein 290	5.76	290151	32	1	3	1	/
Q70F00	Centrosome spindle pole associated protein	6.25	101380	44	2	4	1	/
AAL55733	Centrosome-associated protein	5.99	350722	58	2	4	2	/
AAA51975	Ceruloplasmin	5.29	97637	114	4	8	3	+
CAF25186	Chorein 1st dimension	5.81	347453	59	1	3	1	/
EAL24102	Chromosome 7 Scaffold04	8.71	86341	49	2	3	1	/
A41386	Clusterin precursor	5.89	52461	37	4	2	3	/
Q8IZZ5	Coagulation factor XII	8.03	67691	66	7	4	2	-
ITHUC1	Complement C1 inhibitor precursor*	6.09	55119	298	12	10	3	+/-

Q5ST53	Complement C2 precursor	7.00	11591	26	4	3	3	+/-
C3HU	Complement C3 precursor	6.02	187046	875	17	30	3	+
C4HU	Complement C4a precursor*	6.65	192741	61	1	3	3	+
Q6U2E9	Complement C4b precursor	6.89	192631	187	5	9	3	+
A34372	Complement C6 precursor	6.39	104718	108	4	4	3	+
A27340	Complement C7 precursor	6.09	93454	41	1	2	3	+/-
C9HU	Complement C9 precursor	5.43	63133	40	2	2	3	+
CAA68416	Complement control protein factor I	7.38	63415	268	15	10	3	/
BBHU	Complement factor B precursor	6.67	85479	305	14	13	3	+/-
NBHUH	Complement factor H precursor	6.28	139034	218	6	14	3	-
Q5VXD8	Constitutive photomorphogenic protein	5.95	55648	25	2	3	1	/
AAA52164	Cystatin C	9	15819	35	10	2	1	/
Q6R570	Cytochrome P450 2A13 variant 5	9.31	56665	31	2	2	1	/
IJHUG1	Desmoglein 1 precursor	4.90	113644	35	2	5	1	/
A38194	Desmoplakin	6.36	309797	46	1	2	1	/
Q6F3F7	Developmentally regulated GPCR	8.1	133613	74	4	4	1	/
Q3ZK23	Diaphanous homolog 3	6.41	132318	35	3	3	1	/
B55926	DNA binding protein RFX2	6.29	79953	39	2	2	1	/
A27605	Dystrophin	5.64	426411	78	1	3	1	/
Q3SY90	Elongin A2	9.73	83817	50	2	3	3	/
Q24JU4	Eukaryotic translation initiation factor 3	6.33	166369	63	1	3	2	/
Q8IZ60	Extracellular matrix protein 1	6.25	60695	66	7	4	3	/
1FVDB	Fab fragment of humanized antibody 4d5	8.92	23686	44	12	2	3	/
Q96PQ8	Factor VII active site mutant immunoconjugate	6.60	75504	68	7	4	2	/
Q32Q65	Fibrinogen	8.54	55880	594	28	27	3	+
BAC03643	GAP-associated tyrosine phosphoprotein p62	7.11	45832	41	2	2	1	/
I52300	Giantin	4.96	372015	54	2	6	3	/
AAA63175	Glucose-6-phosphate dehydrogenase	6.62	55168	36	2	2	1	/
GRIP2	Glutamate receptor-interacting protein 2	6.06	112432	44	2	2	1	/
T00743	Glutamyl tRNA synthetase	6.89	35354	64	6	3	1	/

Q5HYX8	GTP binding protein 6	9.60	31679	24	6	2	2	/
OQHU	Hemopexin precursor	6.55	51643	648	32	12	3	+
KGHUGH	Histidine-rich glycoprotein precursor	7.09	59541	531	32	5	3	+
AAF81365	HIV-EP2 enhancer-binding protein	6.50	268869	75	1	4	3	/
T14759	Hypothetical protein DKFZp434A033	5.29	66919	49	2	7	1	/
T34567	Hypothetical protein DKFZp434A128.1	6.02	88175	32	2	2	1	/
Q9H0A2	Hypothetical protein DKFZp434A196	6.47	91691	52	4	5	2	/
CAB66679	Hypothetical protein DKFZp434D1812	9.22	150506	41	2	4	1	/
T42704	Hypothetical protein DKFZp434H177.1	5.47	128024	72	1	2	1	/
Q86T95	Hypothetical protein DKFZp451B0517	5.17	10947	36	6	2	1	/
Q86TE5	Hypothetical protein DKFZp451K1417	9.31	48575	34	3	2	1	/
Q8ND39	Hypothetical protein DKFZp547P028	6.37	57725	32	4	9	1	/
Q7Z374	Hypothetical protein DKFZp686C02218	6.67	53742	58	2	2	1	/
Q6MZU6	Hypothetical protein DKFZp686C15213	7.85	51066	135	9	12	1	/
Q68DA7	Hypothetical protein DKFZp686C2281	9.21	71816	44	3	2	1	/
Q6N093	Hypothetical protein DKFZp686I04196	7.63	46032	67	9	5	1	/
CAH18423	Hypothetical protein DKFZp686I1147	6.23	171598	44	1	2	1	/
Q6MZV6	Hypothetical protein DKFZp686M08189	5.13	51606	212	14	8	1	/
Q7Z351	Hypothetical protein DKFZp686N02209	8.74	52819	101	13	7	2	/
T50614	Hypothetical protein DKFZp761E1415.1	5.49	42921	42	4	2	2	/
Q9NXX7	Hypothetical protein FLJ20001	5.41	33885	37	10	2	1	/
BAA06147	Hypothetical protein KIAA0054	6.99	218933	67	1	3	2	/
BAA25477	Hypothetical protein KIAA0551	6.73	157763	57	1	3	1	/
T00330	Hypothetical protein KIAA0556	5.54	120384	39	0	2	3	/
T00363	Hypothetical protein KIAA0674	5.13	135096	36	3	3	1	/
O94909	Hypothetical protein KIAA0819	5.42	109822	74	3	4	1	/
O94942	Hypothetical protein KIAA0861	6.1	112095	56	2	3	1	/
Q9Y2L0	Hypothetical protein KIAA1007	6.96	206198	38	1	4	1	/
Q9P2P4	Hypothetical protein KIAA1302	6.26	226433	47	1	7	2	/
Q96RY5	Hypothetical protein KIAA1426	8.71	169730	30	2	10	3	/

Q9P219	Hypothetical protein KIAA1509	6.56	146718	54	1	3	1	/
Q9P219	Hypothetical protein KIAA1509	6.65	146718	43	1	2	1	/
BAA96042	Hypothetical protein KIAA1518	5.53	93507	33	1	2	1	/
BAA96055	Hypothetical protein KIAA1531	9.03	128146	36	1	6	1	/
BAB13387	Hypothetical protein KIAA1561	6.6	162404	50	3	3	1	/
Q9C0I3	Hypothetical protein KIAA1680	7.92	99693	36	3	5	1	/
BAB21814	Hypothetical protein KIAA1723	5.89	173441	49	1	3	2	/
Q5T2E0	Hypothetical protein KIAA1751	6.50	80421	35	1	7	1	/
Q8IVF4	Hypothetical protein KIAA2017	5.63	349281	45	1	5	1	/
Q8IVF4	Hypothetical protein KIAA2017	5.63	349281	68	1	7	1	/
Q8WTQ4	Hypothetical protein MGC33367	9.80	30799	31	2	2	2	/
S23741	Hypothetical TPR/TRK mutant fusion protein	6.60	58138	47	4	3	3	/
BAC86456	Immunoglobulins	8.45	51333	127	9	5	3	/
Q6ZQW0	Indoleamine 2,3-dioxygenase	5.88	19597	29	5	2	1	/
INCE	Inner centromere protein	9.46	106049	56	3	5	1	/
Q59ES2	Inositol 1,4,5-trisphosphate receptor type 3 variant	5.93	266852	46	2	4	2	/
Q5W136	Inositol polyphosphate-5-phosphatase F	6.57	128326	40	1	2	2	/
A41915	Insulin-like growth factor-binding complex acid-labile chain precursor	6.33	65994	292	11	7	2	/
BAB17050	Interferon-responsive finger protein 1	7.76	97601	49	2	4	3	/
AAD29952	Intersectin long isoform	7.76	195300	52	1	2	2	/
JC5526	Kinase deficient protein precursor	6.19	109204	39	1	3	2	/
Q17RZ5	Kinectin protein	5.59	150260	47	3	4	3	/
Q2UVF0	Kinesin-like protein KIF21B variant	6.81	186156	34	1	2	1	/
KGHUH1	Kininogen precursor	6.34	71900	182	8	5	3	+/-
Q24K24	killer cell lectin-like receptor subfamily B protein	5.95	25387	37	16	2	1	/
LCHUL	Lacrimal lipocalin precursor	5.39	19238	93	12	2	1	/
AAA59487	Laminin	4.58	47820	39	5	2	1	/
AAF62352	Latent transforming growth factor beta binding protein 3	5.76	134203	38	3	4	1	/
LUZP1	Leucine zipper protein 1	8.67	120202	61	2	3	1	/

Q5VZP9	Matrix metalloproteinase 21	9.19	65003	30	1	2	2	/
O76P96	Matrix metalloproteinase 23B	9.82	38696	36	1	2	1	/
CAA03597	MCSP precursor	5.20	250297	39	1	8	2	/
3FCTB	Metal chelatase catalytic antibody fab fragment	9.29	23059	33	7	3	2	/
Q5VW21	Microtubule-actin crosslinking factor 1	5.20	669721	47	1	4	3	/
Q2KQ73	M-phase phosphoprotein 1	5.16	72591	56	2	2	2	/
MBB1A	Myb-binding protein 1A	9.34	148762	68	1	2	1	/
Q5UON1	Myeloid leukemia factor 2	6.40	28129	26	7	2	2	/
A61231	Myosin heavy chain nonmuscle form A	5.53	226602	68	2	4	3	/
Q1PSK5	Nephrocystin-6	5.75	290207	39	1	3	1	/
AAN60442	Nuclear envelope spectrin repeat protein 1	5.37	1010307	99	1	11	1	/
B55282	Neurofibromatosis-related protein	6.90	316829	54	1	2	2	/
Q96IV0	N-glycanase 1 (PNGase)	6.47	74343	45	2	3	1	/
JC7363	NMDA (N-methyl D-aspartate) receptor	5.47	94723	56	8	4	3	/
Q60FE2	Non-muscle myosin heavy polypeptide 9	5.5	226392	77	2	5	1	/
S78549	Notch3 protein	5.18	243496	58	1	3	2	/
Q6ZQV0	NP220 nuclear protein	4.8	64706	64	10	4	1	/
Q5T1E8	Nuclear receptor coactivator 4	5.73	69682	56	3	2	1	/
Q96F82	Origin recognition complex, subunit 1	9.31	97262	45	4	6	2	/
Q5VVU0	Outer dense fiber of sperm tails 2	8.87	80835	41	3	3	1	/
Q5TD33	Pecanex-like 2	7.55	86573	39	1	3	1	/
Q9P2X9	Peptide transporter 3	9.27	63518	32	1	6	2	/
Q5T1M2	Peptidyl-prolyl cis-trans isomerase	6.34	52941	37	6	2	1	/
PCNT	Pericentrin B (Kendrin)	5.39	377849	81	1	8	1	/
S02004	Phosphoinositol-specific Phospholipase C	6.22	146027	46	2	4	3	/
JC7963	Phospholysine phosphohistidine inorganic pyrophosphate phosphatase	6.00	29175	41	3	5	3	/
AAA60124	Plasminogen*	7.42	57372	122	5	4	3	+
Q6S381	Plectin	5.61	513393	46	1	5	3	/
Q6IPC0	Protein phosphatase 1F	5.02	49671	45	5	2	2	/

Q4QZ40	Prothrombin	5.70	69920	285	16	5	3	+
Q59F38	Purinergic receptor P2X5 isoform A variant	8.49	51681	37	1	3	3	/
PSA	Puromycin-sensitive aminopeptidase	5.49	103211	36	2	2	2	/
I78879	Retinoblastoma binding protein 2	6.42	195690	53	1	4	2	/
AAC34368	Retinoblastoma interacting protein	5.92	101878	41	4	7	2	/
VAHU	Retinol binding protein precursor	5.48	22853	130	15	7	3	-
AAH06133	Ring finger protein 40	5.97	113609	55	7	4	2	/
Q86SS3	RNA binding motif protein 6	8.87	69137	61	5	5	2	/
CAD19037	Sequence 1 from Patent EP1158049	6.44	285075	29	0	2	1	/
CAD12648	Sequence 1 from Patent WO0182948	8.40	199904	39	2	3	2	/
CAD23012	Sequence 1 from Patent WO0190320	7.85	96984	46	2	5	1	/
CAH61633	Sequence 1 from Patent WO2004085474	8.54	51335	217	17	24	1	/
CAD48813	Sequence 10 from Patent WO0246389	10.61	10886	31	6	2	2	/
CAA02876	Sequence 11 from patent WO9521188	8.38	100251	34	2	4	2	/
CAI93502	Sequence 112 from Patent WO2001042451	9.69	9398	45	18	2	1	/
CAC22378	Sequence 13 from Patent WO0075319	6.91	51189	59	6	3	3	/
CAC36461	Sequence 13 from Patent WO0121794	4.95	99305	34	1	2	2	/
CAD33454	Sequence 181 from Patent WO0218424	6.32	32877	161	26	7	1	/
CAD33474	Sequence 201 from Patent WO0218424	9.66	126965	41	1	3	2	/
CAC49990	Sequence 22 from Patent WO0146261	8.83	65476	197	13	23	1	/
CAD48779	Sequence 23 from Patent EP1229047	6.65	130903	47	4	5	1	/
CAF16643	Sequence 2338 from Patent EP1104808	9.37	9816	46	12	4	1	/
CAD48781	Sequence 27 from Patent EP1229047	6.68	103786	63	3	3	1	/
CAF05454	Sequence 3 from Patent WO03097823	5.88	174187	64	1	2	3	/
CAI61680	Sequence 3 from Patent WO2005012512	5.67	222874	46	1	2	1	/
CAD19027	Sequence 31 from Patent EP1158004	7.12	51648	135	9	12	1	/
CAC39844	Sequence 329 from Patent EP1067182	8.35	43778	48	2	2	2	/
CAD19029	Sequence 35 from Patent EP1158004	7.12	51635	79	7	4	1	/
CAC08836	Sequence 38 from Patent WO0006605	6.47	57347	84	8	8	1	/
CAC69723	Sequence 52 from Patent WO0162932	9.36	24692	34	6	2	1	/

CAH05540	Sequence 521 from Patent WO2004058805	9.22	22927	30	6	2	1	/
CAD33357	Sequence 84 from Patent WO0218424	9.91	61143	71	9	5	1	/
CAE90265	Sequence from Patent EP1074617	9.89	14896	34	10	9	2	/
CAD48777	Sequence from Patent EP1229047	6.25	79091	68	7	5	2	/
Q5VWB4	Serine palmitoyltransferase	5.72	52710	52	6	2	1	/
Q59GI0	Serotonin receptor 6	5.23	15491	39	10	3	1	/
ABHUS	Serum albumin precursor	5.92	69321	1211	45	50	3	-
YLHUP	Serum amyloid P component precursor*	6.10	25371	100	11	2	3	+
AAD22973	Silencing mediator of retinoic acid and thyroid hormone receptor	7.49	273235	48	1	2	1	/
Q3MNF0	Smooth muscle myosin heavy chain isoform	5.44	224189	59	3	6	2	/
Q5T9J7	Spastic ataxia of Charlevoix-Saguenay	6.63	520795	56	1	4	2	/
Q7RTM4	Spectrin-like protein	5.40	965738	52	1	5	3	/
Q8NEC5	Sperm-associated cation channel 1	7.22	90121	55	1	2	2	/
CAA28659	S-protein	5.55	54308	100	11	4	3	/
A26366	Steroid 17 alpha-monooxygenase	8.72	57334	39	1	8	2	/
AAA60321	Sulfated glycoprotein-2	5.97	45787	123	10	7	1	/
Q59R70	TBL2 (transducin beta-like 2) protein	9.14	17224	36	13	2	1	/
JC5020	Tetratricopeptide repeat protein	7.63	229746	58	3	4	3	/
THYG	Thyroglobulin precursor	5.42	304536	42	1	5	1	/
AAH36022	Transcription elongation factor B	9.76	83896	38	3	4	2	/
A36368	Transcription factor CBF, CCAAT-binding	5.19	114000	44	2	3	1	/
TFHUP	Transferrin precursor	6.81	77000	194	13	27	3	-
VBHU	Transthyretin precursor*	5.52	15877	213	58	13	3	-
Q5VUI3	Trichohyalin	5.73	253777	63	3	8	1	/
Q9BW51	TTK protein kinase	8.41	97011	53	2	4	3	/
AAT09770	Tyrosine kinase 6	8.72	38293	45	3	2	2	/
Q59H66	Ubiquitin specific protease	5.82	65735	48	5	2	2	/
UN13 A	Unc-13 homolog A	5.21	192876	33	1	4	1	/
VYHUD	Vitamin D-binding protein precursor	5.40	52929	201	15	10	3	-
SGHU1V	Vitronectin precursor	5.55	54328	147	8	7	3	+

YLPM1	YLP motif-containing protein 1	6.14	219849	54	1	4	1	/
AAL85487	Zinc finger protein 298	8.56	169092	46	2	4	1	/
Z3H7B	Zinc finger protein 7B	6.82	111506	35	2	2	3	/
ZN638	Zinc finger protein 638	6.02	220488	51	1	2	2	/
1ZAGD	Zinc-alpha-2-glycoprotein	6.03	30547	450	27	8	3	-

6.2 Biomarker candidates

Supplemental Table 2: Function of the 17 biomarker candidates in inflammation that only detected in diseased plasma specimens. X and O refer to the presence or absence of these candidates in sepsis-related Proteomes S1, N1, S2, and N2, respectively.

Protein name	Function in inflammation	S1	N1	S2	N2
alpha-1-antichymotrypsin precursor	Acute phase protein	x	x	x	x
Inter-alpha trypsin inhibitor	Acute phase protein, Anti-inflammatory agent	x	x	x	x
Urinary protease inhibitor	Anti-inflammatory agent [Inoue et al. 2008]	x	x	x	x
V-myb myeloblastosis viral oncogene	Unknown	x	x	x	x
Lumican	regulate inflammatory responses [Wu et al. 2007]	x	x	x	x
Serum amyloid A protein precursor	Acute phase protein	x	x	O	O
Nuclear mitotic apparatus protein	Unknown	x	x	O	O
Obscurin	Unknown	x	x	O	O
Apolipoprotein B-100	Secretion during hepatic inflammation [Tsai et al. 2009]	x	x	O	O
SNC66 protein	Unknown	x	x	O	x
Leucine-rich alpha-2-glycoprotein	Up-expressed during inflammation [Shirai et al. 2009]	x	x	O	x
C-reactive protein precursor	Acute phase protein	x	x	O	x
HDL-binding protein (110K)	Unknown, Removal of excess cellular cholesterol [Fidge et al. 1999]	x	x	O	x
Protein tyrosine phosphatase 1B	Up-expressed during inflammation [Zabolotny et al. 2008]	x	O	O	O
Lactoferrin	Anti-inflammatory agent [Conneely 2001]	x	O	O	O
Ferritin	Acute phase protein	O	O	O	x
Cationic trypsinogen	Up-expressed during pancreatic inflammation [Whitcomb 2006]	O	O	O	x

Supplemental Table 2 (continued): MS information and the location in proteome profile of the17 biomarker candidates.

Accession in MSDB	Protein name	theo. p*I*	theo. Mw	Mowse Score	Sequence coverage	Peptide hits	Fraction in 1D	RT in 2D (min)
4CAAA	alpha-1-antichymotrypsin precursor	5.38	37707	129	11	4	F27	15.8
HUCU	Inter-alpha trypsin inhibitor	5.95	38974	114	20	9	F20	17
Q9UDI8	Urinary protease inhibitor	5.20	7086	63	16	3	F20	18.4
Q708J0	V-myb myeloblastosis viral oncogene	7.04	76101	42	2	3	F21	15.7
Q53FV4	Lumican	6.16	38389	177	15	7	F27	19.5
YLHUS	Serum amyloid A protein precursor	6.28	13524	213	45	22	F3	15.5
Q4LE64	Nuclear mitotic apparatus protein	5.64	238715	86	3	4	F28	19.5
Q8NHN3	Obscurin	5.41	241828	56	2	3	F24	15.8
CAA28420	Apolipoprotein B-100	6.67	514934	41	3	12	F4	16.5
Q8WY24	SNC66 protein	6.22	53631	217	13	9	F23	19.5
NBHUA2	Leucine-rich alpha-2-glycoprotein	5.66	34325	137	19	6	F28	19.5
1B09A	C-reactive protein precursor	5.45	23033	67	8	3	F21	19.6
A44125	HDL-binding protein (110K)	6.43	141352	54	3	3	F27	19.5
Q96CU0	Protein tyrosine phosphatase 1B	5.55	20026	82	13	3	F28	19.5
AAG30947	Lactoferrin	9.86	9146	92	20	4	F21	19.6
1LFG	Ferritin	8.34	75934	101	4	4	F22	16.3
CAA56563	Cationic trypsinogen	6.01	274805	45	2	3	F22	14.5

6.3 Distribution in chromatofocusing of the remnant 12 target proteins.

Supplemental Table 3: Distribution in chromatofocusing of the remnant target proteins from normal and diseased plasma.

12 target proteins	Fraction Nr. in Proteome R	Fraction Nr. In Proteomes S1 and N1
Serum albumin	F18, F19, F27, F28	F18, F19, F27, F28
IgG, IgA, IgM Total *	F2, F3, F4, F18, F2, F28	F2, F3, F4
Transferrin	F16, F27	N/A
Fibrinogen	F24, F27, F28	F20, F22, F24, F27, F28
α2-Macroglobulin	N/A	N/A
α1-Antitrypsin	F28	F20, F21, F22, F24, F27, F28
Haptoglobin	N/A	F21, F22, F23, F24, F27
Apolipoprotein A-I	F27, F28	F4, F28
Apolipoprotein A-II	F4	N/A
α1-Acid glycoprotein	F28	F23, F24, F27, F28

* Total IgG, IgA, and IgM are considered as one unit due to their similar antibody activity and chemical structure. N/A = detection is not available.

.

6.4 Differential expression of the 37 classical plasma proteins in two states

Supplemental Table 4: 37 classical plasma proteins in Proteome R with documented plasma concentrations in normal state and corresponding peptide hits observed in control samples in relation to patient samples. N/A, detection is not available; ↑/↓ or ↑↑/↓↓ (at least 2-fold changed) describes the grade of up-/down-expression; ~ means no significant differential expression was observed; APP, acute-phase protein; NAP, negative acute-phase protein.

Protein name	Concentration (µg/mL)	Peptide counts in control	Peptide counts in patient [a)]	Expression level [b)]	Acute phase response [c)]
Serum albumin precursor	45000	50	19	↓↓	NAP
Fibrinogen	3000	27	32	↑	APP
Transferrin	2660	27	N/A	↓↓	NAP
Complement C3 precursor	1500	30	64	↑↑	APP
Apolipoprotein A-I precursor	1375	21	14	↓↓	/
Haptoglobin [d)]	1365	N/A	19	↑↑	APP
alpha-1-antitrypsin precursor	1235	23	54	↑↑	APP
alpha-1-acid glycoprotein	870	12	17	↑	APP
alpha-2-HS-glycoprotein precursor	625	13	2	↓↓	NAP
Complement factor H precursor	500	14	7	↓↓	/
Apolipoprotein A-II precursor	460	10	N/A	↓↓	/
Ceruloplasmin	400	8	13	↑	APP
Vitamin D-binding protein precursor	400	10	3	↓↓	/

Transthyretin precursor	345	13	6	↓↓	NAP
Vitronectin precursor	340	7	13	↑	APP
Complement C4 precursor	315	6	8	↑	APP
C4b-binding protein	250	7	5	(↓)	APP
alpha-1-B-glycoprotein	225	10	10	~	/
Hemopexin precursor	200	12	30	↑↑	APP
Complement factor B precursor	200	13	8	(↓)	APP
Complement C1 inhibitor precursor	200	10	7	(↓)	APP
Plasminogen	155	4	4	(~)	APP
Prothrombin	150	5	12	↑↑	/
Antithrombin III precursor	145	6	5	~	/
Apolipoprotein C-III precursor	124	3	3	~	/
Histidine-rich glycoprotein	100	5	8	↑	/
Kininogen precursor	90	5	5	~	/
Zinc-alpha-2-glycoprotein	80	8	5	↓	/
Complement C7 precursor	60	2	3	~	/
Complement C9 precursor	60	2	4	↑↑	APP
Retinol binding protein precursor	55	7	2	↓↓	/
Serum amyloid P component	55	2	4	↑↑	APP
Angiotensinogen	45	4	7	↑	APP

Complement C6 precursor	40	4	7	↑	/
Apolipoprotein E precursor	35	4	2	↓↓	/
Coagulation factor XII	30	4	N/A	↓↓	NAP
Complement C2 precursor	20	3	2	~	/

[a)] The number of peptide hits is average value based on detection in different patient samples.

[b)] Up- or down-expression level based on comparison of peptide hits in different states, those which disagreed with acute phase response are shown in round parenthesis.

[c)] Those proteins which not known as APP or NAP in previous study concerning acute phase response are marked with solidus.

[d)] Haptoglobin is excluded for illustration of Figure 5-3, since it is not detectable in control samples following immunodepletion.

7 Reference

Aderka, D., Le, J., Vilcek, J., et al. (1989) IL-6 inhibits lipopolysaccharide induced tumour necrosis factor production in cultured human monocytes, U937 cells and mice. Journal of Immunology 143: 3517-3523.

Adibhatla, R. M., Dempsey, R., and Hatcher, J. F. (2008) Integration of Cytokine Biology and Lipid Metabolism in Stroke. Front Biosci 13: 1250–1270.

Aebersold, R., and Mann, M. (2003) Mass spectrometry-based proteomics. Nature 422: 198-207.

Anderson, N. L., and Anderson, N. G. (2002) The human plasma proteome: history, character, and diagnostic prospects. Mol Cell Proteomics 1: 845-867.

Anderson, N. L., Polanski, M., Pieper, R., et al. (2004) The human plasma proteome: A non-redundant list developed by combination of four separate sources. Mol Cell Proteomics 3: 311-316.

Angus, D. C., Burgner, D., et al. (2003) The PIRO concept: P is for predisposition. Crit Care 7: 248-251.

Antonelli, M. (1999) Sepsis and septic shock: pro-inflammatory or anti-inflammatory state? J Chemother 11: 536-540.

Astiz, M. E., and Rackow, E. C. (1998) Septic shock. Lancet 351: 1501-1505.

Banaszak, L. J., and Ranatunga, W. K. (2008) The assembly of apoB-containing lipoproteins: a structural biology point of view. Ann Med 40: 253–267.

Baumann, H., and Gauldie, J. (1994) The acute phase response. Immunol Today 15: 74-80.

Bernard, G. R., Vincent, J. L., Laterre, P., et al. (2001) Efficacy and safety of

recombinant human activated protein C for severe sepsis. N Engl J Med 344: 699–709.

Blackwell, T. S., and Christman, J. W. (1996) Sepsis and cytokines: current status. Br J Anaesth 77: 110-117.

Bone, R. C., Balk, R. A., et al. (1992) Definitions for sepsis and organ failure and guidelines for the use of innovative therapies in sepsis. The ACCP/SCCM Consensus Conference Committee. Chest 101: 1644-1655.

Borden, E. C., Chin, P., et al. (1994) Interleukin-6: a cytokine with potential diagnostic and therapeutic roles. Journal of Laboratory and Clinical Medicine 123: 824-829.

Boyanton, B. L., and Blick, K. E. (2002) Stability studies of twenty-four analytes in human plasma and serum. Clin Chem 48: 2242-2247.

Brunkhorst, F. M., Eberhard, O. K., Brunkhorst, R., et al. (1999) Discrimination of infectious and noninfectious causes of early acute respiratory distress syndrome by procalcitonin. Crit Care Med 27: 2172-2176.

Buchud, P.-Y., and Calandra, T. (2003) Pathogenesis of sepsis: new concept and implications for future treatment. BMJ 326: 262-266.

Burdette, S. D., and Parilo, M. A. (2010) Systemic Inflammatory Response Syndrome. eMedicine Critical Care. http://emedicine.medscape.com/article/168943-overview.

Burtis, C. A., and Ashwood, E. R. (2001) Tietz Fundamentals of Clinical Chemistry. 5th Ed. W. B. Saunders Company. Philadelphia.

Calandra, T., Gerain, J., et al. (1991) High circulating levels of interleukin-6 in patients with septic shock: evolution during sepsis, prognostic value, and interplay

with other cytokines. The Swiss-Dutch J5 Immunoglobulin Study Group. Am J Med 91: 23-29.

Ceciliani, F., and Pocacqua, V. (2007) The acute phase protein alpha1-acid glycoprotein: a model for altered glycosylation during diseases. Curr Protein Pept Sci 8: 91-108.

Chen, E. I., Hewel, J., Felding-Habermann, B., and Yates, J. R. (2006) Large Scale Protein Profiling by Combination of Protein Fractionation and Multidimensional Protein Identification Technology (MudPIT). Molecular & Cellular Proteomics 5: 53–56.

Chen, J.-M., and F′erec, C. (2009) Chronic Pancreatitis: Genetics and Pathogenesis. Annu. Rev. Genom. Human Genet 10: 3.1-3.25.

Conneely, O. M. (2001) Antiinflammatory Activities of Lactoferrin. Journal of the American College of Nutrition 20: 389S–395S.

Edwards, K., Davis, T., Marcey, D., Kurihara, J., and Yamamoto, D. (2001) Comparative Analysis of the Band 4.1/ezrin-related Protein Tyrosine Phosphatase Pez from Two Drosophila Species: Implication for Structure and Function. Gene 275: 195-205.

Engel, C., Brunkhorst, F. M., et al. (2007) Epidemiology of sepsis in Germany: results from a national prospective multicenter study. Intensive Care Med 33: 606-618.

Etzioni, R., Urban, N., Ramsey, S., et al. (2003) The case for early detection. Nat Rev Cancer 3:243-252.

Feelders, R. A., Vreugdenhil, G., Eggermont, A. M. M., et al. (1998) Regulation of iron metabolism in the acute-phase response: interferon-g and tumor necrosis factor-a induce hypoferraemia, ferritin production and a decrease in circulating

transferrin receptors in cancer patients. Eur J Clin Invest. 28: 520–527.

Feezor, R. J., Cheng, A., Paddock, H. N., Baker, H. V., and Moldawer, L. L. (2005) Functional Genomics and Gene Expression Profiling in Sepsis: Beyond Class Prediction. Clinical Infectious Diseases 41: 427–435:

Fidge, N. H. (1999). High density lipoprotein receptors, binding proteins, and ligands. J Lipid Res 40: 187-201.

Fröhlich, T., and Arnold, G. J. (2006) Proteome research based on modern liquid chromatography – tandem mass spectrometry: separation, identification and quantification. J Neutral Transm 113: 973-994.

Gabay, C., Kushner, I., et al. (1999) Mechanisms of Disease: Acute-Phase Proteins and Other Systemic Responses to Inflammation. N Engl J Med 340: 448-454.

Giorgianni, F., Desiderio, D. M., and Beranova-Giorgianni, S. (2003) Proteome analysis using isoelectric focusing in immobilized pH gradient gels followed by mass spectrometry. Electrophoresis 24: 253–259.

Glauser, M. P., Zanetti, G., Baumgartner, J. D., and Cohen, J. (1991) Sepstic schock: pathogenesis. Lancet 338: 732-736.

Gonzalez-Chavez, S. A., Arevalo-Gallegos, S., et al. (2009) Lactoferrin: structure, function and applications. Int J Antimicrob Agents 33: 301e1-8.

Griffiths, B., and Anderson, Iain D. (2009) Sepsis, SIRS and MODS. Surgery 27: 446-449.

Hamler, R. L., Zhu, K., et al. (2004). A two-dimensional liquid-phase separation method coupled with mass spectrometry for proteomic studies of breast cancer and biomarker identification. Proteomics 4: 562-577.

Hanash, S. (2003) Disease proteomics. Nature 422: 226-232.

Herzum, I., and Renz, H. (2008) Inflammatory markers in SIRS, sepsis and septic shock. Current Medicinal Chemistry 15: 581-587.

Hotchkiss, R. S., Karl, I. E., et al. (2003) Medical progress: The pathophysiology and treatment of sepsis. 348: 138-150.

Hu, L., Li, X., Jiang, X., Zhou, H., et al. (2007) Comprehensive Peptidome Analysis of Mouse Livers by Size Exclusion Chromatography Prefractionation and NanoLC-MS/MS Identification. Journal of Proteome Research 6: 801-808.

Hu, S., Loo, J. A., and Wong, D. T. (2006) Human body fluid proteome analysis. Proteomics 6: 6326–6353.

Hu, S., Xie, Y., Ramachandran, P., et al. (2005) Large-scale identification of proteins in human salivary proteome by liquid chromatography/mass spectrometry and two-dimensional gel electrophoresis-mass spectrometry. Proteomics 5: 1714–1728.

Huang, L., Harvie, G., Feitelson, J.-S., et al. (2005) Immunoaffinity separation of plasma proteins by IgY microbeads: Meeting the needs of proteomic sample preparation and analysis. Proteomics 5: 3314–3328.

Ikuta, S., Edamatsu, H., Li, M., Hu, L., and Kataoka, T. (2008) Crucial Role of Phospholipase CE in Skin Inflammation Induced by Tumor-Promoting Phorbol Ester Cancer Res 68: 64–72.

Inoue, K.-I., Takano, H., Yanagisawa, R., and Yoshikawa, T. (2008) Protective Effects of Urinary Trypsin Inhibitor on Systemic Inflammatory Response Induced by Lipopolysaccharide. J Clin Biochem Nutr 43: 139–142.

Ishihama, Y. (2005) Proteomic LC-MS systems using nanoscale liquid

chromatography with tandem mass spectrometry. Journal of Chromatography A 1067: 73-83.

Issaq, H. J., Xiao, Z., and Veenstra T. D. (2007) Serum and Plasma Proteomics. Chem Rev 107: 3601-3620.

Kalantar-Zadeh, K., Rodriguez, R. A., and Humphreys, M. H. (2004) Association between serum ferritin and measures of inflammation, nutrition and iron in haemodialysis patients. Nephrol Dial Transplant 19: 141–149.

Koch, A. E., Polverini, P. J., Kunkel, S. L., et al. (1992) Interleukin-8 as a macrophage-derived mediator of angionenesis. Science 258: 1798-1801.

Kolb-Bachofen, V. (1991) A review on the biological properties of C-reactive protein. Immunobiology 183:133–145.

Kontrogianni-Konstantopoulos, A., and Bloch, R. J. (2005) Obscurin: a multitasking muscle giant. Journal of Muscle Research and Cell Motility 26: 419–426.

Lathrop, J. T., Anderson, N. L., Anderson, N. G., and Hammond, D. J. (2003) Therapeutic potential of the plasma proteome. Curr Opin Mol Ther 5: 250-257.

Lee, H.-J., Lee, E.-Y., Kwon, M.-S., and Paik, Y.-K. (2006) Biomarker discovery from the plasma proteome using multidimensional fractionation proteomics. Current Opinion in Chemical Biology10: 42–49.

Lever, A., and Mackenzie, I. (2007) Sepsis: definition, epidemiology, and diagnosis. BMJ 335: 879-883.

Levi, M., ten Cate, H., et al. (1999) Current Concepts: Disseminated Intravascular Coagulation. N Engl J Med 341: 586-592.

Levy, M. M., Fink, M. P., et al. (2003) 2001 SCCM/ESICM/ACCP/ATS/SIS

International Sepsis Definitions Conference. Crit Care Med 31: 1250-1256.

Linke, T., Ross, A. C., Harrison, E. H., et al. (2006) Proteomic analysis of rat plasma by two-dimensional liquid chromatography and matrix-assisted laser desorption ionization time-of-flight mass spectrometry. Journal of Chromatoghraphy A 1123: 160-169.

Liu, T., Qian, W.-J., Mottaz, H. M., et al. (2006) Evaluation of Multiprotein Immunoaffinity Subtraction for Plasma Proteomics and Candidate Biomarker Discovery Using Mass Spectrometry. Molecular & Cellular Proteomics 5: 2167–2174.

Lundblad, R. L. (2005) Considerations for the Use of Blood Plasma and Serum for Proteomic Analysis. The Internet Journal of Genomics and Proteomics. Volume 1. Number 2.

Luzzani, A., Polati, E., Dorizzi, R., et al. (2003) Comparison of procalcitonin and C-reactive protein as markers of sepsis. Crit Care Med 31:1737-1741.

Mann, M., and Jensen, O. N. (2003) Proteomic analysis of post-translational Modifications. Nature biotechnology 21: 255-261.

Martin, G. S., Mannino, D. M., et al. (2003) The epidemiology of sepsis in the United States from 1979 through 2000. N Engl J Med 348: 1546-1554.

Matot, I., and Sprung, C. I. (2001) Definition of sepsis. Intensive Care Med 27: 3-9.

Matthay, M. A. (2001) Severe sepsis — a new treatment with both anticoagulant and antiinflammatory properties. N Engl J Med 344: 759-62.

McDonald, T., Sheng, S., Stanley, B., et al. (2006) Expanding the Subproteome of the Inner Mitochondria Using Protein Separation Technologies. Molecular &

Cellular Proteomics 5: 2392-2411.

Meisner, M. (2005) Biomarkers of sepsis: clinically useful? Current Opinion in Critical Care 11: 473-480.

Michie, H. R., Spriggs, D. R., Manogue, K. R., et al. (1988) Tumor necrosis factor and endotoxin induce similar metabolic responses in human beings. Surgery 104: 280–286

Moshage, H. (1997) Cytokines and the hepatic acute phase response. J Pathol 181: 257-266.

Nakayama, T., Sonoda, S., Urano, T., et al. (1993) Monitoring both serum amyloid protein A and C-reactive protein as inflammatory markers in infectious diseases. Clin Chem 39: 293–297.

Nijsten, M. W., Olinga, P., The, T. H., et al. (2000) Procalcitonin behaves as a fast responding acute phase protein in vivo and in vitro. Crit Care Med 28: 458-461.

Norkina, O., Kaur, S., Ziemer, D., and De Lisle, R. C. (2004) Inflammation of the cystic fibrosis mouse small intestine. Am J Physiol Gastrointest Liver Physiol 286: 1032–1041.

O'Donnell, L. C., Druhan, L. J., and Avalos, B. R. (2002) Molecular characterization and expression analysis of leucine-rich α2-glycoprotein, a novel marker of granulocytic differentiation. J Leukoc Biol 72: 478–485.

Oberhoffer, M., Vogelsang, H., Rußwurm, S., Hartung, T., and Reinhart, K. (1999) Outcome Prediction by Traditional and New Markers of Inflammation in Patients with Sepsis. Clin Chem Lab Med 37: 363–368.

Pieper, R., Gatlin C. L., Makusky, A. J., et al. (2003) The human serum

proteome: Display of nearly 3700 chromatographically separated protein spots on two-dimensional electrophoresis gels and identification of 325 distinct proteins. Proteomics 3: 1345–1364.

Pratt, C. W., Swaim, M. W., and Pizzo, S. V. (1989) Inflammatory cells degrade inter-alpha inhibitor to liberate urinary proteinase inhibitors. J Leukoc Biol 45: 1–9.

Pugia, M. J., and Lott, J. A. (2005) Pathophysiology and diagnostic value of urinary trypsin inhibitors. Clin Chem Lab Med 43: 1–16.

Qian, W.-J., Jacobs, J. M., Camp II, D. G., et al. (2005) Comparative proteome analyses of human plasma following in vivo lipopolysaccharide administration using multidimensional separations coupled with tandem mass spectrometry. Proteomics 5: 572–584.

Rebecchi, M. J., and Srinivas, N. P. (2000) Structure, Function, and Control of Phosphoinositide-Specific Phospholipase C. Physiol Rev 80: 1291–1335.

Recalcati, S., Invernizzi, P., Arosio, P., and Cairo, G. (2008) New functions for an iron storage protein: The role of ferritin in immunity and autoimmunity. J Autoimmun 30: 84–89.

Reddy, K. S., and Perrotta, P. L. (2004) Proteomics in transfusion medicine. Transfusion 44: 601-604.

Rello, J., Díaz, E., Rodríguez, A., et al. (2009) Management of Sepsis: the PIRO Approach. Springer.

Remick, D. G. (2007) Pathophysiology of sepsis. The American Journal of Pathology 170: 1435-1444.

Ren, Y., Wang, J., Xia, J., et al. (2007) The Alterations of Mouse Plasma Proteins during Septic Development. Journal of Proteome Research 6: 2812-2821.

Rivers, E., Nguyen, B., Havstad, S., et al. (2001) Early goal-directed therapy in the treatment of severe sepsis and septic shock. N Engl J Med 345: 1368– 1377.

Saha, S., Harrison, S. H., Shen, C., Tang, H., et al. (2008) An online Database of human plasma proteins from healthy individuals. BMC Medical Genomics.

Scott, M. J., Godshall, C. J., et al. (2002) Jaks, STATs, Cytokines, and Sepsis. Clin Diagn Lab Immunol 9: 1153-1159.

Sheng, S., Chen, D., and Van Eyk, J. E. (2006) Multidimensional Liquid Chromatography Separation of Intact Proteins by Chromatographic Focusing and Reversed Phase of the Human Serum Proteome. Molecular & Cellular Proteomics 5: 26-34.

Shin, Y.-K., Lee, H.-J., Lee, J.S., and Paik, Y.-K. (2006) Proteomic analysis of mammalian basic proteins by liquid-based two-dimensional column chromatography. Proteomics 6: 1143–1150.

Shirai, R., Hirano, F., Ohkura, N., Ikeda, K., and Inoue, S. (2009) Up-regulation of the expression of leucine-rich α2-glycoprotein in hepatocytes by the mediators of acute-phase response. Biochemical and Biophysical research communications. 382: 776-779.

Simonian, M. H., and Betgovargez, E. (2003) Proteome analysis of human plasma with the ProteomeLab PF2D system. Beckman Coulter application information bulletin A-1963A.

Specialty Laboratories (2001) Directory of Services, and Use and Interpretation of Tests. Santa Monica. CA.

Steel, D. M., and Whitehead, A. S. (1994) The major acute phase reactants: C-reactive protein, serum amyloid P component and serum amyloid A protein. Immunology Today 15: 81-88.

Steinwald, P. M., Whang, K. T., Becker, K. L., et al. (1999) Elevated calcitonin precursur levels are related to mortality in an animal model of sepsis. Crit Care 3: 11-16.

Strieter, R. M., Kunkel, S. L., and Bone, R. C. (1993) Role of tumour necrosis factor-α in disease and inflammation. Critical Care Medicine 21: 447-463.

Suffredini, A. F., Fromm, R. E., Parker, M. M., et al. (1989) The cardiovascular response of normal humans to the administration of endotoxin. N Engl J Med 321: 280–287.

Takala, A., Nupponen, I., et al. (2002). Markers of inflammation in sepsis. Ann Med 34: 614-623.

Thadikkaran, L., Siegenthaler, M. A., Crettaz, D., et al. (2005) Recent advances in blood-related proteomics. Proteomics 5: 3019–3034.

Tracy, R. P. (2003) Thrombin, Inflammation, and Cardiovascular Disease. Chest 124: 49S-57S.

Tsai, J., Zhang, R., Qiu, W., Su, Q., Naples, M., and Adeli, K. (2009) Inflammatory NF-κB activation promotes hepatic apolipoprotein B100 secretion: evidence for a link between hepatic inflammation and lipoprotein production. Am J Physiol Gastrointest Liver Physiol 296: 1287-1298.

Tsiotou, A. G., Sakorafas, G. H., et al. (2005) Septic shock; current pathogenetic concepts from a clinical perspective. Med Sci Monit 11: 76-85.

Van Amersfoort, E. S., Van Berkel, T. J., et al. (2003) Receptors, mediators, and mechanisms involved in bacterial sepsis and septic shock. Clin Microbiol Rev 16: 379-414.

Van der Westhuyzen, D. R., de Beer, F. C., et al. (2007) HDL cholesterol

transport during inflammation. Curr Opin Lipidol 18: 147-151.

Veenstra, T. D., Conrads, T. P., Hood, B. L., et al. (2005) Biomarkers: Mining the Biofluid Proteome. Molecular & Cellular Proteomics 4: 409–418.

Venu, G. L. (2008) A study of foci of infection on admission in patients with sepsis in multidisciplinary intensive care unit. Dissertation.

Vermeire, S., Van Assche, G., and Rutgeerts, P. (2006) Laboratory markers in IBD: Useful, magic, or unnecessary toys? Gut 55: 426–431.

Walsh, G., and Jefferis, R. (2006) Post-translational modifications in the context of therapeutic proteins. Nature biotechnology 24: 1241-1252.

Wendel, M., Paul, R., and Heller, A. R. (2007) Lipoproteins in inflammation and sepsis. II. Clinical aspects. Intensive Care Med 33: 25–35.

Whitcomb, D. C. (2006) Acute pancreatitis. N Engl J Med 354: 2142–2150.

Wu, F., Vij, N., et al. (2007). A novel role of the lumican core protein in bacterial lipopolysaccharide-induced innate immune response. J Biol Chem 282: 26409-26417.

Young, B., Gleeson, M., Cripps, A. W., et al. (1991) C-reactive protein: a critical review. Pathology 23: 118–124.

Zabolotny, J. M., Kim, Y.-B., Welsh, L. A., et al.(2008) Protein-tyrosine Phosphatase 1B Expression Is Induced by Inflammation in Vivo. Journal of biological chemistry 283: 14230–14241.

Zeng, C. (2000) NuMA: A Nuclear Protein Involved in Mitotic Centrosome Function. Microsc Res Tech 49: 467–477.

Zhang, W. W. (2003) The use of gene-specific IgY antibodies for drug target discovery. Drug Discov Today 8: 364-371.

Zhang, X., Li, L., and McNaughton, P. A. (2008) Proinflammatory Mediators Modulate the Heat-Activated Ion Channel TRPV1 via the Scaffolding Protein AKAP79/150. Neuron 59: 450–461.

Zhou, L., Beuerman, R. W., Chew, A. P., Koh, S. K., et al. (2009) Quantitative Analysis of N-Linked Glycoproteins in Tear Fluid of Climatic Droplet Keratopathy by Glycopeptide Capture and iTRAQ. Journal of Proteome Research 8: 1992–2003.

Zhu, K., Zhao, J., et al. (2005) Protein pI shifts due to posttranslational modifications in the separation and characterization of proteins. Anal Chem 77: 2745-2755.